Universitat Autònoma de Barcelona

ROLE OF IRON CONTENT AND ENDOSTATIN EXPRESSION IN THE PROGRESSION OF DIABETIC RETINOPATHY

Aina Bonet Arribas

Universitat Autònoma de Barcelona

ROLE OF IRON CONTENT AND ENDOSTATIN EXPRESSION IN THE PROGRESSION OF DIABETIC RETINOPATHY

Thesis presented by:

Aina Bonet Arribas

To apply for the degree:

PhD in Animal Medicine and Health by the Universitat Autònoma de Barcelona

UNDER THE DIRECTION OF:

Dr. Jesús Ruberte París

DEPARTMENT OF ANIMAL HEALTH AND ANATOMY, VETERINARY FACULTY, UNIVERSITAT AUTÒNOMA DE BARCELONA AND CENTER OF ANIMAL BIOTECHNOLOGY AND GENE THERAPY

Bellaterra, 2022

JESÚS RUBERTE PARÍS, full professor of the Department of Animal Health and Anatomy at the Veterinary Faculty of Universitat Autònoma de Barcelona

CERTIFIES THAT:

AINA BONET ARRIBAS has carried out the study "**Role of iron content and endostatin expression in the progression of diabetic retinopathy"** under my direction at the Universitat Autònoma de Barcelona

Bellaterra, 2022

Dr. JESÚS RUBERTE PARÍS

ACKNOWLEDGMENTS

Primero de todo quiero agradecer esta tesis a mi director y mentor, Jesús Ruberte, que me ha guiado durante estos años con dedicación, profesionalidad y empatía y ha hecho que tuviera más confianza en mí misma como investigadora y como persona.

En segundo lugar, dar infinidad de gracias a todas las personas que han pasado por el laboratorio durante el tiempo en el que he estado. Desde Andreia y David, que me guiaron cuando estaba empezando, hasta Vero, Ángel y Lore, que han sido unos verdaderos pilares. Gracias Ángel por hacer más amenos los días con tu buen humor inacabable y tu alegría. Gràcies Vero per escoltar-me, preguntar-me, aconsellar-me i ajudar-me tantes vegades. Mil gràcies també a la Judit, que ha sigut aire fresc i que tant m'ha ajudat amb les seves idees, la seva experiència i les seves ganes d'innovar i avançar cada dia. I al Guillem, amb qui he compartit feina, però amb qui continuaré compartint vida com sempre i per sempre.

Agrair també a tota la gent del Cbateg, especialment a l'Alba, que m'ha il·luminat en tants moments. També a tota la gent de la Facultat de Veterinària, en especial al Marc, a l'Ana i al Víctor, amb qui he compartir molts bons moments en les practiques d'anatomia. També un especial agraïment a l'Eduard Cunilleras per haver invertit temps i coneixement en aquesta tesi. Gràcies també al personal dels serveis de microscòpia i al laboratori de luminescència i espectroscòpia de biomolècules de la UAB per tota l'ajuda.

Gracias Lore por ser mi ángel de la guarda y mi hermana mayor durante este tiempo y por toda la paciencia, la complicidad, las risas y el apoyo permanente. Vaya tesoro me llevo.

A tots els meus amics que tan enamorada em tenen. A la meva família, tant la que m'ha tocat com la que he triat. Al meu pare i a les meves dues increïbles mares que sempre m'han recolzat incondicionalment i m'han fet ser qui soc. A la meva àvia que és un sol enorme. I a l'Albert, l'amor de la meva vida que m'estima, em comprèn i em fa créixer cada dia.

I finalment, el més sentit agraïment i respecte a tots els animals que fan possible que la ciència avanci cada dia.

SUMMARY

Diabetic retinopathy (DR) is a leading cause of visual impairment in adults and its prevalence is expected to increase in the next years. DR can be divided into non-proliferative (NPDR), in which the retina suffers from microvascular changes and blood-retinal barrier (BRB) breakdown, and proliferative diabetic retinopathy (PDR), characterized by neovascularization. Although DR has been extensively studied, it has a complex and multifactorial pathogenesis that challenges the development of effective therapies. In this regard, new mechanisms involved in DR should be studied to increase the knowledge of the disease. Diabetes mellitus has been related to an increase of systemic iron content which could affect the retina causing oxidative damage and exacerbating the pathogenesis of DR. However, how systemic iron excess and BRB status determine retinal iron dysregulation during DR remains unclear. Furthermore, pathological neovascularization during PDR takes place due to an imbalance between angiogenic and antiangiogenic factors. In this regard, endostatin, the most powerful antiangiogenic factor known in the retina, could have a key role in PDR development. The main objectives of the present work have been the analysis of the role of BRB in retinal iron homeostasis and the characterization of endostatin expression in the retina during DR. The experiments have been performed in the db/db mice, a model that develops type 2 diabetes, and in human samples.

The results of this work support the fact that diabetes courses with systemic iron overload. Furthermore, this research demonstrated that the retina is tightly protected against systemic iron overload by the BRB, which only allows massive entry of iron when is compromised. Moreover, the retina is capable to detect systemic iron overload and increase its ferritin expression, an iron storage protein with antioxidant activity, suggesting an autonomous regulatory mechanism prior to BRB breakdown and iron increase in the retina.

This work also showed for the first time intracellular expression of endostatin in the retina, mainly in bipolar cells and photoreceptors, in both human and mouse. Furthermore, endostatin was decreased in db/db mouse retinas, creating an environment prone to neovascularization. Accordingly, intravitreal vessels protruding from the optic disc mimicking neovascularization were found in db/db mouse.

Overall, this thesis provides an insight on the understanding of the role of the BRB during iron overload and the decrease of endostatin during DR. Thus, offering a guidance on the potential therapies that could be used.

RESUM

La retinopatia diabètica és la principal causa de ceguera en la població adulta i s'espera que la seva prevalença continuï augmentant en els propers anys. Està dividida en una fase no proliferativa, en la que es donen alteracions vasculars i la ruptura de la barrera hematorretiniana, i una fase proliferativa, caracteritzada per la neovascularització. Tot i que la retinopatia diabètica ha estat extensament estudiada, la seva patogènesis és complexa i multifactorial, fet que dificulta el desenvolupament de teràpies efectives i fa necessari ampliar el coneixement sobre possibles nous mecanismes involucrats. En aquest sentit, la diabetis mellitus ha estat relacionada amb un increment de ferro sistèmic, el qual podria causar dany oxidatiu en la retina i empitjorar la progressió de la retinopatia diabètica. Malgrat això, encara no se sap com l'excés de ferro sistèmic i la barrera hematorretiniana determinen el contingut de ferro en la retina durant la retinopatia diabètica. Pel que fa a la neovascularització pròpia de la fase proliferativa, es considera que està causada per un desequilibri entre factors angiogènics i antiangiogènics. L'endostatina és el factor antiangiogènic més potent conegut en la retina i podria tenir un paper clau en el desenvolupament de la neovascularització. Els objectius principals d'aquest treball han estat l'anàlisi de la funció de la barrera hematorretiniana en l'homeòstasi del ferro en la retina i la caracterització de l'expressió d'endostatina durant la retinopatia diabètica. Els experiments s'han desenvolupat en un model de diabetis tipus 2, el ratolí db/db, i en mostres de pacients humans.

Els resultats donen suport al fet que durant la diabetis hi ha un increment de ferro sistèmic. A més, aquesta investigació demostra que la retina està estretament protegida per la barrera hematorretiniana en front als augments de ferro sistèmic i que el ferro només entra massivament a la retina quan aquesta es trenca. La retina podria també detectar el augment del ferro sistèmic augmentant l'expressió de ferritina, proteïna encarregada d'emmagatzemar ferro i evitar el dany oxidatiu. Aquest fet suggereix la existència d'un mecanisme de regulació autònom en la retina previ al trencament de la barrera hematorretiniana i a l'augment de ferro en la retina.

Aquesta treball també ha mostrat per primera vegada l'expressió d'endostatina a nivell intracel·lular en cèl·lules bipolars i en fotoreceptors, tant en humà com en ratolí. A més a més, les retines dels ratolins diabètics presenten una disminució en l'expressió d'endostatina, el què provocaria un ambient propens a la neovascularització. D'acord amb això, els ratolins db/db presenten vasos en el vitri sortint del disc òptic amb característiques de neovasos.

En conclusió, aquesta tesi proporciona coneixement sobre el paper de la barrera hematorretiniana en condicions de sobrecàrrega de ferro i sobre la disminució de l' endostatina durant la retinopatia diabètica. Aquesta recerca, per tant, obre la porta a possibles teràpies que es podrien fer servir per combatre la progressió de la malaltia.

RESUMEN

La retinopatia diabética es la principal causa de ceguera en la población adulta y se espera que su prevalencia continue aumentando en los próximos años. Se divide en una fase no proliferativa, en la que se dan alteraciones vasculares y la rotura de la barrera hematorretiniana, y una fase proliferativa, que se caracteriza por la neovascularización. Aunque la retinopatia diabética ha sido extensamente estudiada, su patogénesis es compleja y multifactorial, hecho que dificulta el desarrollo de terapias efectivas y hace necesario ampliar el conocimiento sobre posibles nuevos mecanismos involucrados. En este sentido, la diabetes mellitus se ha relacionado con un incremento de hierro sistémico, el cual podría causar daño oxidativo en la retina y empeorar la progresión de la enfermedad. Sin embargo, aún no se sabe cómo el exceso de hierro sistémico y la barrera hematorretiniana determinan el contenido de hierro en la retina durante la retinopatia diabética. En cuanto a la neovascularización propia de la fase proliferativa, se considera que está causada por un desequilibrio entre factores angiogénicos y antiangiogénicos. La endostatina es el factor antiangiogénico más potente conocido en la retina y podría tener un papel clave en el desarrollo de la neovascularización. Teniendo esto en cuenta, los objetivos principales de este trabajo han sido el análisis de la función de la barrera hematorretiniana en la homeostasis del hierro en la retina y la caracterización de la expresión de endostatina durante la retinopatia diabética. Los experimentos se han desarrollado en un modelo de diabetes tipo 2, el ratón db/db, y en muestras de pacientes humanos.

Los resultados apoyan el hecho de que durante la diabetes hay un incremento de hierro sistémico. Además, esta investigación demuestra que la retina está estrechamente protegida por la barrera hematorretiniana frente a aumentos de hierro sistémico, ya que el hierro sólo entra masivamente en la retina cuando la barrere se rompe. La retina podría también detectar el augmento de hierro sistémico aumentando la expresión de ferritina, proteína encargada de almacenar hierro y evitar el daño oxidativo. Este hecho sugiere la existencia de un mecanismo de regulación autónomo en la retina previo a la rotura de la barrera hematorretiniana y al aumento de hierro en la retina.

Este trabajo también ha mostrado por primera vez la expresión de endostatina a nivel intracelular en las células bipolares y en los fotorreceptores, tanto en humano como en ratón. Además, las retinas de los ratones diabéticos presentan una disminución en la expresión de endostatina, lo que provocaría un ambiente propenso a la neovascularización. De acuerdo con esto, los ratones db/db presentan vasos intravítreos que protruyen del disco óptico con características de neovasos.

En conclusión, esta tesis proporciona conocimiento sobre el papel de la barrera hematorretiniana en condiciones de sobrecarga de hierro sistémico y sobre la disminución de la endostatina durante la retinopatia diabética. Esta investigación abre la puerta a posibles terapias que se podrían utilizar para combatir la progresión de la enfermedad.

TABLE OF CONTENTS

LIST OF FIGURES

A) LITERATURE REVIEW

B) CHAPTER I

C) CHAPTER II

LIST OF ABBREVIATIONS

AGEs: advanced glycation products

ATP: adenosine triphosphate

b-FGF: basic fibroblast growth factor

bi: bipolar cell

BRB: blood-retinal barrier

BCA: bicinchoninic acid

BSA: bovine serum albumin

CBATEG: Center for Animal Biotechnology and Gene Therapy

cGMP: cyclic guanosine monophosphate

db/db: BKS.Cg-Dock7^{m} +/+ Lepr^{db}/J diabetic mouse

db/+: BKS.Cg-Dock7^{m} + Lepr^{db}/+ non-diabetic mouse

DMO: diabetic macular oedema

DMT1: divalent metal cation transporter

DNA*:* deoxyribonucleic acid

DR: diabetic retinopathy

ELM: external limiting membrane

FcR: antibody Fc receptors

GCL: ganglion cell layer

GFAP: glial fibrillary acidic protein

H/E: haematoxylin and eosin

HIF-1: hypoxia-inducible factor 1

HFE: homeostatic iron regulator gene

HRP: horseradish peroxidase

iBRB: inner blood-retinal barrier

ICP-MS: inductively coupled plasma mass spectrometry

IGF-1: insulin-like growth factor 1

ILM: internal limiting membrane

INL: inner nuclear layer

IPL: inner plexiform layer

IREs: iron responsive elements

IRPs: iron regulatory proteins

IS: photoreceptor inner segment

JAM: junction adhesion molecules

MMPs: metalloproteinases

mRNA: messenger ribonucleic acid

NADPH: nicotinamide adenine dinucleotide phosphate

NPDR: non-proliferative diabetic retinopathy

oBRB: outer blood-retinal barrier

ONL: outer nuclear layer

OPL: outer plexiform layer

OS: photoreceptor outer segment

PBS: phosphate buffer saline

PBI: phosphate buffer igepal

PDGF: platelet-derived growth factor

PDR: proliferative diabetic retinopathy

PKC: protein kinase C

PEDF: pigment epithelium-derived factor

PVDF: polyvinylidene difluoride

RIPA: radioimmunoprecipitation assay

RPE: retinal pigmented epithelium

ROS: reactive oxygen species

SCARA5: scavenger receptor class A member *5*

SDS-page: sodium dodecyl sulfate polyacrylamide gel electrophoresis

SEM: standard error of the mean

SLO: scanning laser ophthalmoscope

TBST*:* Tris buffered saline- Tween

TIBC: total iron binding capacity

TIM2: T-cell immunoglobulin mucin *receptor 2*

TGF-β: transforming growth factor

UK: United Kingdom

USA: United States of America

VEGF: vascular endothelial growth factor

VEGFR: vascular endothelial growth factor receptor

WT: wild type

ZO: Zonula occludens

LIST OF SYMBOLS AND UNITS OF MEASUREMENT

AU: arbitrary units

Fe^{2+}: ferrous iron

Fe^{3+}: ferric iron

G*:* gauge

g: gram

HO^-: hydroxyl ions

H_2O_2: hydrogen peroxide

kDA: kilodalton

Kg: kilogram

M: molar

ml: milliliter

mm^2: square millimiter

mM: millimolar

NaCl: sodium chloride

nm: nanometer

$OH^·$: hydroxyl radicals

pH: potential hydrogen

µm: micrometer

ºC: degree Celsius

%: percentage

INTRODUCTION

Diabetes mellitus affects over a 573 million people and its prevalence is predicted to increase to 783 million by 2045 (IDF, 2021). Diabetic retinopathy (DR), a major complication of diabetes, is a leading cause of visual impairment and blindness worldwide in working-age population (WHO, 2021). It has been estimated that 35% of diabetic patients will develop some form DR during their life (WHO, 2020). DR is a complex and multifactorial disease associated with genetic and environmental factors that has been widely studied (Warpeha and Chakravarthy, 2003; Reddy and Natarajan, 2011; Petrovič, 2013); however, its pathogenesis is still not fully understood.

DR is a progressive microvascular disease that can be divided in a non-proliferative and a proliferative phase (Duh et al., 2017). The non-proliferative phase represents an early stage of the disease and is characterized by the blood-retinal barrier (BRB) breakdown that results in increase of vascular permeability and vascular leakage (Klaassen et al., 2013). Excess of retinal iron content has been pointed out as a key factor for non-proliferative DR, since it causes oxidative damage that harms the retina (Rogers et al., 2007; Chaudhary et al., 2018; Shu et al., 2020). However, the relation between iron efflux into the retina and BRB breakdown during DR remains unclear.

Proliferative diabetic retinopathy is the most advanced phase of the disease, and courses with retinal neovascularization triggered by retinal ischemia (Silva et al., 2012). Retinal neovascularization is induced by an imbalance between angiogenic and antiangiogenic factors (Simo et al., 2006; Praidou et al., 2010; Abcouwer, 2013; Behl and Kotwani, 2015), being vascular endothelial growth factor (VEGF) the main factor for retinal angiogenesis (Zhang et al., 2018). However, the role of antiangiogenic factors such as endostatin, could be crucial to understand the angiogenic switch that occurs during DR.

In this scenario, the present work has been divided in two parts:

1. Analysis of the **role of the BRB in retinal iron overload** during DR.
2. Characterization of the **expression and activity of endostatin** during DR.

For this research work, human samples, as well as the db/db mouse, have been used. Mouse models are still essential for the study of DR since they offer advantages compared with other species (Olivares et al., 2017). Both human and mouse retinas have a similar vascular pattern in which retinal vessels arise from the optic disc and spread the periphery nourishing only the inner retina (Ruberte et al., 2017). Furthermore, mice can be genetically modified to mimic DR lesions (D. Ramos et al., 2013b). The db/db mouse has a mutation in the gene that encodes the leptin receptor, which causes obesity and insulin resistance (Robinson et al., 2012), and is a widely used model to study DR (Bogdanov et al., 2014; Chaudhary et al., 2018; Hanaguri et al., 2021).

LITERATURE REVIEW

A. ANATOMY OF THE MOUSE EYE AND RETINA

The eye is a specialized sensory organ that captures light and transforms it into visual images, which relay into the brain. It is located at the cranial part of the skull, inside the orbit, and surrounded by accessory organs such as the eyelids, the conjunctiva, the eyeball muscles, and the lacrimal apparatus (Ruberte et al., 2017).

A.1. Parts of the eyeball and topography of the retina

The eyeball is covered and protected by three different tunics from outside to inside: the fibrous layer, the vascular layer, and the retina (Treuting and Dintzis, 2012).

The outer part is formed by the **fibrous tunic**, which is divided in the cornea and the sclera. The **cornea** is the anterior part of the eye and acts as an external barrier that protects the eye from the environment. It is an avascular and densely innervated layer composed by keratocytes, epithelial cells, endothelial cells, and acellular components such as collagen (DelMonte and Kim, 2011). The distribution of collagen and the absence of vessels gives transparency to the cornea and allows the transmission of the light into the retina with minimum optical scatter (Lee Ann, 2012; Sridhar, 2018). The cornea meets the **sclera** in a structure called **limbus**, and then the sclera is extended in the posterior part of the eye (Van Buskirk, 1989). The sclera is a thick and opaque layer formed by fibrous tissue rich in type I collagen and elastic fibers that maintains the shape of the eye bulb (de la Maza et al., 2012).

The **vascular tunic***,* also called uvea, is formed by the iris and the ciliary body in the anterior portion, and the choroid in the posterior portion. The **iris** is a contractile structure located behind the cornea that presents a circular aperture in the middle called the **pupil,** which can dilate (mydriasis) or contract (myosis), regulating the light that enters the eye (Bloom and Czyz, 2018). Laterally, between the iris and the vitreous chamber, there is the **ciliary body**, which consist of the ciliary muscle, the ciliary epithelium, and the ciliary blood vessels. The ciliary muscle supports and accommodates the lens inside the eyeball to adjust the vision, although in mice it is not well developed. The ciliary body folds to form the ciliary processes and produce **aqueous humour.** The aqueous humour is secreted to the **posterior chamber**, which is the space delimited by the iris and the lens, goes through the pupil into the **anterior chamber**, which is delimited by the cornea and the iris, and finally drains into the **trabecular meshwork** located in the angle of the anterior chamber (Overby et al., 2014; Ruberte et al., 2017). Among other functions, the aqueous humour maintains the intraocular pressure and provides nutrients to the avascular tissues such as the cornea. Mouse and human eyes have a similar production

rate of aqueous humour (Aihara et al., 2003). Both anterior and posterior chamber are in the anterior part of the eye, while the **vitreous chamber,** which is behind the lens, is in the posterior part of the eye (Ruberte et al., 2017). The **choroid** is in the back of the eye between the retina and the sclera, and its function is to provide oxygen and nutrients to the outer retina. It is highly pigmented, which allows the light absorption and prevents reflections within the retina (Smith, 2002).

The inner layer of the eyeball is the **retina**, which constitutes the neural part of the eye that receives the light and initiates the process of vision. In its outer surface, the retina is in contact with the choroid, while its inner part is in contact with the vitreous body (Schaller and Constantinescu, 2007). In the middle of the retina there is the optic disc, from where the optic nerve emerges (Smith, 2002; Ruberte et al., 2017). The retina is capable to capture light and turn it into neural impulses that travel thought the **optic nerve** to the brain, where are integrated and interpretated (Chaffee et al., 1923).

Inside the eyeball, between the iris and the vitreous chamber, there is the **lens**, bathed by the aqueous humour anteriorly and by the vitreous body posteriorly. It is transparent, biconvex, avascular, and can adjust its shape (accommodation) to refract the light and focus objects on the retina, like a photographic camera. The mouse lens is much bigger and spherical than human lens, occupying the 75% of the intraocular area, which explains why the vitreous chamber in mouse is proportionally smaller than in human (D. Ramos et al., 2013a; Ruberte et al., 2017). The parts of the mouse eyeballs are shown in detail in Figure 1.

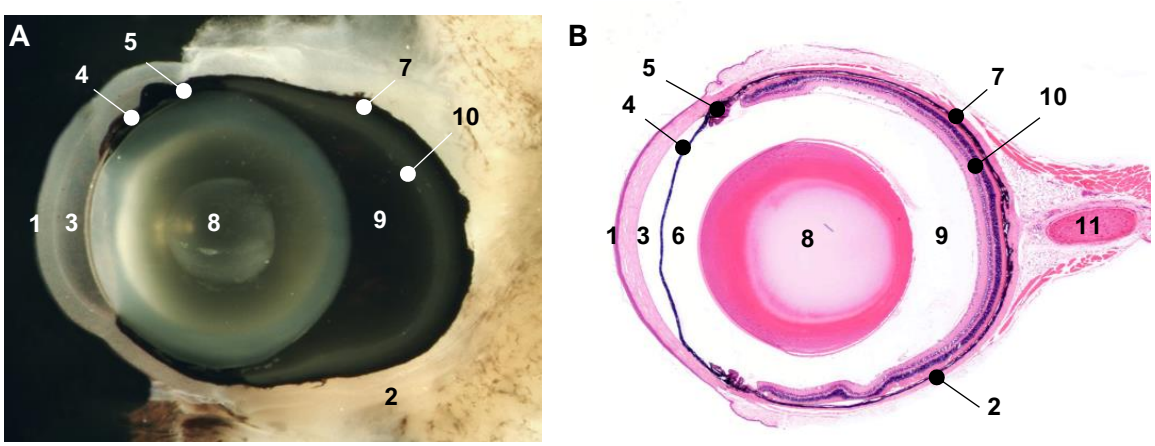

Figure 1. Anatomy of the mouse eye. Topographical **(A)** and histological **(B)** sections of the mouse eye. 1: cornea; 2: sclera; 3: anterior chamber; 4: iris; 5: ciliary body; 6: posterior chamber; 7: choroid; 8: lens; 9: vitreous chamber; 10: retina; 11: optic nerve. (Ruberte et al., 2017).

The anatomy of the vertebrate retina was described in detail for the first time by Santiago Ramón y Cajal in 1893. All vertebrates have in common that the retina is formed by different and highly organized groups of neurons and glial cells with specific roles that allow the visual function. Structurally, the retina presents a neuronal part, which is organized in different cell layers with specialized functions, and a pigmented epithelium, which supports and nourish the neurosensory retina. As shown in figure 2, the retina is composed by the following layers from the inner to the outer part (Remington, 2012; Ruberte et al., 2017):

- **Internal limiting membrane (ILM):** is the boundary between the retina and the vitreous and represents the basal lamina of the inner retina. The ILM is composed of proteoglycans, collagen IV, and collagen XVIII, among others, and is lined by Müller cells endfeet.
- **Nerve fiber layer:** composed by ganglion cells axons surrounded by astrocytes, retinal vessels, and Müller cells terminals.
- **The ganglion cell layer (GCL):** formed by ganglion cells, whose axons converge in the optic disc, and Müller cells processes. It is also possible to observe displaced amacrine cells and astrocytes.
- **The inner plexiform layer (IPL)**: consists of bipolar cell axons and ganglion cell dendrites along with their synapsis.
- **The inner nuclear layer (INL):** composed mainly by bipolar cells, but also by horizontal cells in the external part and amacrine cells in the internal part.
- **The outer plexiform layer (OPL)**: is a dense synaptic network between cells from the inner nuclear layer and photoreceptors.
- **The outer nuclear layer (ONL)** contains the cellular bodies of **rods** and **cones** photoreceptors.
- **External limiting membrane (ELM):** formed by Müller cells processes. It lays between the outer nuclear layer and the internal segments of the photoreceptors.
- The photoreceptor **inner segment (IS)** contains the soma, the axon, the organelles, and the synaptic terminals. The cytoplasm of photoreceptors is rich in mitochondria.
- The photoreceptor **outer segment (OS)** is formed by disc membranes that harbour the phototransduction cascade.
- The retina is supported by a single layer of pigmented cells called the **retinal pigmented epithelium (RPE)**.

A.2.1. Neurons

The neurons that detect light in the first place and transform it into electrical signal are the **photoreceptors.** More precisely, light absorption takes place in the **outer segment,** a specialized disc membrane filled with photosensitive pigments, such as rhodopsin (Lem et al., 1999). These discs allow the enlargement of the membrane surface and maximize the chances of capturing photons. In 1967, Richard Young described how photoreceptors discs are continually renewed during lifetime (Young, 1967). The outer segment follows with the **inner segment**, which contains the cytoplasm with the cell machinery, mainly mitochondria, and the synaptic terminal of the photoreceptor. This organization is similar in all vertebrates, with only slightly morphological variations (Peichl, 2005).

There are two types of photoreceptors: rods and cones. **Rods** are activated at low levels of light, whereas **cones** are responsible for daylight and coloured vision. In mice, the average ratio between rods and cones is 35:1 (Jeon et al., 1998) while in humans is 20:1 (Mustafi et al., 2009), but the biggest difference is that human retinas present the macula, a high visual acuity area with a small depression in its centre, the fovea, that exclusively contains cones (Jonas et al., 1992). This characteristics corelate with the nocturnal and diurnal habits that mice and humans have, respectively (Kaskan et al., 2005). Rods can be distinguished because they have a denser chromatin nucleus than cones (Carter-Dawson and Lavail, 1979).

Horizontal cells are interneurons in charge of laterally connections between photoreceptors and bipolar cells. They cause inhibitory feedback to photoreceptors, and are believed to be implicated in contrast and light intensity discrimination (Peichl et al., 1998).

Bipolars cells are so named as they present a central body and two processes that arise in opposite directions: the dendrites, in contact with the outer retina, and the axon, connected with the inner retina. Bipolar cells synapse with both rods and cones and then transmit the electric signal to the ganglion cells, directly or indirectly (via amacrine cells). They also receive lateral synapses from horizontal cells. There are many types of bipolar cells, differentiating between cone bipolar cells and rod bipolar cells, and each one encodes different actions, such as polarity or chromatic composition (Ghosh et al., 2004).

Amacrine cells are neurons that interact laterally with bipolar cells and ganglion cells and have inhibitory effect. There are also many types of amacrine cells depending on their dendrite morphology and length, which is related to the specific functions that these

cells can carry out. Some of their functions include release of neurotransmitters, regulation of the circadian rhythm, and modulation in vision of movement objects (Kolb et al., 1995).

The last neurons in the retinal visual circuit are the **ganglion cells,** which form a layer in the inner part of the retina. All ganglion cells synapse with bipolar and amacrine cells and their long axons converge at the centre of the retina to form the optic nerve that is directed into the brain (Masland, 2011).

A.2.2. Glia

There are three types of glial cells in the mouse retina: Müller cells, astrocytes, and microglia. These cells maintain retinal homeostasis, provide support to the neurons, and participate in metabolism processes (Kolb, 1995).

The **Müller cell** was first described by Heinrich Müller in 1851 and represents the 90% of the glia in the retina. These cells cross the retina from the inner border to the outer nuclear layer and form the outer limiting membrane. Müller cells maintain retinal structure, controls nutrients supplies, and regulates the composition of extracellular fluid, among other functions. Müller cells present cell processes, also called “endfeets”, that surround the retinal vessels and help in the preservation of the BRB tightness (Vecino et al., 2016).

Astrocytes are located at the nerve fiber layer, where they escort the trajectory of axons that will form the optic disc (Stone and Dreher, 1987). As Müller cells, astrocytes are intimately related to blood vessels and have endfeets that surround and preserve the BRB integrity (Coorey et al., 2021). In fact, astrocytes modulate the development of retinal vasculature (Zhang and Stone, 1997) and, interestingly, are absent in species with avascular retinas (Schnitzer, 1988). Astrocytes also participate in neuronal homeostasis and in the maintenance of retinal architecture (Holländer et al., 1991).

Microglial cells are resident macrophages of the central nervous system, which includes the retina. Microglia are distributed in the inner layers of the retina and are involved in retinal surveillance, phagocyting pathogens, cellular debris, and apoptotic cells when needed (Thanos, 1991).

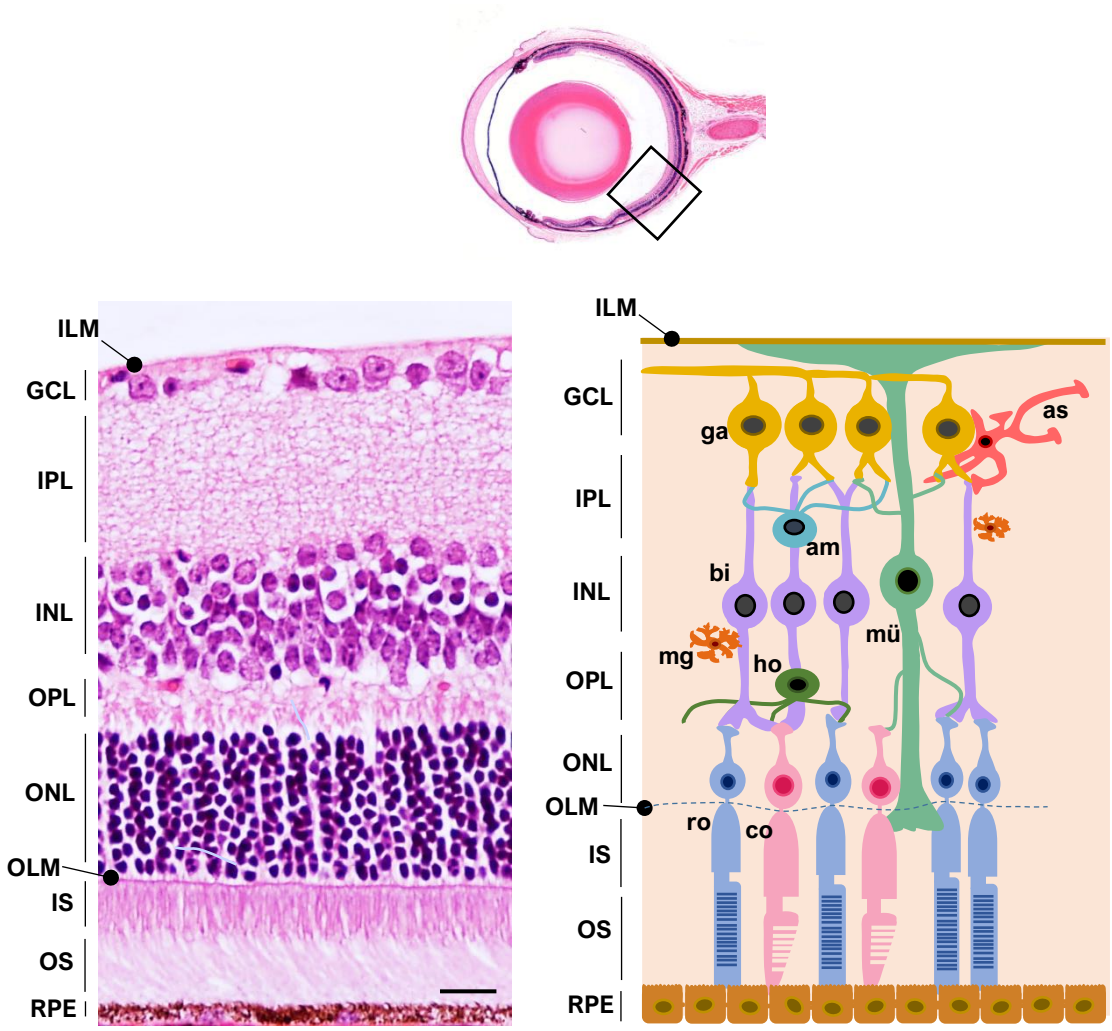

Figure 2. Anatomy of the mouse retina. ILM: internal limiting membrane; GCL: ganglion cell layer; IPL: inner plexiform layer; INL; inner nuclear layer; OPL: outer plexiform layer; ONL; outer nuclear layer; ELM: external limiting membrane; IS: photoreceptor inner segments; OS: photoreceptor outer segments; RPE: retinal pigmented epithelium. Scale bar: 22.93 µm.

A.3. Retinal vascular system

The retina and its related structures need a proper blood supply to assure their functions. Depending on the phase of development and part of the retina, it can be nourished by three vascular beds: the hyaloid, the retinal, and the choroidal vasculature. During the embryonic development and soon after birth, mice retina receives oxygen and nutrients exclusively from the hyaloid vessels; after birth, these vessels start to regress while retinal vascularization develops. Retinal vascularization supplies oxygen and nutrients to the inner retina and the choroids to the outer retina (Fruttiger, 2002; Saint-Geniez and D'Amore, 2004).

A.3.1. Development of retinal vasculature

During foetal development, the retina is nourished by the hyaloid vasculature, which arises from the **hyaloid artery** and extends from the optic disc to the lens, crossing the vitreous chamber (Figure 3 and 4A). In mid-gestation in humans (Birnholz and Farrell, 1988) and within two weeks after birth in mouse (Ito and Yoshioka, 1999), the hyaloid vasculature regresses and is replaced by the retinal vasculature (Fruttiger, 2007) (Figure 3). Normally, at day P21 hyaloid vasculature has disappeared, but in some cases, this regression is not completed and remains as a persistent hyaloid artery (Z. Wang et al., 2019) (Figure 4B). In fact, previous studies have described that hyaloid artery persists in 15% of mice (McLenachan et al., 2015).

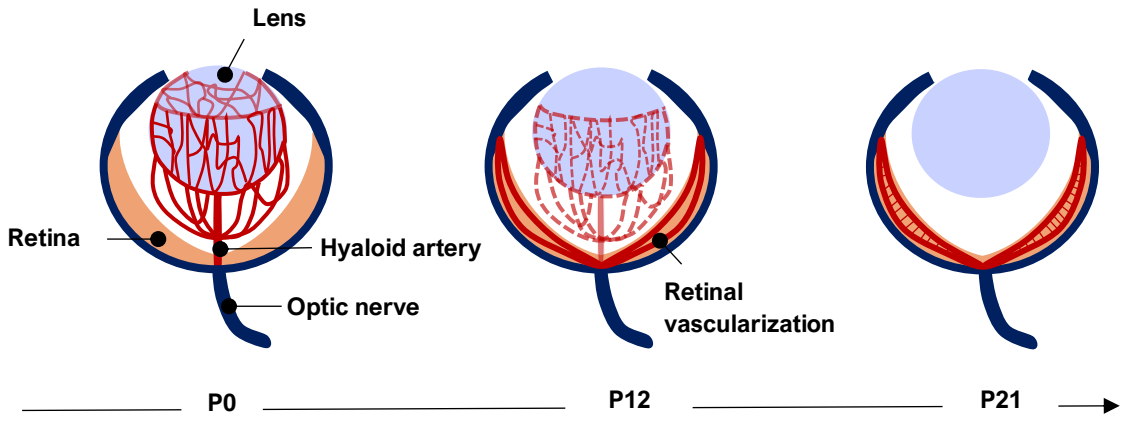

Figure 3. Regression of the hyaloid system. At P0, hyaloid vessels are still extended to the lens and occupy the vitreous to nourish the immature retina. By P12, hyaloid vessels involute while retinal vascularization is developing, being the superficial retinal vascular layer the first one to form. Around P21, the hyaloid vessels are completely regressed and substituted by retinal vascularization. (Adapted from Wang et al., 2019).

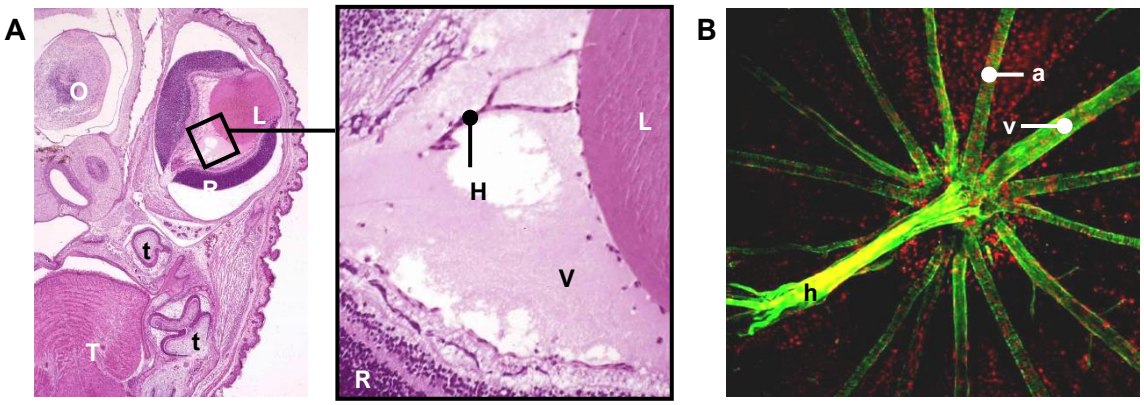

Figure 4. Hyaloid vasculature in a newborn mouse (A) and persistent hyaloid vessel in an adult mouse (B). **(A)** Transverse histological section of the head at P0 showing hyaloid vessels in the vitreous attached to the lens (2X and 20X, respectively). **(B)** Confocal microscopy image of a whole mount retina immunodetecting blood vessels, including a persistent hyaloid artery, with collagen IV (green) (200X). L: lens; R: retina; HA: hyaloid artery; ON: optic nerve; a: arteriole; v: venule OB: olfactory bulb; T: tongue; t: tooth; R: retina; L: lens; V: vitreous; HA: hyaloid artery. (Ruberte et al., 2017).

In addition to the hyaloid artery regression, the **central retinal artery**, which comes from the ophthalmic branch of the carotid artery in both mouse and human, enters the retina through the optic nerve and branches radially to nasal and temporal directions to supply the different quadrants of the retina. This process follows a pre-existing template of astrocytes that guide vessel formation (Dorrell et al., 2002). In the way to the periphery, retinal arterioles become smaller and form an arteriovenous capillary network that merge into venules that return towards the optic disc to join the **central retinal vein,** which finally drains into the retro-orbital venous plexus (McLenachan et al., 2015).

A.3.2. Adult vascular pattern

The retina is a high oxygen demanding tissue but also requires transparency, thus, retinal vessels are very well-organized. Compared with capillary beds in other tissues, retinal capillaries have a higher microhematocrit and velocity, which means that more oxygen can be delivered in the retina with less vascular density (Paques et al., 2003a).

In both humans and mice, retinal vessels branch in three layers: the **superficial vascular plexus** at the level of the ganglion cell layer, and the **intermediate vascular plexus** and **deep vascular plexus** along each side of the inner nuclear layer (Connolly et al., 1988; Paques et al., 2003). In fact, the intermediate vascular plexus is constituted by the anastomosis between the superficial and the deep plexus (Ruberte et al., 2017) (Figure 5A). In the superficial plexus there are fewer and thicker vessels compared to the deep plexus (Figure 5B). There are also variations in vessel density and branching between individuals or between eyes of the same animal (McLenachan et al., 2015).

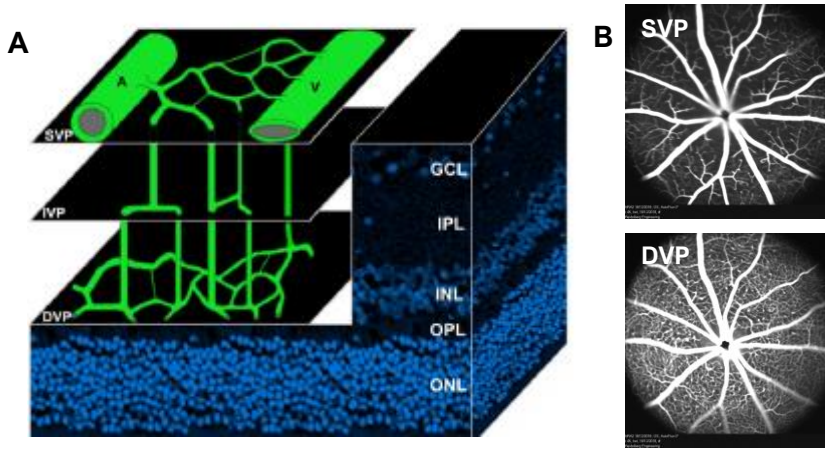

Figure 5. **Retinal vascular plexi in mouse. (A)** Schematic representation of the distribution of retinal blood vessels. **(B)** Fluorescein s**c**anning laser ophthalmoscope images of the retinal fundus showing the superficial and deep vascular plexus. SVP: superficial vascular plexus; IVP: intermediate vascular plexus; DVP: deep vascular plexus; GCL: ganglion cell layer; IPL: inner plexiform layer; INL: inner nuclear layer; OPL: outer plexiform layer; ONL; outer nuclear layer. (Ramos, 2014).

Another characteristic is that whereas in mice the centre of the eye axis matches with the optic disc, in human, the central part of the retina presents an avascular area called **macula** (Curcio et al., 1990). Blood vessels distribution in the retina varies between species, but in human and mice, retinal vessels follow a **holangiotic** pattern, meaning that the vessels are only in the inner retina and absent in the photoreceptor layer (D. Ramos et al., 2013b) (Figure 6).

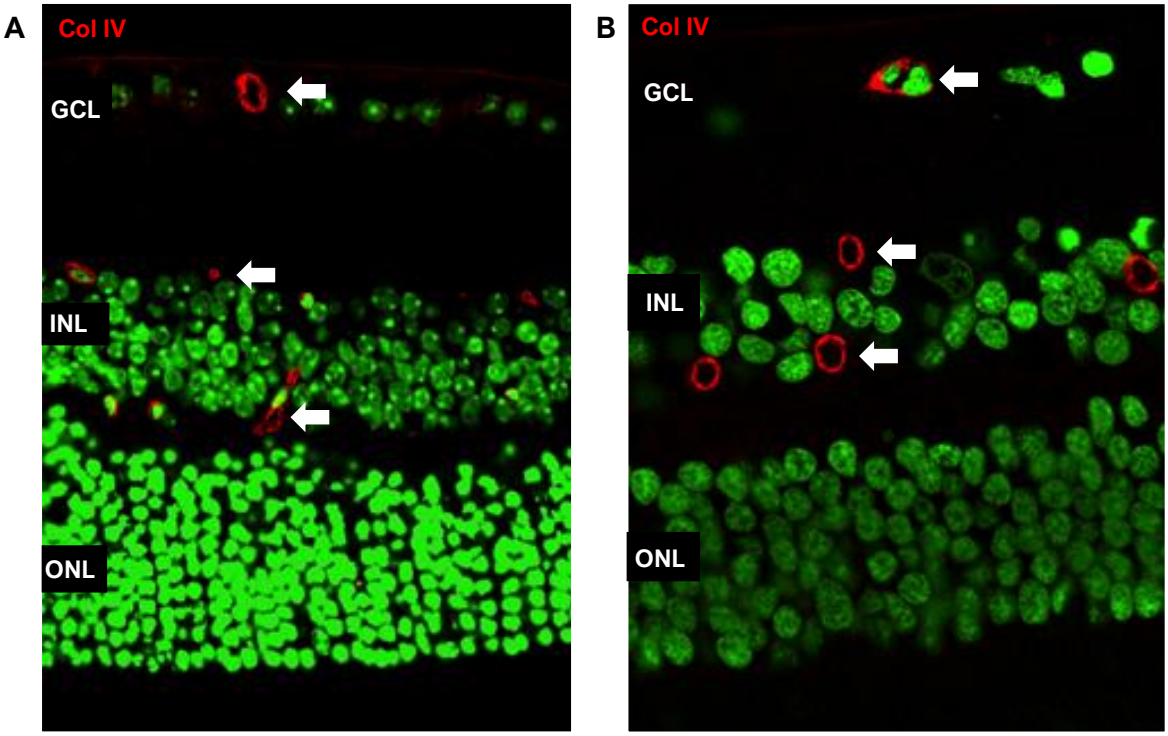

Figure 6. Retinal vascular topography in mouse vs. human. Paraffin sections of mouse **(A)** and human **(B)** retinas stained against collagen IV (red) by immunohistochemistry showing the three superficial, intermediate, and deep vascular plexi (arrows). Nuclei were counterstained with Sytox green (green). GCL: ganglion cell layer; INL: inner nuclear layer; ONL: outer nuclear layer. Scale bar: A: 16.92 µm; B: 13.73 µm. (Ruberte et al. 2017).

A.3.3. Structure of blood vessels

Retinal arterioles and venules, like in other tissues, are composed of three layers. In the luminal surface there is the ***Tunica intima*****,** which is a monolayer of endothelial cells and its basement membrane connected to a subendothelial layer of connective and elastic tissue. Surrounding the tunica intima is the ***Tunica media***, which presents concentric layers of smooth muscle cells and pericytes that encircle the vessels. In big arterioles, the tunica media is much ticker, as they need enough contractability to regulate vessel calibre and blood pressure. In contrast, veins present fewer smooth muscles cells. The tunica externa o ***Tunica adventitia*** is formed by connective tissue that covers the outermost surface of the vessel (Saint-Geniez and D'Amore, 2004; Tucker and Mahajan,

2018). Retinal capillaries are formed exclusively of a single layer of endothelial cells and covered by pericytes embedded in the vessel basement membrane (Ruberte et al., 2017). There are three types of capillaries depending on the blood exchange: pre-capillaries, mid-capillaries, and postcapillaries (Nehls and Drenckhahn, 1991).

Endothelial cells are flattened cells organized in single layers, the endothelium, that line all blood vessels in the organism, from the aorta to the smallest capillaries in the retina (Figure 7A-B). These cells present a typical elongated nucleus with a high condensed heterochromatin and a cytoplasm that extends around the vessel and houses the organelles, mainly distributed in the perinuclear region of the cytoplasm (Bharadwaj et al., 2013). Endothelial cells are full of vesicles that allow the molecular transport from the blood to the surrounding tissue (Gardiner and Archer, 1986). They also modulate blood pressure and blood flow by releasing specific substances, participate in angiogenesis, and are involved in the cellular immune response (Haller, 1997). Endothelial cells phenotype can differ depending on the organ and blood vessel type (Kumar et al., 1987).

At the abluminal surface, surrounding endothelial cells and embedded with their basement membrane, there are specific cells, the **pericytes,** named after their perivascular location (Zimmermann, 1923) (Figure 7B). Pericytes cover the vessels with their cytoplasmatic processes, which can have different morphologies, and become a part of the BRB. In this regard, pericytes act as vascular stabilizers and control retinal homeostasis and vascular permeability. Moreover, pericytes are contractile cells that, together with smooth muscle cells, can regulate the blood flow (Attwell et al., 2016; Gonzales et al., 2020). Pericytes also control endothelial proliferation (Birbrair et al., 2014) and are involved in tissue repair (Özen et al., 2012; Birbrair et al., 2013).

Endothelial cells and pericytes are supported by the **basement membrane**, which is a specialized extracellular matrix formed by proteoglycans and other substances such as type IV collagen, laminin, and fibronectin (Yurchenco and Schittny, 1990). In the retina, type IV collagen is expressed exclusively in vessels basement membranes, becoming a great marker for retinal vessels (Ramos et al., 2013). Basement membrane supports the endothelium, maintains the compartmentalization within tissues, and contributes to BRB function and endothelial cell proliferation (Timpl et al., 1981; Roy and Kim, 2021).

Smooth muscle cells surround the vessels and control the vascular calibre and, thus, the blood pressure, by contracting or relaxing in response to stimuli, assuring that blood is distributed within the retina. Near the optic disc, retinal vessels present several layers of smooth muscle cells and, as they branch peripherally the number of smooth muscle cells decrease (Hogan et al. 1971) (Figure 7C).

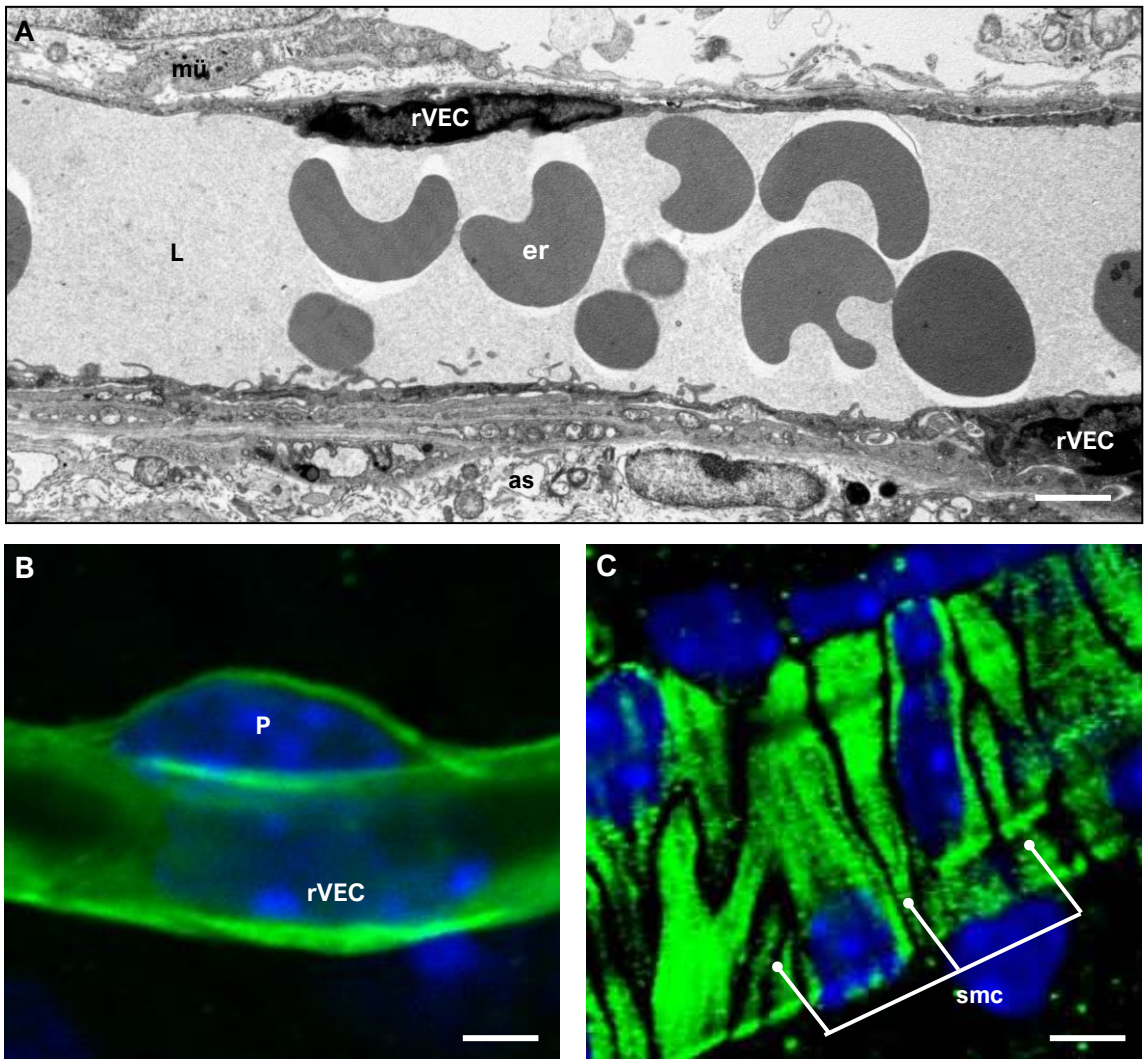

Figure 7. Components of retinal blood vessels. **(A)** Transmission electron microscopy micrograph of a retinal vessel. **(B)** Immunohistochemistry against collagen IV (green) to visualize retinal blood vessels using confocal laser microscopy **(C)** Immunohistochemistry against α-smooth muscle actin (green) to detect vascular smooth muscle cells by confocal laser microscopy. Nuclei were counterstained with ToPro3. mü: Müller cell; L: vascular lumen; rVEC: retinal vascular endothelial cell; er: erythrocyte; as: astrocyte; P: pericyte; smc: smooth muscle cell. Scale bar: 1.62 µm (A); B: 2.25 µm (B); 6.86 µm (C). (Ruberte et al., 2017).

A.3.4. Choroidal vasculature

The outer layer of the retina, formed by photoreceptors, has an enormous need of adenosine triphosphate (ATP) and nutrients to perform the phototransduction and the constant shedding of the outer segments (Okawa et al., 2008), however, it is completely avascular in mouse and depends on **choroidal circulation** for its viability (Anderson and McIntosh, 1967). The choroid can be divided in three layers: the lamina choriocapillaris, that forms part of the Bruch's membrane between the choroids and the pigmented epithelium; the lamina vasculosa, where posterior ciliary artery branches, vortex veins, and nerves pass through; and the lamina suprachoroidea, which is avascular and in

contact with the sclera. Ciliary arteries branch from the ophthalmic artery, as well as the central artery of the retina, and vortex veins drain in the ophthalmic veins (Ruberte et al., 2017). Choroid not only provides blood flow to the RPE and photoreceptors, but also accounts for the 85% of the total vascular support in the eye (Ehrlich et al., 2016).

Some species with nocturnal habits like the cat, present a reflective layer in the choroid called the ***Tapetum lucidum****,* which reflects light back to the retina to increase the possibility of catching photons (Ruberte et al., 2017). However, even mice are nocturnal animals, they do not present this feature.

A.4. The Blood Retinal Barrier

In 1947, Erik Palm performed an experiment injecting intravenous trypan blue to rabbits and found that all organs were stained except for the central nervous system, which included the retina. This experiment demonstrated that the retina and the brain presented specific barriers that regulate the entry of substances from the blood (Palm, 1947). The retinal parenchyma is protected by the BRB, which is composed by two distinct barriers; the inner BRB (**iBRB**), which control transport across the retinal capillaries, and the outer BRB (**oBRB**), formed by the RPE that regulates molecular diffusion from the choroid to the retina (Figure 8). BRB preserve retinal integrity from the variations that occur in the systemic circulation and prevents the entry of harmful agents (Campbell and Humphries, 2013).

A.4.1. Inner and outer BRB

As happens in the brain, iBRB is formed by retinal capillaries with a non-fenestrated endothelium, a basement membrane, and a pericyte coverage, all sustained by glia endfeets. These endothelial cells are connected by tight junctions, which shape the inner BRB and regulate the flux of molecules intercellularly (Díaz-Coránguez et al., 2017).

In contrast to retinal vessels, the choriocapillaris are highly fenestrated, so the retina is protected by a single layer of RPE cells with intercellular tight junctions that form the oBRB. The oBRB regulates paracellular diffusion from the choroid to the outer retina regulating photoreceptors nutrition and removing waste products (Naylor et al., 2020). RPE also transports fluid from the apical to the basal border that creates negative pressure and maintains retinal adhesion to the RPE (Frambach and Marmor, 1982).

Any alteration in vascular endothelial cells or in their tight junction conformation will compromise the BRB integrity and will produce an increase of vascular permeability.

Without BRB regulation, fluid could enter the retina indiscriminately and cause retinal oedema (Campbell and Humphries, 2013).

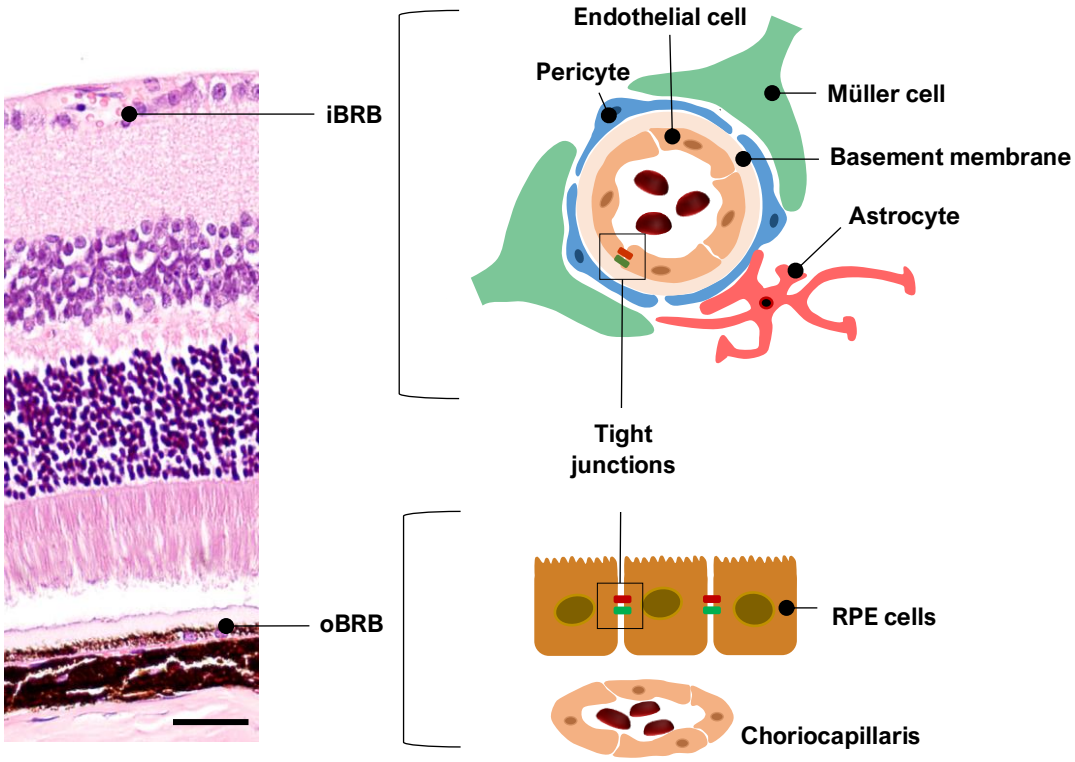

Figure 8. Schematic view of the BRB. BRB is composed by the iBRB formed by tight junctions between vascular endothelial cells surrounded by a basement membrane with a coverage of astrocytes and Müller cells processes. The oBRB is formed by tight junctions between RPE cells. Scale bar: 36.36 µm.

A.4.2. Tight junctions

Tight junctions, also known as *Zonula occludens*, are well organized transmembrane complexes of at least 40 proteins that maintain the connection between retinal vascular endothelial cells in the iBRB or between retinal pigmented epithelial cells in the oBRB. Tight junctions are expressed in endothelial cells as soon as the vascular network is developing in the retina, even before BRB is completely assembled (Van Der Wijk et al., 2019). Tight junction's proteins include occludin, claudins, and junction adhesion molecules (JAMs) (Figure 9).

Occludin was the first protein to be isolated from the tight junction complex and its responsible for tight junction stability (Furuse et al., 1993). **Claudins** are believed to be the backbone proteins in tight junctions' formation. There are 27 subtypes of claudins identified in mammals (Liu et al., 2016), differently expressed depending on the tissue, being claudin-5 the most abundant in iBRB endothelial cells (Morita et al., 1999; Luo et

al., 2011). Both claudins and occludin present four transmembrane domains that form loops between adjacent cells, which, in turn, contact with the intracellular scaffold proteins of the Zonula occludens family (ZO-1, ZO-2, and ZO-3).This complex is anchored to the actin of the cytoskeleton and maintain cell adhesion (Balda and Matter, 2000; Suzuki et al., 2015) (Figure 9).

JAMs belong to the immunoglobulin superfamily and, unlike claudins and occludins, only have one transmembrane domain (Balda and Matter, 2000). JAMs interact with scaffolding proteins and participate in cell signalling and regulation (Chavakis et al., 2004; Martìn-Padura et al., 1998).

Apart from sealing the paracellular space, tight junctions maintain cell polarity by regulating the transport of proteins and lipids between the apical and basolateral membrane (Köhler and Zahraoui, 2005). Other functions have also been reviewed, such as signal transmitting, gene expression and cell proliferation (Zihni et al., 2016; Bhat et al., 2019; Díaz-Coránguez et al., 2019).

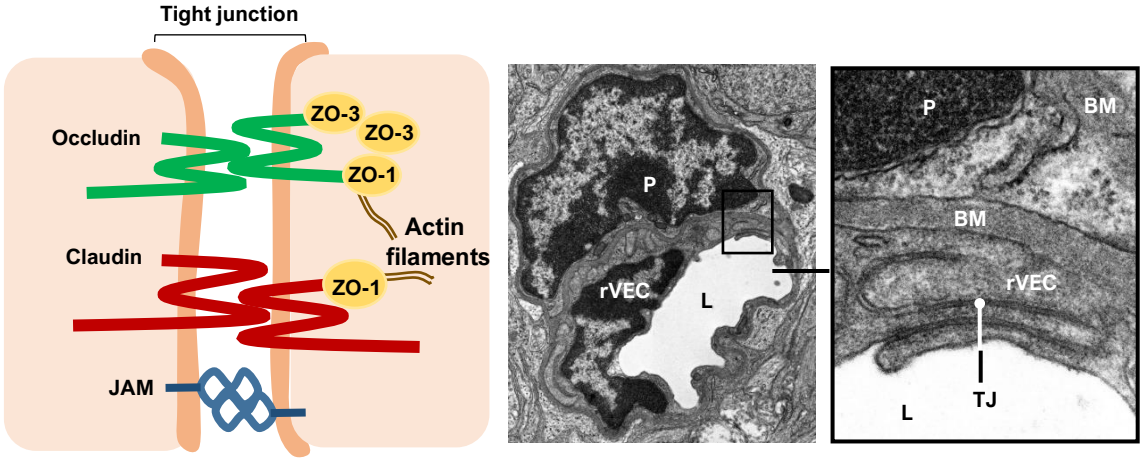

Figure 9. BRB tight junctions (A) Representation of tight junctions claudin, occludin, JAM, and Zonula occludens (ZO's) in retinal vascular endothelial cells. **(B)** Tight junction observed in a retinal micrograph using transmission electron microscopy (15,000X and 80,000X, respectively). Tight junctions appear as an electrodense line between neighbouring endothelial cells. P: pericyte; rVEC: retinal vascular endothelial cell; L: vascular lumen; BM: blood vessel basement membrane; TJ: tight junction. (Ruberte et al., 2017).

A.4.3. Transport across the blood-retinal barrier

Movements of molecules across BRB can occur through the vascular endothelial cells by **transcellular transport** or between cells by **paracellular transport** (Figure 10). Both routes can happen simultaneously (Díaz-Coránguez et al., 2017).

Molecules are transported across the retinal endothelium following gradients of concentration by different mechanisms. Depending on the size, chemical properties, and charge, molecules will be transported in one way or another (Toda et al., 2011) (Figure 10). For example, liposoluble molecules and gases, such oxygen, cross the cell by passive diffusion; plasma proteins are transported via transcytosis; other proteins like transferrin, insulin or albumin need to bind to a receptor in the cell membrane; glucose and aminoacids use specific carriers; and ions cross through channels. Except from passive diffusion, the rest of transports require energy (Díaz-Coránguez et al., 2017; Zhi et al., 2021).

In **transcytosis**, transport is mediated by the vesicular system, in which macromolecules are endocytosed in the apical (luminal) membrane, transported in vesicles across the cell, and exocytosed in the basolateral (abluminal) membrane (Karnovsky, 1967; Raviola, 1977).Transcytosis is higher in early stages of BRB development and is supressed gradually to form a functional barrier (Knowland et al., 2014).

Apart from crossing the endothelial cell, molecules can move between cells by paracellular transport. Under physiological conditions, intercellular spaces of the retinal endothelium are blocked by tight junctions and paracellular trafficking is almost inexistent (Raviola, 1977).

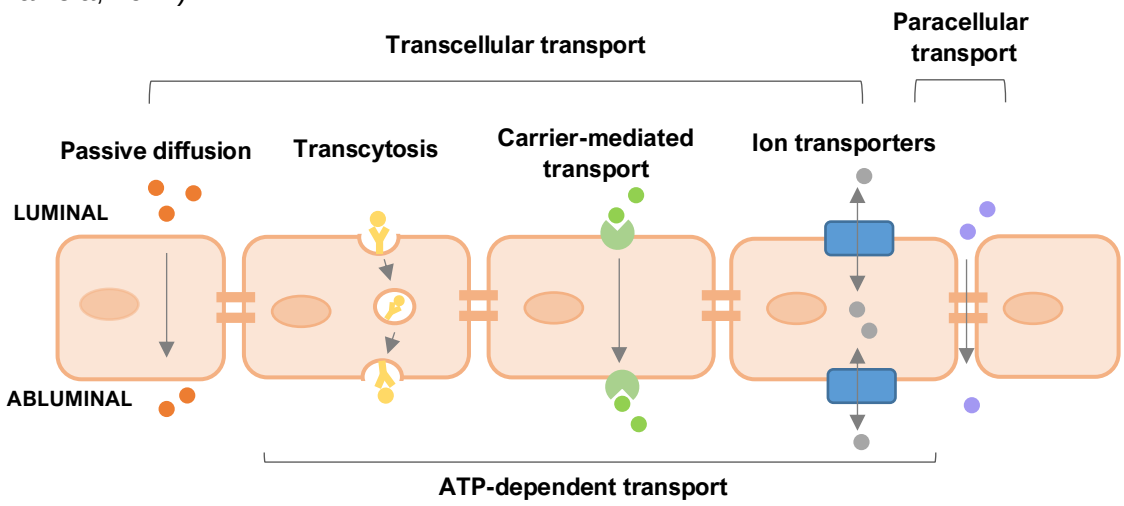

Figure 10. Transport across the BRB. Molecules are transported across the retinal endothelium (transcellular transport) or between neighbouring endothelial cells (paracellular transport) from the luminal to the abluminal surface. Transport can be through passive diffusion or by active transport requiring energy, which include transcytosis, carrier-mediated transport, and ion transporters.

A.4.4. BRB breakdown

BRB breakdown is a multifactorial and interrelated process that can be caused by tight junction dysfunction, increased transcellular transport, and by alterations in the cells that participate in the formation of the barrier, such as pericytes and glia (Vinores, 2010).

Changes in tight junction expression, location, and interaction can lead to an increase of BRB permeability (Antonetti et al., 1998; Muthusamy et al., 2014). In ischemic conditions, VEGF induces vascular permeability by uncoupling tight junctions, specially by occludin phosphorylation, causing retinal oedema in diseases such as diabetic retinopathy (Antonetti et al., 1999; Murakami et al., 2009, 2012). Other molecules such as metalloproteinases (MMPs), mostly MMP-2 and –9, cause BRB disruption by the degradation of the extracellular matrix and by the cleavage of tight junctions proteins (Feng et al., 2011). Pericyte depletion (Ogura et al., 2017) and glia dysfunction (Shen et al., 2010) also cause BRB breakdown by altering the its structure, by inducing VEGF expression, and by affecting tight junctions such as claudin-5 (Nitta et al., 2003; Koto et al., 2007; Argaw et al., 2009). Alterations in the cytoskeleton can affect the anchorage of ZO-1 with claudin and occludin and affect BRB tightness (Hicks et al., 2010). Reactive oxygen species have also been described to cause rearrangements in claudin-5 and occludin location, affecting the BRB (Schreibelt et al., 2007).

Although it is known that paracellular transport alteration is more important in BRB dysfunction, several studies have demonstrated that the increase of vesicular transport (transcytosis) across endothelial cells also determine BRB permeability (Knowland et al., 2014; Valença et al., 2021).

B. DIABETIC RETINOPATHY

Diabetes mellitus is considered the pandemic of this century and is expected to keep increasing in the next decades to 783 million people (IDF, 2021). Diabetes mellitus can be roughly divided in type 1 and type 2. In **type 1 diabetes**, the pancreas is uncapable to produce enough insulin due to pancreatic β-cell destruction and it is usually detected early in life (Kaul et al., 2012). **Type 2 diabetes**, which affects 95% of diabetic patients (WHO, 2021), is characterized by insulin resistant, meaning that the pancreas produces insulin, but the body does not use it efficiently. It is very related to the lifestyle and tends to develop at older ages (Kaul et al., 2012). In fact, many studies have demonstrated the unquestionable relation between obesity and the risk of developing type 2 diabetes (Sasai et al., 2010; Nguyen et al., 2011; Wang et al., 2016).

Diabetes mellitus can carry several complications, affecting to a wide range of tissues in the body. Macrovascular complications include cerebrovascular, cardiovascular, and peripheral disease, in which patients are in risk of developing strokes, heart attacks, and circulation problems in the limbs, respectively. Microvascular complications include diabetic retinopathy, nephropathy, and neuropathy (Beckman and Creager, 2016). This thesis is focused on **diabetic retinopathy**, which is the leading cause of visual impairment and blindness in adult population all over the word.

B.1. Pathogenesis

DR can be divided in **non-proliferative** (NPDR) and **proliferative** (PDR) stages. NPDR is an early phase of DR characterized by an increase in vascular permeability (Lechner et al., 2017). Histologically, the earliest alterations in DR are pericyte loss (Cogan et al., 1961; Speiser et al., 1968) and thickening of the basement membranes (Toussaint and Dustin, 1963), which lead to the formation of microaneurysms and jeopardizes BRB integrity, causing lesions that go from mild haemorrhages to extended exudates and cotton wool spots (Garner, 1993; Lechner et al., 2017). When the accumulation of fluid is localized in the macula, it causes the **diabetic macular oedema** (DMO), which can occur in any stage of DR (Bhagat et al., 2009). Loss of pericytes and endothelial cells ends up causing capillary occlusion and hypoxia in the retinal tissue that led to neovascularization (Hamanaka et al., 2001; Hammes, 2005) (Figure 11). Thus, PDR is an advanced stage characterized by the formation of new vessels that might protrude and bleed into the vitreous cavity and even cause retinal detachment by traction. PDR is the most vision-threatening stage of DR (Lechner et al., 2017).

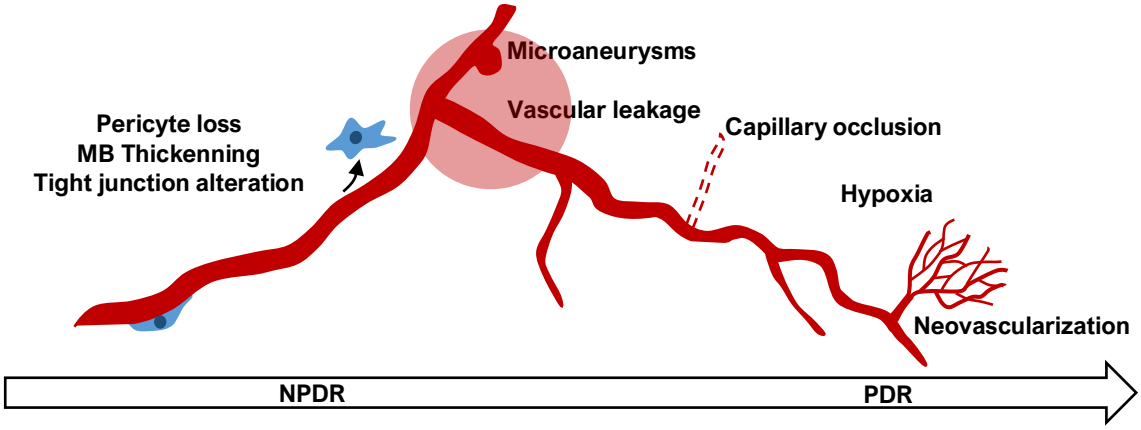

Figure 11. Microvascular changes in the progression of DR. Alterations of the vascular unit such as pericyte loss, BM thickening, and tight junction dysfunction lead to the formation of microaneurysms and BRB breakdown, which in turn cause vascular leakage in the retinal parenchyma. These alterations can occlude the capillaries and cause retinal hypoxia, which induces the expression of vascular growth factors that guide neovascularization. NPDR: non-proliferative diabetic retinopathy; PDR: proliferative diabetic retinopathy. (Adapted from Kusuhara et al., 2018).

DR is a multifactorial disease caused by the hyperglicemia-induced activation of several pathways, such as the formation of advanced glycation end products (AGEs), the polyol pathway, the protein kinase C (PKC) activation, and the hexosamine pathway.

Hyperglycaemia causes an increase in **AGEs formation** (Xu et al., 2018) which alter protein structure and function of the vascular unit by inducing oxidative damage, inflammation (Kanda et al., 2017), leukostasis (Moore et al., 2003), and pericyte apoptosis (Chen et al., 2006), that results in BRB weakening. Excess of glucose also activates the **polyol pathway** to reduce glucose into sorbitol with expenses of nicotinamide adenine dinucleotide phosphate (NADPH), thus, decreasing cellular antioxidant protection (Barnett et al., 1986; Lee and Chung, 1999). Moreover, hyperglycaemia increase glycolysis, which leads to **PKC activation** increasing VEGF expression, endothelial permeability and leukostasis (Ishii et al., 1998). Altogether, these pathways not only cause oxidative damage but also make the retina more vulnerable to suffer oxidative stress from other agents with redox activity (Lee and Chung, 1999; Tang et al., 2012). In turn, oxidative stress activates back these pathways, becoming a self-reinforcing cycle that ends up causing the lesions of DR (Kowluru and Chan, 2007).

Accumulation of reactive oxygen species (ROS) causes mitochondrial dysfunction, inflammation, lipid peroxidation, and apoptosis, damaging the retinal tissue (Kowluru and Chan, 2007). In the mitochondria, ROS alter protein synthesis, induce NF-kB activation, and increase MMP-2 and -9 expression, which damage the mitochondrial membrane and cause the release of cytochrome c into the cytoplasm. These events trigger the caspase cascade, responsible of apoptosis (Kowluru et al., 2011; Mohammad and

Kowluru, 2011). ROS also promote lipid peroxidation by the oxidation and degradation of cell membrane phospholipids that causes cell damage and is believed to be responsible for retinal neurodegeneration (Armstrong and Al-Awadi, 1991; Augustine et al., 2021).

Oxidative damage is caused by ROS, specially by hydroxyl radicals. In this regard, any molecule with redox activity, such as iron, represents a threat in the retina. Iron in ferrous form is capable to generate hydroxyl radicals that could be involved in the pathogenesis of DR in a situation of iron overload (Song and Dunaief, 2013), which will be reviewed in detail later in this thesis.

All the mechanisms involved in DR pathogeny create an inflammatory environment that contribute to the exacerbation of the disease. Inflammation causes cytokines upregulation, VEGF signalling, leukostasis, and nitric oxide secretion among others, that magnifies vascular damage, increases vascular permeability, and causes capillary occlusion (Tang and Kern, 2011; Nagineni et al., 2012).

During retinal ischemia, the hypoxia-inducible factor 1 (HIF-1) activates and upregulates the expression of VEFG (Ozaki et al., 1999; Yan and Su, 2014; Zhang et al., 2018), which increases vascular permeability by altering tight junctions (Antonetti et al., 1999) and promotes neovascularization by the recruiting and proliferation of endothelial cells (Cai et al., 2006).

Although DR is considered a microvascular disease, it also causes **neurodegeneration**. Indeed, oxidative stress, imbalance of neuroprotective factors, and metabolites produced due to hyperglycaemia cause neuronal apoptosis and glia activation (Bogdanov et al., 2014). It is believed that neurodegeneration occurs before microvascular abnormalities, and it has been described that patients without noticeable signs of diabetic retinopathy presented already a decrease of visual electrophysiological responses and retinal neurodegeneration (Villarroel et al., 2010). Ganglion cells are the first neurons to be affected, causing nerve fiber layer loss in diabetic patients (Lopes de Faria et al., 2002), although it has been reported that neurons in the inner retina and photoreceptors are also affected (Park et al., 2003; Yi et al., 2005; Gastinger et al., 2006; Bogdanov et al., 2014).

Reactive gliosis is a common response to inflammation and oxidative damage in the retina and is characterized by the overexpression of the glial fibrillary acidic protein (GFAP) (Lewis and Fisher, 2003). In physiological conditions, GFAP is only expressed by astrocytes; however, in retinopathies, Müller cells “activate” and start expressing

GFAP (Lieth et al., 1998). Reactive Müller cells GFAP-positive release VEGF and exacerbate the disease (Wang et al., 2010).

Overall, DR has a complex pathophysiology and, although it has been widely studied, there are many aspects that remain unclear. The appearance and study of new factors that could be involved in the progression of DR is crucial for the complete understanding of the disease.

B.2. Neovascularization

The word neovascularization refers to the formation of new blood vessels from the *de novo* (vasculogenesis) or from pre-existing vessels (angiogenesis) (Risau, 1997). In DR, vascular growth develops from pre-existing vessels, however, there are studies that have shown that circulating levels of endothelial precursors cells could also play a role in neovascularization during DR (Lee et al., 2005; Abu El-Asrar et al., 2013).

Microvascular changes in the retina during DR create a hypoxic environment that induces the upregulation of angiogenic factors to form new vessels. HIF-1 is a transcription factor thar responds to low concentrations of oxygen and stimulates **VEGF** expression (Ozaki et al., 1999; Yan and Su, 2014; Zhang et al., 2018), which has been widely demonstrated to promote angiogenesis in the retina in vitro and in vivo (Ozaki et al., 1997; Pe'er et al., 1998; Gerhardt et al., 2003; Kinnunen et al., 2006; Rezzola et al., 2014). During retinal development, VEGF guides angiogenesis of new vessels, which arise from the optic disc and extend to the peripherical retina, whereas in DR, new vessels growth is aberrant and directed to the vitreous (Ishibazawa et al., 2016).

MMPs are proteases responsible of the degradation of extracellular matrix and are crucial for retinal neovascularization (Rodrigues et al., 2013). MMPs substrates include collagen IV, which is present in the basement membrane of retinal blood vessels (Essner and Lin, 1988). During DR, MMPs, and specially MMP-2 and -9 (Das et al., 1999; Noda et al., 2003; Rodrigues et al., 2013), trigger basement membrane degradation, allowing the sprouting of new blood vessels and the formation of a new vascular lumen. Indeed, patients with PDR present MMP-2 and -9 overexpression in the epiretinal vessels (Abu El-Asrar et al., 2013a; Rodrigues et al., 2013). In physiological conditions, pericytes would be recruited and basement membrane established, however, pathological vessels lack of a solid structure in the basement membrane and tight junctions, making them prone to leak plasma proteins and blood into the retina and vitreous (Miller et al., 1984).

DR therapies are focused on the prevention and treatment of the most vision-threating stages of the disease, namely macular oedema and neovascularization. Laser

photocoagulation was first proposed as a tool to stop the growth of new vessels by thermal exposure in the ischemic retina, however, it can cause the loss of the peripheral vision, along with other side effects like haemorrhages, oedema or loss of lens accommodation (McDonald and Schatz, 1985; Larsson and Nuija, 2001; Patel et al., 2002). Currently, anti-VEGF intravitreal injections have proved to be an effective mechanism to treat both DME and PDR without affecting peripheral vision (Sivaprasad et al., 2017; Zhao and Singh, 2018; Brown et al., 2021). However, it is still an invasive treatment that require monthly injections and in substantial occasions patients do not respond adequately (Blinder et al., 2017; Bressler et al., 2012). In those cases, intravitreal use of corticosteroids is gaining popularity in the treatment of DME (Lattanzio et al., 2017).

B.2.1. Angiogenic factors

It has been extensively proven that VEGF is the most potent growth factor in blood vessel formation. The VEGF family is formed by 5 VEGF types (A-E), being VEGF-A the responsible of neovascularization during DR. VEGF-A binds to its receptor VEGFR and promotes endothelial cell proliferation and migration, as well as vascular permeability (Aiello et al., 1994; Kant et al., 2009). Although VEGF is the most important angiogenic factor in PDR, other pro-angiogenic factors such as angiopoietins, platelet-derived growth factors (PDGFs), basic fibroblast growth factor (b-FGF), insulin-like growth factor 1 (IGF-1), and transforming growth factor (TGF)-β could be involved in the angiogenic switch during DR (Kaštelan et al., 2020).

Angiopoietins are growth factors involved in blood vessel remodelling and maturation, but they are also believed to play a role in PDR. Increase in angiopoietin 2, which is typically expressed in the tip of new vessels sprouts, has been found in eyes with active PDR correlating with VEGF and MMP-9 upregulation (Watanabe et al., 2005; Loukovaara et al., 2013). Angiopoietin 2 has also been associated with pericyte loss (Park et al., 2014). In addition, drugs acting against VEGF-A and angiopoietin 2 simultaneusly have resulted effective in clinical trials (Sahni et al., 2019). Furthermore, overexpression of angiopoietin-like 4 has been localized in areas of retinal neovascularization (Babapoor-Farrokhran et al., 2015) and described to participate in BRB breakdown (Yang et al., 2019).

PDGF control cell proliferation and movement, and can be synthetized by activated endothelial cells. Overexpression of PDGF has been detected in the vitreous of patients with PDR (Freyberger et al., 2000) and is believed to play a role in neovascularization

and fibrovascular tissue formation (Klaassen et al., 2017; Lefevere et al., 2021). In this regard, anti-PDGF drugs could be used in PDR treatment (Zhou et al., 2018).

b-FGF has also been proposed to participate in DR neovascularization, since it is a potent factor for cell proliferation, but its role remains unclear. Although its increase has been related to the severity of DR (Lin et al., 2014), it has also been described to supress retinal pathologic angiogenesis in mouse (Fu et al., 2017). Another recent study revealed that treatment with FGF-1 ameliorated oxidative stress and inflammation in the retina (Huang et al., 2021).

Another growth factor that may be implicated in DR by promoting retinal endothelial proliferation could be the **IGF-1**. Intraocular expression of IGF-1 increases VEGF expression (Poulaki et al., 2004; Ruberte et al., 2004), but, again, other studies have seen an inverse relationship with IGF-1 levels and the severity of the disease (Raman et al., 2019), which generates contradictions. The same happens with TGF-b, which is involved in vascular remodelling and potentially involved in microvascular changes of DR, but also believed to have a protective effect against DR progression, thus having a dual function as pro-angiogenic and antiangiogenic (Braunger et al., 2015; Dagher et al., 2017). More factors involved in the pro-angiogenic function during DR could be the placental growth factor, erythropoietin, and inflammatory cytokines, among others (Kaštelan et al., 2020).

B.2.2. Antiangiogenic factors

It is believed that an imbalance between angiogenic and antiangiogenic factors is determinant in PDR rather than just the upregulation of angiogenic factors (Perrin et al., 2005; Simo et al., 2006; Praidou et al., 2010). Thus, the study of antiangiogenic factors in the retina is crucial to understand the angiogenic switch prior to neovascularization. One part of this thesis is based on the study of endostatin in the diabetic retina, the most powerful endogenous antiangiogenic factor.

Endostatin is a 20 kDa protein with antiangiogenic activity first described in a murine hemangioendothelioma (O'Reilly et al., 1997). The first studies were performed in tumours, in which endostatin showed the capacity to counteract pathological neovascularization (O'Reilly et al., 1997; Hajitou et al., 2002). Endostatin is generated by the protein cleavage of **collagen XVIII** at the C-terminal by MMPs, cathepsin L, and elastases (Ferreras et al., 2000) (Figure 12). In the developing retina, endostatin is responsible for the regression of the hyaloid vessels (Ohlmann et al., 2004). In this regard, endostatin knockout mice shows hyaloid vessel persistence (Fukai et al., 2002).

During neovascularization, endostatin binds to VEGFR-2 and interferes VEGF signalling (Kim et al., 2002), as well as inhibits MMPs activity (Kim et al., 2000).

The antiangiogenic capacity of endostatin have been recently tested as a potential therapeutic agent. Intravitreal injection of endostatin prevented BRB breakdown in a study using diabetic rats (Zhou and Xie, 2022) and therapy with endostatin transfected endothelial progenitor cells turned effective in preventing pathological retinal neovascularization (Ai et al., 2020). Although several studies have focused on the role of endostatin, none have described its detailed location in the human nor mouse retina yet, which could be very important to understand its role in preventing retinal angiogenesis. So far, endostatin has only been located as part of collagen XVIII in the vessel's basement membrane and in the internal limiting membrane (Bhutto et al., 2004; Ramesh et al., 2004; May et al., 2006; Määttä et al., 2007).

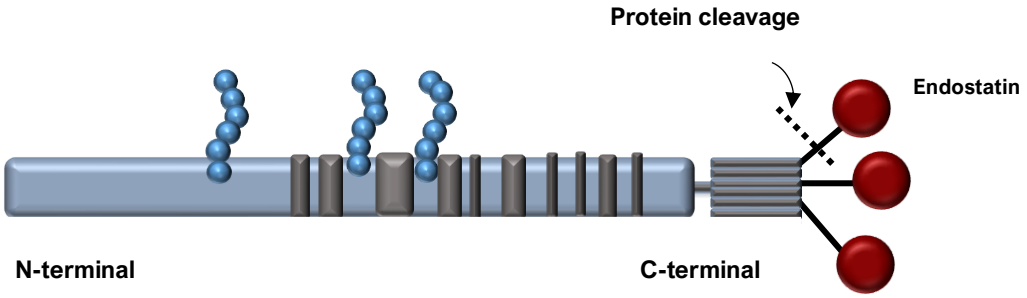

Figure 12. Structure of collagen XVIII. Endostatin is cleaved at the C-terminal region of collagen XVIII by proteases.

Other antiangiogenic factors include pigment epithelium-derived factor (PEDF), angiostatin, thrombospondin, and somatostatin.

PEDF inhibits endothelial cell proliferation and migration and has been shown to be decreased in DR (Spranger et al., 2001). In fact, it is suggested that low content of PEDF could be a good predictor of DR progression (Boehm et al., 2003). Other studies have demonstrated that PEDF could prevent neuronal damage and vascular changes in permeability by protecting the cells from oxidative stress (Amano et al., 2005; Yoshida et al., 2009; Haurigot et al., 2012; Wang et al., 2019). Treatment with PEDF by eyedrops amelliorates inflammation, apoptosis, and vascular leakage in diabetic mice (Liu et al., 2012).

Angiostatin is a proteolytic fragment of plasminogen that inhibits endothelial cells proliferation by blocking VEGF expression among other mechanisms (Sima et al., 2004). Recombinant angiostatin was proposed as a potential therapeutic agent for PDR, as it

also prevents retinal vascularization (Meneses et al., 2001; Igarashi et al., 2003), however, not many studies have been recently performed in this direction. Another antiangiogenic factor present in the eye is **thrombospondin-1**, which deficiency has been directly related with PDR progression in both human and mice (Sheibani et al., 2000;; Wang et al., 2006; Sorenson et al., 2013). **Somatostatin** is an antiangiogenic factor abundant in the retina, mostly secreted by the RPE, that is also downregulated in diabetic retinas (Carrasco et al., 2007; Hernández et al., 2014). Finally, somatostatin have neuroprotective effect in ischemic retinas and prevents neurodegeneration (Kiagiadaki et al., 2010; Kokona et al., 2012; Beltramo et al., 2016).

B.3. Models to study DR. The db/db mouse

Animal models are still essential for the study of diseases such as DR. Although several species have been used to study DR, such as dogs, pigs, cats, and non-human primates, rodents and, especially mouse, are still the most used model to study human DR (Quiroz and Yazdanyar, 2021). Mouse genome is 90% identical to human's, it has a short lifespan that allows the study of chronic diseases in a relative short amount of time, and it is easy to breed and obtain a large offspring, becoming more affordable than larger animals. Furthermore, mouse can be conveniently genetically modified to obtain more accurate models for diseases (D. Ramos et al., 2013b).

There is a wide variety of mouse models to study DR (D. Ramos et al., 2013b); however, not even one is able to reproduce all the features of human DR together. Classically, DR has been studied in models that develop hyperglicemia (spontaneously or chemically) and in models that are non-diabetic but present PDR features such as neovascularization DR (Ramos et al., 2013b; Quiroz and Yazdanyar, 2021).

Experimental hyperglicemia can be induced chemically, genetically or through the diet. Intraperitoneal injection of drugs streptozotocin or alloxan destroys pancreatic β-cells (Lenzen, 2008), obtaining a model of type I diabetes that is still being used in multiple studies (Danilova et al., 2018; Liu et al., 2018; Saadane et al., 2020; Seo et al., 2020). Spontaneous and genetically modified models are also used to study DR. For example, the akita mouse, which courses with pancreatic β-cell death, shows signs of early diabetic retinopathy (Barber et al., 2005), and the kimba mouse overexpresses VEGF mimicking PDR (Ali Rahman et al., 2011). Additionally, the crossing of akita with kimba mouse generates the akimba mouse, which shows both diabetes and neovascularization (Rakoczy et al., 2010). Other mouse models such as ob/ob and db/db develop spontaneous type 2 diabetes induced by obesity due to mutations in the leptin and leptin receptor gene, respectively, which is responsible to control the appetite (Suriano et al.,

2021). In addition, diabetes development can be accelerated with a high fat diet (Zhang et al., 2008). For the study of advanced PDR, non-diabetic models of oxygen induced neovascularization are used, in which there is a high exposure of oxygen during retinal development followed by ischemia that causes abnormal blood vessels growth (Scott and Fruttiger, 2009). The list of mouse models for the study of DR is extensive and more precise genetic engineering is being developed.

As mentioned, there are different models that mimic the different types of diabetes mellitus and the different stages of DR. During the thesis, the db/db mouse was used since it naturally develops morbid obesity at 3-4 weeks of age and hyperglicemia at 4-8 weeks of age (Robinson et al., 2012). The **db/db mice** is extensively used to study DR (Figure 13) as it presents the main vascular complications that occur in human, namely pericyte loss, basement membrane thickening, acellular capillaries, glia activation, and vascular leakage (Clements et al., 1998; Cheung et al., 2005; Bogdanov et al., 2014; Xiong et al., 2017). Although *a priori* this model does not resemble PDR it might be an interesting model to study the changes in the angiogenic balance that occur before neovascularization.

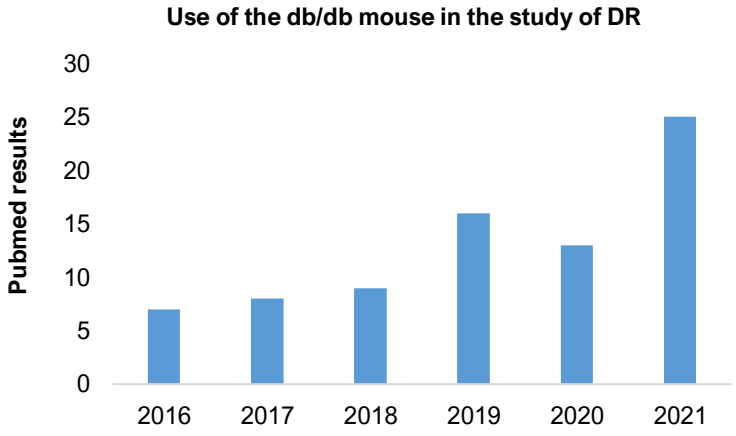

Figure 13. Use of db/db mouse in the study of DR. Graphic with data obtained from Pubmed representing the increase in the use of the db/db mouse model to study DR in the past five years.

C. IRON METABOLISM

C.1. Iron homeostasis

Iron is an essential element for the organism of all mammals and plays a key role in many metabolic functions due to its redox activity. There are numerous iron-requiring proteins involved in deoxyribonucleic acid (DNA) synthesis and repair (helicases, ribonucleotide reductase, nucleases) (Puig et al., 2017) and haemoglobin needs iron to bind and transport oxygen through blood (Gao et al., 2019). Furthermore, iron is indispensable for the course of the electron transport chain and ATP production in the mitochondria, which provides energy to many processes in the body (Paul et al., 2017). In the central nervous system, oligodendrocytes use iron for myelin synthesis and maintenance and, moreover, iron acts as a cofactor for catecholamine neurotransmitters synthesis, such as dopamine (Ward et al., 2014).

Iron is physiologically found in ferrous (**Fe^{2+}**) or ferric (**Fe^{3+}**) state. Fe^{2+} iron is soluble and has the capacity to donate electrons and oxidize while Fe^{3+} is found binding to proteins (Miller and Berner, 1989). Within the organism, iron is mostly found in haemoproteins, which include haemoglobin, myoglobin, and cytochromes, or in non-heme proteins, such as ferritin or transferrin. Over 70% of the iron is found binding to haemoglobin, 20% is stored in ferritin, primarily in the liver and in the spleen, and about 3% of iron is bound to myoglobin in the muscle. The remaining iron is distributed in the rest of the tissues as a **labile iron pool** (LIP) (Zhang and Enns, 2008).

Since the body doesn't produce iron, it needs to be obtained through the diet. Diet iron is absorbed in the duodenum and proximal jejunum (Muir and Hopfer, 1985). The low pH produced by the gastric fluids allows the conversion of Fe^{3+} to Fe^{2+} iron by duodenal cytochrome B (Dcytb) (Lane et al., 2015), which can be then absorbed by the enterocytes at the apical membrane through the protein divalent metal cation transporter 1 (DMT1) (Przybyszewska and Zekanowska, 2014). Once inside the enterocyte, iron can be stored in molecules of **ferritin** or exported to the bloodstream by the protein **ferroportin**, located in the basolateral membrane (Ganz and Nemeth, 2006). In the bloodstream, iron is bound to the carrier **transferrin**, which can allocate two atoms of iron, and distributed to the tissues for utilization (Brock et al., 1995). Most of the iron in the body is used for erythropoiesis in the bone marrow and then recycled by the phagocytosis of senescent erythrocytes (Beaumont and Canonne-Hergaux, 2005) (Figure 14).

Since there is no physiological mechanism for iron excretion, iron levels are regulated in the absorption process depending on the iron need, erythropoiesis rate, and oxygen

levels (Moos et al., 2002) (Raja et al., 1988; Gulec et al., 2014). In a situation of iron excess, **hepcidin**, the most important iron regulatory hormone, is produced in the liver inhibiting iron absorption and iron recycling (Ganz and Nemeth, 2006). However, even though iron has a tight regulation, it tends to accumulate during aging, causing iron overload and consequent tissue damage (Pirpamer et al., 2016; Sato et al., 2022).

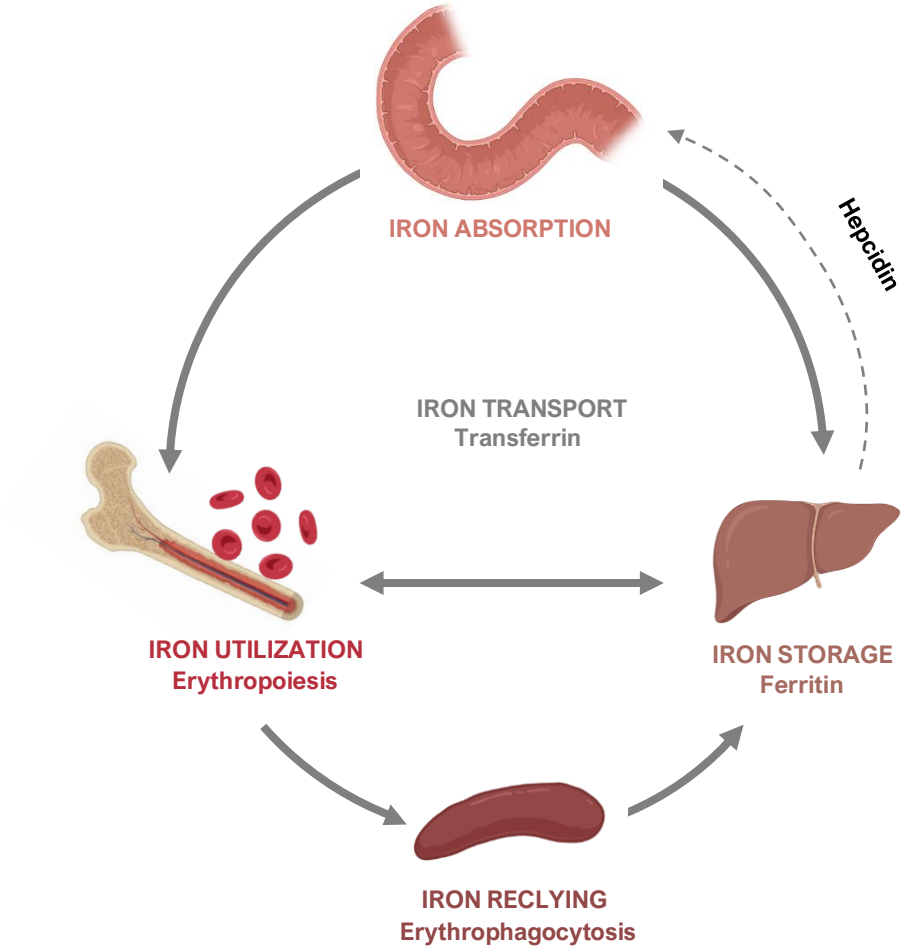

Figure 14. Iron cycle in the organism. Iron is absorbed in the duodenum and release into the bloodstream, where binds to transferrin and is distributed along the organism. Excess of iron is intracellularly stored by ferritin. In iron overload, the liver secretes hepcidin, which downregulates iron absorption in the intestines and triggers ferroportin internalization. At the end of the cycle, iron is recycled from senescent erythrocytes.

C.1.1. Cellular iron import

Several pathways of iron import into the tissues have been described (Richardson and Ponka, 1997; Li et al., 2009; Knutson, 2017). Most of the non-heme iron circulates in the bloodstream bound to transferrin, which binds to the transferrin receptor on the cell surface and mediates iron entrance into the cells. Once transferrin binds to its receptor, an endosome is formed and, both subtract and receptor, are internalized into the cell. Inside the endosome, a bomb of H^+ assembles an acidic environment that allows the

enzyme streap 3 to convert Fe^{3+} in Fe^{2+}, which is then released in the cytoplasm by DMT1, located in the endosome. Then, Fe^{2+} is either rapidly captured by ferritin and oxidized to Fe^{3+} for storage or stays as a labile pool of iron in the cytoplasm membrane (Dautry Varsat et al., 1983) (Figure 15).

Serum ferritin has also been proposed as a new iron-carrier protein able to mediate iron import into the cell. It is formed by light chains (L-ferritin) and heavy chains (H-ferritin), although in the serum ferritin is mostly composed by L subunits. L- and H-ferritin bind the receptors scavenger receptor class A member 5 (**SCARA5**) (Li et al., 2009) and T-cell immunoglobulin mucin receptor 2 (**TIM2**) (Todorich et al., 2008; Han et al., 2011), respectively. Additionally, ferritin can bind to transferrin receptor. The advantage of this alternative pathway is that ferritin can allocate up to 4500 iron atoms while transferrin can incorporate only 2 atoms (Harrison and Arosio, 1996).

C.1.2. Cellular iron storage

Fe^{2+} is toxic for the cells due to its redox activity, thus, cells need a mechanism to store iron excess in Fe^{3+} state. Ferritin is the primary protein responsible for iron storage in the cells and prevents ferrous-induced oxidative damage. When iron is imported in a cell, apoferritin (iron-free ferritin) captures Fe^{2+}, which is oxidized to Fe^{3+} and stored in holoferritin (iron-loaded ferritin) (Balla et al., 1992) (Figure 15).

Ferritin is a ubiquitous protein found in animals, plants, and bacteria. In mammals, it consists of 24 subunits of **L-** and **H-ferritin** that have complementary functions: H-ferritin has ferroxidase activity that allows rapid iron uptake by the conversion of Fe^{2+} into Fe^{3+} form and L-ferritin is involved in protein core stability and iron mineralization (Levi et al., 1992). The ferritin complex is assembled in different proportions depending on the tissue. Tissues that need iron rapidly available like the heart or the brain, are formed by H-rich ferritin, while tissues that are more involved in iron storage like the liver or the spleen, have L-rich ferritin (Worwood et al., 1975; Zhang and Knez, 2011). Ferritin is mostly found in the cell cytosol, although it is also present in the nucleus and in the mitochondria (Guaraldo et al., 2016; Surguladze et al., 2005). Mouse L- and H-ferritin functionality and structure are very similar to human (Rucker et al., 1996).

C.1.3. Cellular iron export

The only known iron exporter in mammals is **ferroportin**, a transmembrane protein that pumps intracellular Fe^{2+} out of the cell. During iron export, Fe^{2+} is oxidized to Fe^{3+} by the ferroxidases hephaestin and ceruloplasmin so iron can bind with transferrin in the blood

again. Ferroportin expression is negatively regulated by hepcidin, which binds to the ferroportin extracellular domain inducing its internalization and degradation. Ferroportin inhibition avoids iron export and prevents iron increase in the extracellular fluid and in the blood (Figure 15).

.

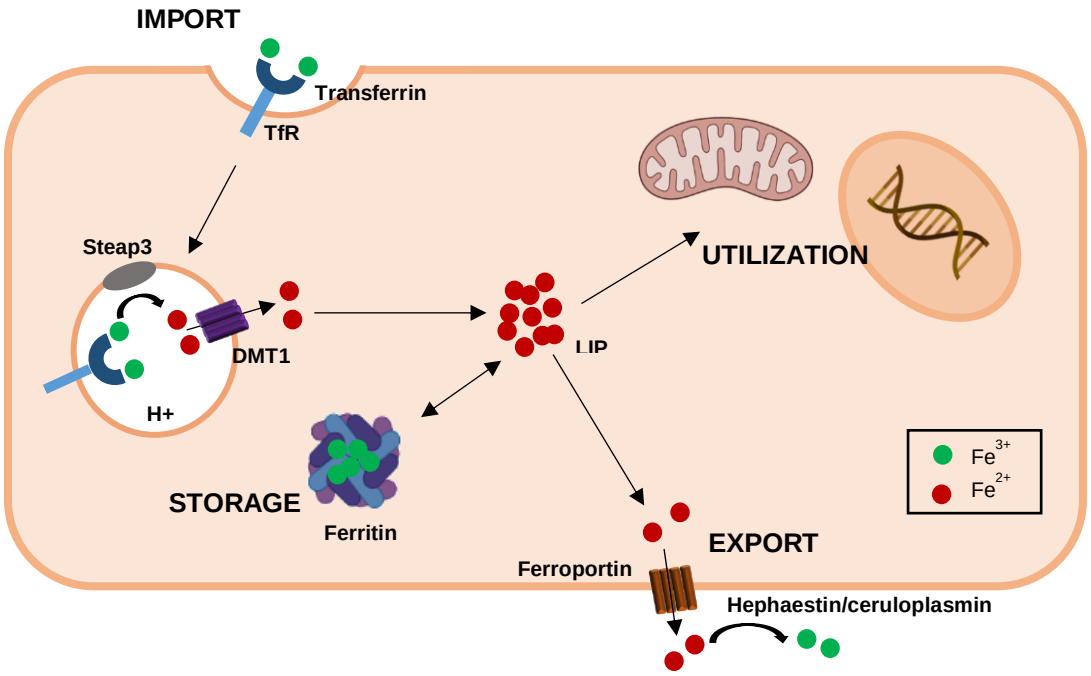

Figure 15. Cellular iron metabolism. Schema showing iron import into the cell by transferrin, iron storage in the cytoplasm by ferritin, and iron export into the extracellular space by ferroportin. In the cytoplasm, the LIP is used for cellular functions in the mitochondria and the nucleus.

C.1.4. Iron deficiency and iron overload

It is important to have the right amount of iron in the body because both iron deficiency and overload can be very harmful. As mentioned before, iron is obtained from the diet, and when iron absorption is not enough or there is a blood loss, it can trigger iron deficiency. When there is a lack of iron, erythropoiesis production and consequent oxygen delivery to the tissues is decreased, causing anaemia. The most common symptoms of anaemia include weakness, fatigue, and difficulty to concentrate, although it can become more dangerous and present cardiac alterations in severe anaemias. Anaemia caused by iron deficiency is treated with dietary iron supplements that help to restore iron levels in the organism (Miller, 2013).

On the other side, excess of iron in the body can be extremely toxic and, since there is no active mechanism for its excretion, it can accumulate more easily. Iron overload occurs when transferrin and ferritin are unable to capture all the iron (Murphy and Oudit, 2010; Milic et al., 2016), which accumulates in a intracellular LIP and act as a catalyst in

the **Fenton reaction** and produce oxidative damage. In the Fenton reaction, Fe^{2+} reacts with hydrogen peroxide generating Fe^{3+} and hydroxyl radicals that cause oxidative damage (Chevion, 1988a) (Figure 16).

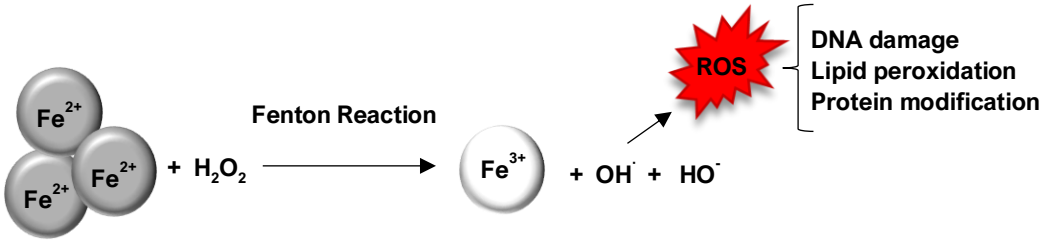

Figure 16. Fenton Reaction. Iron overload triggers the Fenton reaction in which Fe^{2+} is oxidized by hydrogen peroxide (H_2O_2), generating Fe^{3+}, hydroxyl radicals ($OH^{\cdot}$), and hydroxyl ions (HO^{-}), causing DNA damage, lipid peroxidation, and protein modification that ends up in cell death and tissue damage.

There are several causes that induce iron overload such as multiple blood transfusions, iron poisoning, chronic liver disease, and genetic disorders that alter iron metabolism, such as hereditary hemochromatosis, a group of disorders characterized by an increase in iron absorption, mostly due to a mutation in the homeostatic iron regulator gene (HFE) (Siah et al., 2006). Depending on the amount of iron accumulated and the oxidative damage produced, iron overload can affect the liver, pancreas, and heart, causing secondary complications such as liver disease or diabetes (Batts, 2007; Belhoul et al., 2013). Iron excess has also been involved with the progression of cancer (Steegmann-Olmedillas, 2011; Fonseca-Nunes et al., 2014) and neurological disorders like Alzheimer's (Smith et al., 1997; Du et al., 2018). Iron overload has also been associated with retinopathies, especially with age-related macular oedema and diabetic retinopathy, which will be discussed later.

C.2. Iron in the retina

As happens in other tissues, in the retina iron participates in many functions such as DNA repair, cell proliferation, and ATP production in the mitochondria. Furthermore, in the visual cycle, iron is crucial for the enzyme guanylate cyclase, which synthetizes cyclic guanosine monophosphate (cGMP) synthesis, the second messenger in the photo-transduction cascade (Derbyshire and Marletta, 2012). Additionally, RPE65 is an iron-dependent protein in the retinal pigment epithelium that catalyses the conversion of all-trans-retinyl ester to 11-cis-retinol in the visual cycle, an unavoidable step for normal vision (Moiseyev et al., 2006a). Iron-containing enzymes are also required in the retina for shedding and synthesizing disc membranes of photoreceptor outer segments.

Moreover, iron enhances aconitase activity, which is essential to secrete the neurotransmitter glutamate (McGahan et al., 2005).

C.2.1. Retinal iron traffic

Any molecule, including iron, must cross the BRB before entering the retina, but the mechanism by which iron crosses the BRB and the direction of iron efflux within the retina remains unclear. There are different pathways proposed for iron import into the retina (Picard et al., 2020) (Figure 17).

The classical theory suggests that iron enters the retina by transferrin transcytosis across the vascular retinal endothelial cells in the iBRB and through RPE cells in the oBRB. In this regard, transferrin receptor is found in the luminal membrane of retinal vascular endothelial cells (Baumann et al., 2019) and in the basolateral membrane of RPE cells (Hunt et al., 1989; Hunt and Davis, 1992).

A part from transferrin transcytosis-mediated transport, iron could be transport by transferrin endocytosis followed by ferroportin export, given that ferroportin is expressed in the abluminal membrane of retinal vascular endothelial cells (Theurl et al., 2016). Another evidence that supports this hypothesis is that deletion of ferroportin in endothelial cells causes iron accumulation in those cells (Baumann et al., 2019a). Ferroportin expression has also been detected in Müller cells and in the basolateral membrane of RPE cells, suggesting that iron enters the retina crossing the iBRB, is distributed throughout the retinal parenchyma by Müller cells and, finally, is excreted by the RPE cells into the bloodstream (Theurl et al., 2016).

Although iron bound to transferrin is believed to be the main pathway to cross the BRB, iron delivery mediated by ferritin can also occur (Fisher et al., 2007). In addition to this, our group described the expression of SCARA5 in the retinal vascular endothelium (Mendes-Jorge et al., 2014), suggesting the role of serum L-ferritin in iron delivery. Supporting this hypothesis, a model of TIM2 deficiency developed in our laboratory resulted in SCARA5 overexpression and consequent retinal iron increase (Valença et al., 2021).

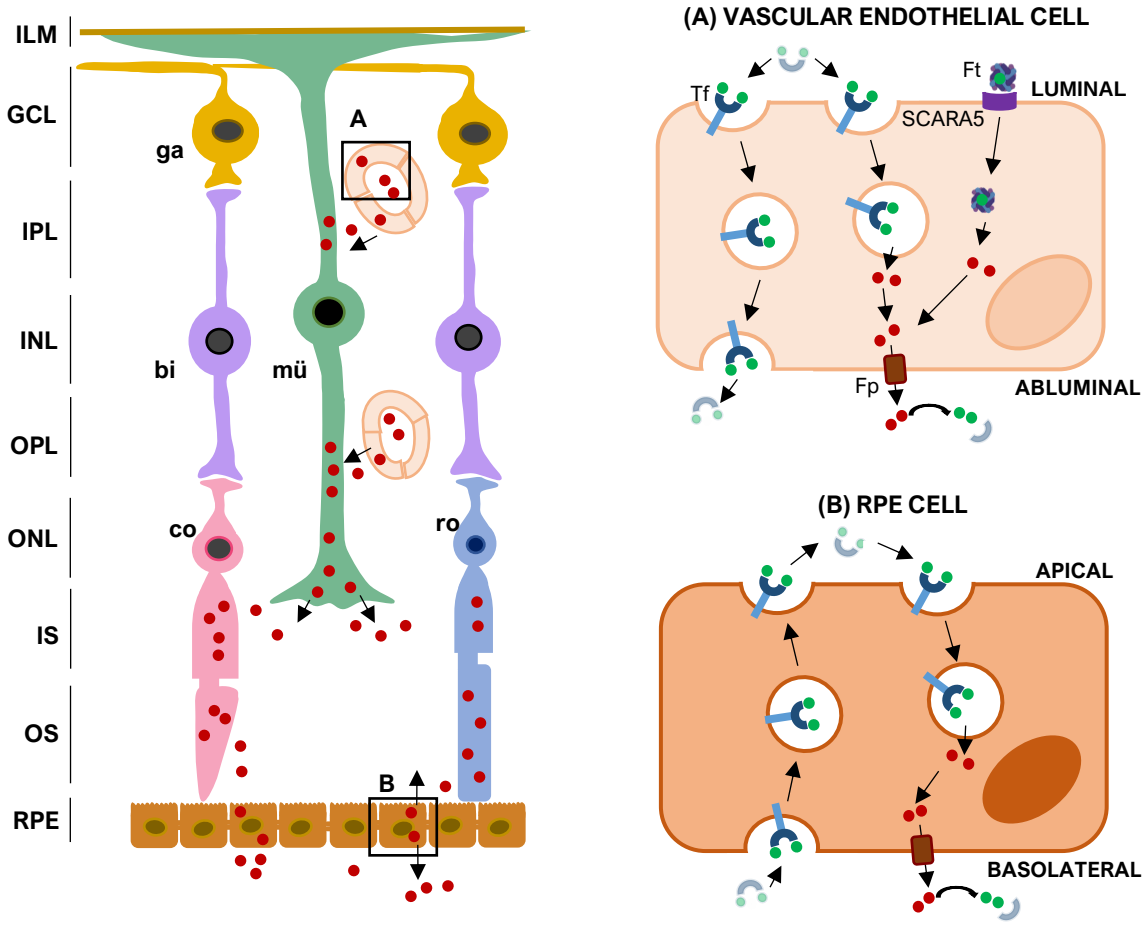

Figure 17. Iron traffic in the retina. (A) Iron transport across the iBRB can occur by both transcytosis of iron loaded transferrin or by endocytosis of iron loaded transferrin, release of iron, and following export mediated by ferroportin. Serum L-ferritin can also bind to the receptor SCARA5 located in the luminal membrane of endothelial cells. **(B)** Iron enters the retina from the choroid crossing RPE cells by transferrin transcytosis. Interestingly, ferroportin expression is in the basolateral membrane of RPE cells, suggesting iron export from the outer retina to the choroid. ga: ganglion cell; bi: bipolar cell; co: con; mü: Müller cell; ro: rod; Tf: transferrin; TfR: transferrin receptor; Fp: ferroportin; Ft: ferritin. (Adapted from Theurl et al., 2016).

C.2.2. Retinal iron regulation

In iron overload, the liver secretes **hepcidin** to the circulation, which inhibits ferroportin and iron export in the tissues. However, in the retina, BRB is not permeable to hepatic hepcidin, which suggests that there must be an autonomous mechanism for iron regulation. In this regard, hepcidin expression was observed in Müller cells and photoreceptors (Gnana-Prakasam et al., 2008). Moreover, retinal hepcidin knockout mouse presents retinal iron metabolism dysregulation (Hadziahmetovic et al., 2011), suggesting the importance of this hormone in retinal iron homeostasis. Supporting this, recent studies have found iron overload that triggers hepcidin secretion by the glia and

induce ferroportin internalization in BBB endothelial cells preventing iron entry into the brain (McCarthy and Kosman, 2015; Mezzanotte et al., 2021).

Along with hepcidin regulation, iron in the retina is controlled by **iron regulatory proteins** (IRPs) 1 and 2. These proteins bind to iron responsive elements (IREs) presents in the messenger ribonucleic acid (mRNA) of iron handling proteins such as ferritin, transferrin, ferroportin, and DMT1, regulating its expression. In iron overload, intracellular iron content increases and IRPs are not able to bind to ferritin mRNA, preventing ferritin degradation (Hentze and Kühn, 1996). The exact location of IRPs in the retina has not been yet elucidated, but an experiment using IRP deficiency retinas showed an increase in ferroportin and ferritin expression, suggesting its key role in retinal iron regulation (Paul Hahn et al., 2004a; Picard et al., 2020).

C.3. Iron overload in diabetic retinopathy

Iron overload is toxic for the organism as Fe^{2+} catalyses the Fenton reaction and generates damaging radical oxygen species. The retina is particularly susceptible to oxidative damage due to its high metabolic rate, high oxygen tension, and elevated concentration of polyunsaturated fatty acids (Nita and Grzybowski 2016).

In the retina, iron overload causes neuronal toxicity and BRB breakdown by oxidative stress. As mentioned, oxidative damage is one of the hallmarks in DR pathogenesis. Iron overload not only harms the retina increasing oxidative stress, but also reinforces the different pathways involved in the pathogenesis of DR. In this regard, HFE knockout mice, a model of iron overload, was injected with streptozotocin to induce diabetes and showed neuronal cell death and BRB breakdown compared with the diabetic wild type, indicating that iron exacerbates DR (Chaudhary et al., 2018). Furthermore, intravitreal injection of Fe^{2+} has been proved to cause photoreceptors death (Imamura et al., 2014; Shu et al., 2020), being cones more susceptible to iron oxidative damage (Rogers et al., 2007).

There are several mouse models that course with iron overload and that have showed features of DR. In this regard, TIM2 deficient mouse with retinal iron overload develops tight junction impairment and vascular leakage (Valença et al., 2021) and mouse deficient in ceruloplasmin and hephaestin genes presents retinal iron overload, photoreceptors degeneration, and subretinal neovascularization (Hahn et al., 2004b). Furthermore, mouse models with hereditary hemochromatosis present retinal degeneration (Gnana-Prakasam et al., 2012). Another evidence that iron exacerbates

retinopathies is that treatment with iron chelators significatively prevents retinal damage (Charkoudian et al., 2008; Gnana-Prakasam et al., 2016).

Apart from the association between retinal iron overload and retinal lesions, there are studies that have found a correlation between the increase of iron in the organism and the risk of developing diabetes (Misra et al., 2016; Liu et al., 2020). Furthermore, patients with PDR present higher levels of iron (Konerirajapuram et al., 2004) and iron-binding proteins (Weller et al., 1990; Kimura et al., 2017) in their vitreous fluid. Similarly, serum iron and retinal ferritin increase have been described in mouse models for type 1 and 2 diabetes (Chaudhary et al., 2018). However, the homeostasis between serum and retinal iron and the mechanisms that induce retinal iron overload are poorly understood. Therefore, is essential to continue studying iron metabolism in the retina during diabetes to elucidate its role in the pathogenesis of the disease.

Overall, the study of the risk factors involved in the exacerbation of DR, such as iron content and endostatin expression, is crucial for the development of new non-invasive, long-lasting, and more affordable treatments to prevent DR. Future therapies using iron chelators to prevent oxidative damage during NPDR and antiangiogenic drugs to prevent neovascularization during PDR could be key in the treatment of the disease.

OBJECTIVES

BACKGROUND

- Iron overload is associated with diabetes mellitus.
- The mechanisms by which systemic iron overload causes retinal iron increase are unclear.
- Ferritin is used as an indirect measurement to assess iron content in the tissues.
- Endostatin is a part of collagen XVIII with antigiogenic activity.
- In the retina, endostatin has only been localized forming part of collagen XVIII in blood vessels basement membranes and in the internal limiting membrane.

HYPOTHESIS

- BRB has a role in the regulation of retinal iron content during DR.
- Endostatin plays a role in the angiogenic switch during DR.

MAIN OBJECTIVES

- To understand the mechanisms underlying retinal iron overload during DR.
- To study the effect of endostatin expression in the development of DR.

SPECIFIC OBJECTIVES

- To evaluate systemic and retinal iron content during DR.
- To assess BRB status in diabetic mouse retinas.
- To prove if BRB protects the retina from systemic iron overload.
- To characterize endostatin expression in human and mouse retinas.
- To analyse endostatin expression in diabetic mouse retinas.
- To assess the relation between endostatin expression and vascular alterations in diabetic mouse retinas.

CHAPTER I

BRB PROTECTS THE RETINA FROM SYSTEMIC IRON OVERLOAD DURING EARLY DIABETIC RETINOPATHY

Authors: Aina Bonet[1,2], Judit Pampalona[1], Eduard Jose-Cunilleras[3], Víctor Nacher[2], Jesús Ruberte[1,2]

[1]Center of Animal Biotechnology and Gene Therapy (CBATEG), Universitat Autònoma de Barcelona, Bellaterra, Spain.

[2]Department of Animal Health and Anatomy, Faculty of Veterinary Medicine, Universitat Autònoma de Barcelona, Bellaterra, Spain.

[3]Department of Animal Medicine and Surgery, Faculty of Veterinary Medicine, Universitat Autònoma de Barcelona, Bellaterra, Spain

[*]Corresponding author. CBATEG - Center of Animal Biotechnology and Gene Therapy, Autonomous University of Barcelona, C/ de la Vall Morona, 08193, Bellaterra (Cerdanyola del Vallès), Spain.

Declarations of interest: **A. Bonet**, None; **J. Pampalona,** None; **E. Jose-Cunilleras,** None; **V. Nacher**, None; **J. Ruberte**, None.

Sent for publication to Investigative Ophthalmology & Visual Science

Abstract

Iron overload causes oxidative damage in the retina, and it has been involved in the pathogeny of diabetic retinopathy, which is one of the leading causes of blindness in the adult population worldwide. However, how systemic iron enters the retina during diabetes and the role of blood retinal barrier (BRB) in this process remains unclear.

The db/db mouse, a well-known model of type 2 diabetes, and a model of systemic iron overload induced by iron dextran intraperitoneal injection, were used. Perls stain and mass spectrophotometry were used to study iron content. Western blot and immunohistochemistry of iron handling proteins were performed to study systemic and retinal iron metabolism. BRB function was assessed by analyzing vascular leakage in fundus angiographies and in retinal sections, and by studying the status of tight junctions using transmission electron microscopy and western blot.

20-week-old db/db mice with systemic iron overload presented ferritin overexpression without iron increase in the retina and did not show any sign of BRB breakdown. These findings were also observed in iron dextran injected mice. In those animals, after BRB breakdown induced by cryopexy, iron entered massively in the retina

Our results suggested that BRB protects the retina from excessive iron entry in early stages of diabetic retinopathy. Furthermore, ferritin overexpression prior to iron increase may prepare the retina for a potential BRB breakdown and iron entry from the circulation.

Key words: iron overload, ferritin, diabetic retinopathy, BRB breakdown, eye cryopexy.

1. INTRODUCTION

Iron is one of the most abundant elements in the Earth's crust and is essential for organism's development and survival (Morgan et al., 1980). As a metal, iron has the capacity to donate and accept electrons in redox reactions that are required in vital enzymatic processes such as oxygen transport, energy production, DNA replication, neurotransmitter signaling, myelin shedding, and steroid hormones synthesis (Abbaspour et al., 2014). In the retina, iron is a co-factor for guanylate cyclase and RPE65 synthesis, both involved in the phototransduction cascade (Yau and Baylor, 1989; Moiseyev et al., 2006). Furthermore, iron-containing enzymes are responsible of the shedding and renewal of the photoreceptor outer segments disc membranes (Adijanto et al., 2014).

After iron absorption in the duodenum, iron is released into the bloodstream and bound to the iron carrier transferrin for tissue delivery (Gulec et al., 2014b). Once in the cell membrane, transferrin binds to its transferrin receptor, and the entire complex enters the cell by endocytosis (Mayle et al., 2012). Then, iron is used for cellular functions, while excess of iron is stored in ferritin (Arosio et al., 2017). When needed, iron exits the cells through the iron exporter ferroportin (Dunaief et al., 2004). In addition, it has been described that ferritin can act as a retinal iron importer by binding its L and H subunit to the receptors SCARA5 and TIM2, respectively (Chen et al., 2005; Li et al., 2009). In fact, our group has showed that this iron import alternative mechanism also works in the retina (Mendes-Jorge et al., 2014; Valença et al., 2021).

In states of iron overload, the IRPs initiate a series of mechanisms to protect the cells, increasing the expression of ferritin to store more iron (Gray and Hentze, 1994; Zhou and Tan, 2017). However, when iron levels exceed the limit, free ferrous ion triggers the production of oxygen free radicals via the Fenton reaction (Chevion, 1988b), which are toxic and can cause DNA alterations, protein damage, and lipid peroxidation (Meneghini, 1997; Zhao et al., 2021). This can be especially harmful in the retina, which presents a high oxygen tension and metabolic rate (Hughes et al., 2010).

Diabetes has been widely associated with systemic iron overload (Ciudin et al., 2010; Wu et al., 2020). In fact, recent studies have showed a positive correlation between iron in serum and the risk of developing diabetes (Misra et al., 2016; Liu et al., 2020). Supporting this association, several mice models of iron overload have been described to develop retinal lesions resembling diabetic retinopathy (P. Hahn et al., 2004; Gnana-Prakasam et al., 2011; Arjunan et al., 2016; Valença et al., 2021). Furthermore, iron overload in diabetic mouse exacerbates the progression of diabetic retinopathy

(Chaudhary et al., 2018). Nevertheles, wild type mice in which iron overload was experimentally induced by iron dextran injection, exhibited that systemic iron had minimal penetration in the retina (Shu et al., 2019).Thus, the mechanism by which systemic iron overload induces retinal iron overload remains unclear.

The aim of this study is to analyze the relation between systemic and retinal iron during diabetes and the implication of the BRB, as it has been suggested to have a role in the regulation of iron transport into the retina (Shu et al., 2019). For this purpose, two mouse models have been used: (i) the db/db mouse, a widely accepted model for type 2 diabetes (Belke and Severson, 2012; Bogdanov et al., 2014; Burke et al., 2017) and (ii) iron dextran injected mice, a model of systemic iron overload (Musumeci et al., 2014; Wichaiyo et al., 2015; Shu et al., 2019).

2. MATERIALS AND METHODS

2.1. Mice

Male diabetic mice db/db (BKS.Cg-Dock7^{m} +/+ Lepr^{db}/J), non-diabetic littermates db/+ (BKS.Cg-Dock7^{m} + Lepr^{db}/+) and C57BL/6J wild type (WT) mice of 20 weeks old were used in this work. The animal facility had a controlled environment (20ºC temperature, 60% humidity, and 12 hours light/dark cycles) and mice were feed *ad libitum* with a standard diet (2018S TEKLAD Global, Harlan Teklad, Madison, WI, USA). Mice were euthanized with an overdose of inhaled isoflurane or anesthetized with an injected solution of ketamine (100mg/kg) and xylazine (12mg/kg) followed by cervical dislocation. Experiment procedures were performed following the ARVO Statement for the Use of Animals in Ophthalmic and Vision Research and the ARRIVE (Animal Research: Reporting In Vivo Experiments) guidelines 2.0 (du Sert et al., 2020). All the procedures were approved by the Ethics Committee in Animal and Human Experimentation of the Universitat Autònoma de Barcelona (UAB) (FUE-2018-00717286).

2.2. Glycaemia measurement

The db/db mice start to show hyperglycemia at 4-8 weeks of age (Robinson et al., 2012). Glycaemia was measured in non-fasted conditions with a glucometer (Bayer, Leverkusen, Germany) in blood collected from the tail vein. Mice were considered diabetic when glycaemia values were greater than 250 mg/dl in, at least, in two consecutive measurements (Leiter, 2009). According to this, 20-week-old mice presented a significant statistical difference in body weight (30.21±0.665 g, n=16, in db/+ vs. 52.69±1.117 g, n=13, in db/db; $p<0.0001$) and glycaemia (121.2±3.204 mg/dl, n=16,

in db/+ vs. 519.1±21.12 mg/dl, n=13, in db/db; p<0.0001), confirming that db/db mice used in this study were type 2 diabetic.

2.3. Analysis of iron parameters in systemic blood

Mice were anesthetized using inhaled isoflurane and blood samples were collected by intracardiac puncture, placed in a lithium heparin tube, and centrifuged to obtain plasma for biochemistry analysis. Serum iron concentration and unsaturated iron binding capacity (UIBC) were determined with an automated biochemistry analyser (Chemistry Analyzer AU400, Olympus) and enzymatic colorimetric assays (Beckman Coulter). Total iron binding capacity (TIBC) was calculated adding serum iron concentration to the UIBC values.

2.4. Perls Prussian Blue iron staining

Perls stain (Perls, 1868) was performed in 3 µm paraffin sections of eyeballs, that were sectioned along their axis, and spleens, that were cut transversally. Samples were deparaffinated, rehydrated, and immersed in a solution of 5% potassium ferrocyanide (Sigma-Aldrich, St Louis, MO, USA) and 5% hydrochloric acid (Panreac Química SLU, Castellar del Vallés, Spain). Nuclear fast red (Sigma-Aldrich) was applied for nuclear counterstaining. Sections were washed, dehydrated, and mounted in DPX medium (Sigma-Aldrich) before analysis. To assess iron content in the spleen, Prussian Blue precipitate was quantified with ImageJ software (National Institutes of Health, Bethesda, MD, USA).

2.5. Detection of retinal ferrous iron (Fe^{2+})

The iron sensing probe 575 Red Fe2+ Dye or FeRhoNox-1™ (Goryo Chemical, Japan) staining was performed in frozen sections (10µm) along the eyeball axis, as previously described (Léger et al., 2019). FeRhonox-1 was diluted following manufacture instructions and incubated for 30 minutes at 37ºC. Next, nuclei were counterstained with Hoechst (Sigma-Aldrich) at 1:100 dilution for 10 minutes. Finally, sections were mounted with Fluoromount media (Sigma-Aldrich) and visualized with a SP5 confocal laser scanning confocal microscope (Leica Microsystems GmbH, Heidelberg, Germany). Fluorescence emission was quantified using ImageJ software.

2.6. Detection of total retinal iron by inductively coupled plasma mass spectrometry (ICP-MS)

Eyes were enucleated and retinas were dissected in 1x phosphate buffered saline (PBS) and collected in vials. A blank with 1x PBS was also included to normalize the values.

For retinal digestion, samples were treated with 65% nitric acid and heated at 120ºC for 30 minutes. Retinal iron concentration was determined by inductively coupled plasma mass spectrometer Agilent 7500ce (Agilent, Santa Clara, CA, USA).

2.7. Injection of iron dextran and BRB breakdown by cryopexy

To induce acute systemic iron overload, 1g/kg of iron dextran (Sigma-Aldrich) was injected intraperitoneally in WT mice. Saline solution was injected instead of iron dextran in a control group. After 4 hours, BRB breakdown by cryopexy was induced in half of the mice injected with iron dextran, by applying a piece of dry ice in the scleral conjunctiva at the lateral palpebral commissure for 10-20 seconds (Derevjanik et al., 2002). Eye and spleen samples were collected for paraffin embedding and for ICP-MS analysis. For ICP-MS analysis, mice were subjected to a vascular washout to avoid measuring the iron inside the retinal blood vessels, which could modify the results of iron content in the retinal parenchyma homogenates. For this purpose, thorax was opened to expose the heart, 2 ml 1x PBS were injected in the left ventricle, and the caudal vena cava was cut to interrupt venous return.

2.8. Western Blot

Retina and spleen samples were first dissected in 1x PBS and homogenized in RIPA lysis buffer (25 mM Tris base, pH 8.2, 150 mM NaCl, 0.5% NP-40, 0.1% SDS, 0.5% sodium deoxycholate) with a protease inhibitor (Roche, Basel, Switzerland) and centrifuged at 8000 *g* for 10 minutes. For sample preparation, 50 mg of protein were resuspended in 2x Laemmli loading buffer (140 mM Tris base, 6.8% SDS, 33% glycerol, 0.004% bromophenol blue, 10% β-mercaptoethanol, pH 6.7) (Sigma-Aldrich) and heated at 95°C for 5 minutes. Electrophoresis was performed by loading 112 µl of each sample in a 12% pre-cast SDS-PAGE gel (Bio-Rad Laboratories, Hercules, CA, USA), which was later transferred to a polyvinylidene difluoride (PVDF) membrane (Merck Millipore, Billerica, MA, USA). For immunoblotting, PVDF membranes were previously blocked with either 5% non-fat dried milk or 2% bovine serum albumin (BSA) (Sigma-Aldrich) diluted in TBST (Tris buffered saline, 0.05% Tween 20) for 1 hour. After blocking, membranes were incubated with the following primary antibodies: rabbit anti-mouse L-ferritin (ab69090, Abcam, Cambridge, UK) at 1:1000 dilution; rabbit anti-mouse H-ferritin (ab65080, Abcam) at 1:1000 dilution; rabbit anti-mouse SCARA5 (ab76720, Abcam) at 1:1000 dilution; rabbit anti-mouse transferrin (ab84036, Abcam) at 1:2000 dilution; rat anti-mouse transferrin receptor (ab63333, Abcam) at 1:1000 dilution; rabbit anti-mouse claudin-5 (34-1600, Thermo Fisher Scientific, Wilmington, DE, USA) at 1:1000 dilution; and rabbit anti-mouse VEGF (ab46154, Abcam) at 1:100 dilution. For protein

normalization, rabbit anti-mouse α-tubulin (ab4074, Abcam) at 1:80000 dilution or rabbit anti-human α smooth muscle actin (ab5694, Abcam) at 1:10000 were used as a loading control. Primary antibodies were incubated overnight at 4ºC. After several washes in TBST, the membranes were incubated with goat anti-rabbit (Bionova Scientific, Fremont, CA, USA) and sheep anti-rat (LifeSpan, Providence, RI, USA) horseradish peroxidase secondary antibodies at 1:5000 dilution for 45 minutes. All antibodies were also diluted in blocking solution. The reagent Immobilon Crescendo Western horseradish peroxidase (HRP) Substrate (Merck Millipore) and the ImageJ software were used for band detection and quantification, respectively.

2.9. Immunohistochemistry

Paraffin embedded mice eyes and spleens were sectioned, deparaffinized, and rehydrated. For antigen retrieval, samples were immersed in a citrate solution (3.38% citric acid, 24.4% sodium citrate), 4 minutes at boiling temperature and 20 minutes at room temperature. After washing samples with PBI (1x PBS, 0.05% Igepal), sections were incubated with the following primary antibodies overnight at 4ºC: rabbit anti-mouse L-ferritin (ab69090 Abcam) at 1:100 dilution; rabbit anti-mouse H-ferritin (ab65080, Abcam) at 1:100 dilution; goat anti-mouse collagen IV (AB769, Merck Millipore) at 1:20 dilution; and rabbit anti-mouse albumin (A001, DAKO, Glostrup, Denmark) at 1:2000 dilution. To prevent antibody unspecific binding, all primary antibodies were diluted in wash buffer (1x PBS, 0.5% BSA, 0.05% Igepal) with 10% of donkey serum (Sigma Aldrich), except anti-albumin antibody that was diluted in PBI to avoid unspecific binding with the BSA from the wash buffer. Negative controls were included by omitting the primary antibody in sequential tissue sections. After primary antibody, samples were incubated with donkey anti-goat Alexa 488 (Life Technology, Carlsbad, Ca, USA) and goat anti-rabbit 568 (Invitrogen, Carlsbad, CA, USA) secondary antibodies, both at 1:1000 dilution for 2 hours. Finally, samples were counterstained with Hoechst (Sigma-Aldrich) at 1:100 dilution for 10 min and slides were mounted in Fluoromount (Sigma-Aldrich) and analyzed in a SP5 laser scanning confocal microscope (Leica Microsystems GmbH).

2.10. In vivo observation of eye fundus vascularization

Mice were anaesthetized with an intraperitoneal injection of a ketamine and xylazine cocktail. During anesthesia, viscofresh (Allergan, Dublin, Ireland) was applied in the eyes to prevent them from drying. Eye drops of tropicamide (Alcon, Barcelona, Spain) were used to induce mydriasis, and 10 µl of 5% sodium fluorescein (Sigma-Aldrich) were injected subcutaneously in each mouse to observe the eye fundus vascularization.

Custom-made mouse lenses were placed on the corneas while visualizing retinal blood vessels in the HRA2 scanning laser ophthalmoscope (Heidelberg Engineering, Heidelberg, Germany). Angiography was performed in both eyes and in the three retinal vascular plexi (Paques et al., 2003b).

2.11. Transmission electron microscopy

Retinas were dissected in 1x PBS and cut into 1 mm^2 fragments. Retinal fragments were fixed in 2,5% glutaraldehyde and 2% paraformaldehyde for 2 hours at 4ºC and then washed in PBI. Post fixation was performed with 1% osmium tetroxide for 2 hours. Samples were dehydrated in a graded acetone solution and infiltrated with Spurr resin (Sigma-Aldrich). Ultra-sections of 60-80nm were obtained with ultramicrotome Leica EM UC6 and contrasted with Reynolds' stain (Soliman et al., 2010) and 2% aqueous uranyl acetate. Finally, samples were analysed with a transmission electron microscope Jeol JEM-1400 (Jeol Ltd., Tokyo, Japan).

2.12. Retinal thickness measurement

To evaluate retinal thickening, an indicator of retinal oedema (Goebel and Kretzchmar-Gross, 2002), paraffined eyes were sectioned through their axis and were stained with Haematoxylin/Eosin (H/E). Retinal thickness was measured between the internal limiting membrane and the outer limiting membrane. A total of six areas, at 100 µm, 500 µm, and 1000 µm on each side of the optic nerve head, were analysed. ImageJ was used for morphometric analysis by an operator blinded to the experimental groups.

2.13. Statistical analysis

For statistical analyses R Software (version 4.1.0; R Foundation for Statistical Computing, Vienna, Austria) was used. Shapiro-Wilk test was performed for evaluation of the data distribution and F test for the variance homogeneity. Data with normal distribution was analyzed using the parametric method unpaired *t*-test and data not normally distributed was analyzed with Wilcoxon test. Data are expressed as mean ± standard error of the mean (SEM). Differences between groups were considered significant at P-value<0.05.

3. RESULTS

3.1. Systemic iron was increased in 20-week-old diabetic mice

The spleen accumulates high concentrations of iron due to haemoglobin catabolism from senescent erythrocytes (Kolnagou et al., 2013), becoming a useful organ to assess systemic iron status. In this regard, we first analysed the iron content in the spleen using Perls stain, which revealed that db/db mice presented a significant increase of iron content compared to db/+ (0.452±0.136 arbitrary units (AU) in db/+ mice vs. 1.489±0.387 AU in db/db mice; p=0.0142; n=9) (Figure 1A). As expected, iron was mostly accumulated in the red pulp (Figure 1A), where erythrophagocytosis takes place. Another widely used indicator to assess iron content in tissues is ferritin concentration (Daru et al., 2017). When intracellular iron levels increase, IRPs enhance ferritin synthesis as a compensatory mechanism (Munro, 1990; Wang and Pantopoulos, 2011). More specifically, during iron overload, L-ferritin is predominant, since L-rich ferritin granules are more efficient for iron storage (Levi et al., 1994). To assess if the increment of iron in db/db spleen correlated with a higher L-ferritin expression, western blot was performed and as expected, db/db mice exhibited higher amounts of L- ferritin (0.372±0.133 AU in db/+ mice vs. 2.123±0.364 AU in db/db mice; p=0.0107; n=3) (Figure 1B). Immunohistochemistry showed that the increase of L-ferritin expression occurred also in the red pulp, where iron is accumulated (Figure 1C).

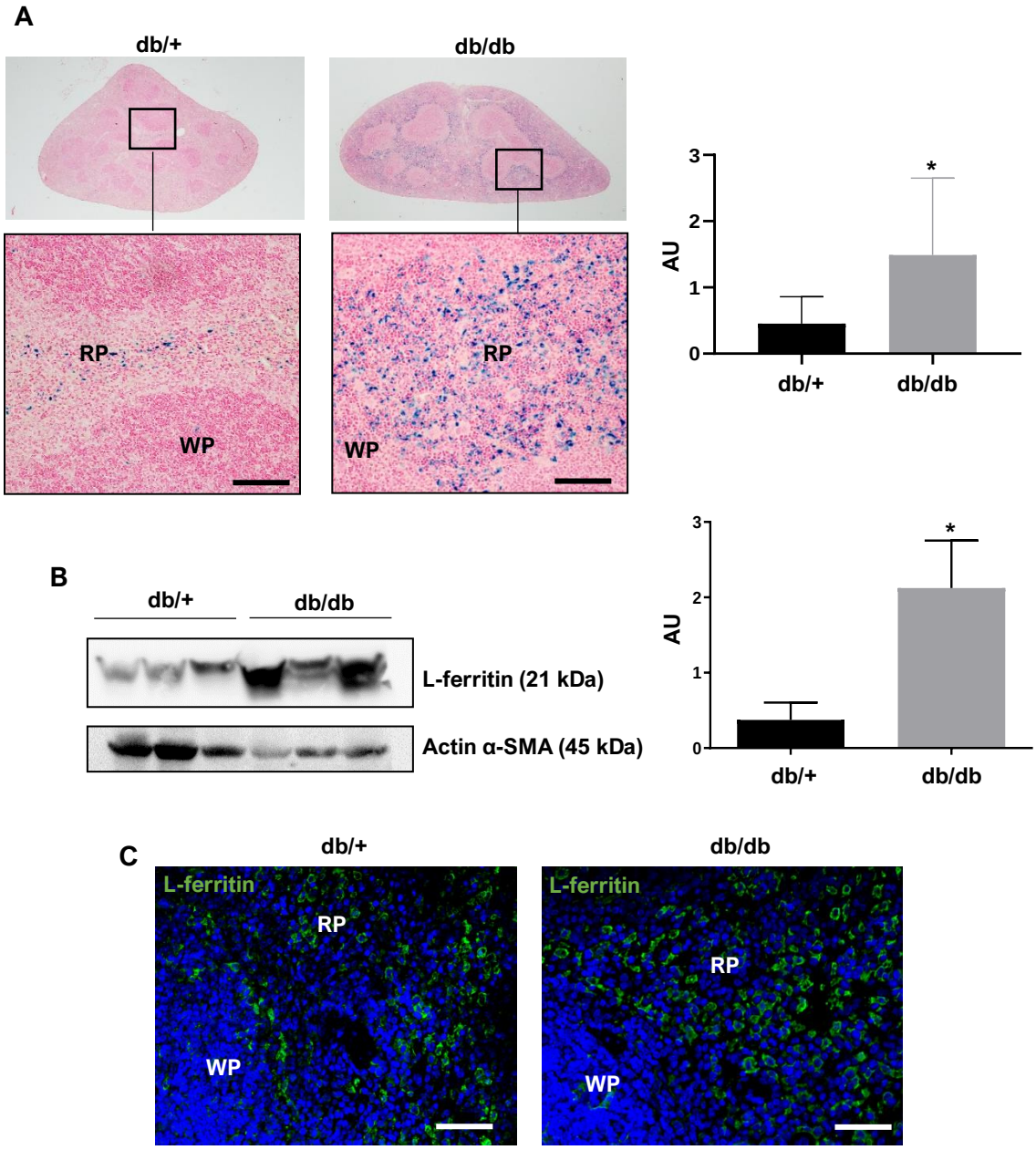

Figure 1. Spleen iron and ferritin were increased in 20-week-old db/db mice. (A) Perls stain showed a significant increment in iron content in the spleen of db/db mice, mostly in the red pulp (0.452±0.136 AU in db/+ mice vs. 1.489±0.387 AU in db/db mice; p=0.0142; n=9). **(B)** Western blot analysis also revealed higher levels of L-ferritin expression in spleen of db/db mice (0.372±0.133 AU in db/+ mice vs. 2.123±0.364 AU in db/db mice; p=0.0107; n=3). α-smooth muscle actin was used as a loading control. **(C)** Immunofluorescence representative images showed increased L-ferritin expression in the red pulp of db/db mouse spleen. Nuclei were counterstained with Hoechst. RP: red pulp; WP: white pulp. Scale bar: 100 µm (A), 30 µm (C).

The increment in iron and ferritin content found in the db/db mouse spleen showed concordance with the high levels of serum iron (20.17±1.072 µmol/L in db/+, n=15 vs. 28.92±2.323 µmol/L in db/db, n=9; p=0.0008) (Figure 2). This finding was accompanied by an increase of serum total iron binding capacity (TIBC) in db/db mice (48.90±0.932 µmol/L in db/+, n=15 vs. 65.28±3.006 µmol/L in db/db, n=9; p<0.0001) (Figure 2), which

is an indicator of serum transferrin concentration and iron delivery into the tissues (Faruqi and Mukkamalla, 2020).

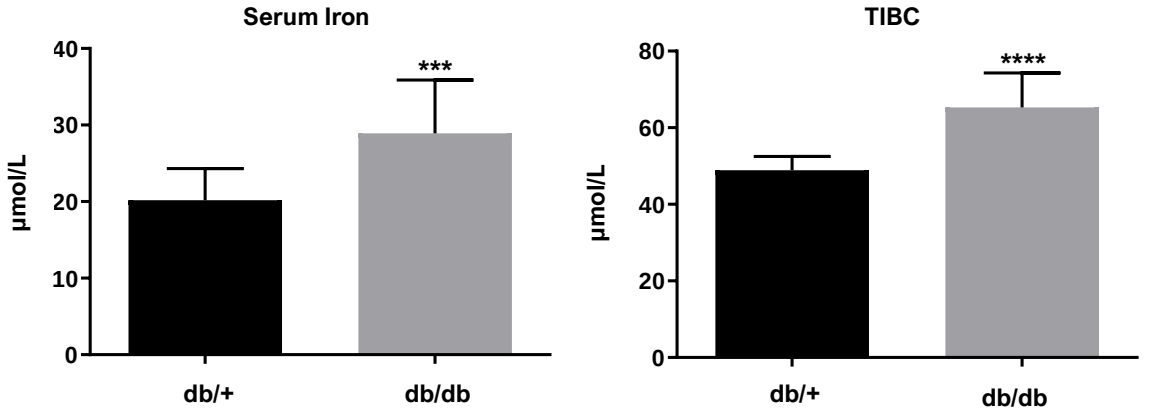

Figure 2. Serum iron and TIBC were increased in 20-week-old db/db mice. Serum iron (20.17±1.072 µmol/L in db/+, n=15 vs. 28.92±2.323 µmol/L in db/db, n=9; p=0.0008) and TIBC, which is an indicator of serum transferrin concentration, (48.90±0.932 µmol/L in db/+, n=15 vs. 65.28±3.006 µmol/L in db/db, n=9; p<0.0001) were significatively increased in db/db mice.

3.2. Retinas showed increased ferritin, but not iron overload in 20-week-old diabetic mice.

To assess if, as happened in the spleen, retinas from diabetic mice presented an elevated expression of ferritin, levels of both L- and H-ferritin were analysed by western blot in db/+ and db/db retinas. An increase of 2-fold change in L-ferritin (0.484±0.488 AU in db/+ vs. 0.9947±0.146 AU in db/db; n=3, p=0.029) and a 3.3-fold change in H-ferritin (0.3168±0.051 AU in db/+ vs. 0.986±0.052 AU in db/db; n=3, p=0.0008) were observed in diabetic retinas (Figure 3A). Immunohistochemistry confirmed an increase in the expression of both ferritin subunits in diabetic retinas (Figure. 3B). These results agreed with those obtained by a previous study (Chaudhary et al., 2018).

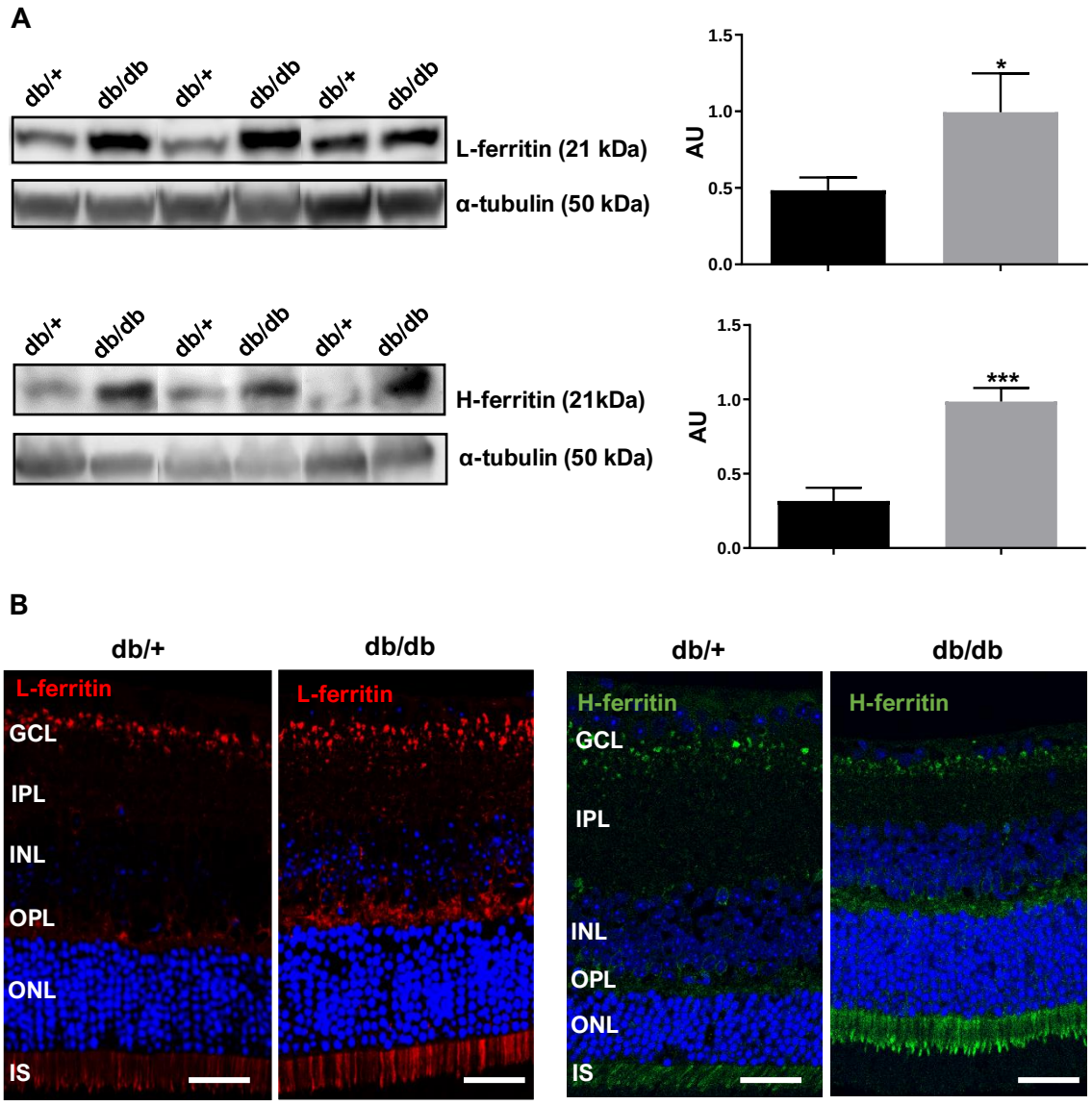

Figure 3. **L and H-ferritin were increased in 20-week-old db/db mouse retinas. (A)** Western blot analysis revealed that L-ferritin expression was 2-fold increased (0.484±0.488 AU in db/+ vs. 0.9947±0.146 AU in db/db; n=3, p=0.029) and H-ferritin was 3.3-fold increased (0.3168±0.051 AU in db/+ vs. 0.986±0.052 AU in db/db; n=3, p=0.0008) in db/db mouse retinas. α-tubulin was used as a loading control. **(B)** Immunofluorescence representative images showed an increase in both L and H-ferritin expression in db/db mouse retinas. Nuclei were counterstained with Hoechst. GCL: ganglion cell layer; IPL: inner plexiform layer; INL, inner nuclear layer; OPL: outer plexiform layer; ONL: outer nuclear layer; IS: inner segments of photoreceptors. Scale bar: 32.05 µm.

In the retina, ferritin expression has been largely used as an indirect measurement of iron content (Hahn et al., 2004; Zhao et al., 2014; Chaudhary et al., 2018; Shu et al., 2019). Since Perl's stain was not sensitive enough to detect iron in db/+ and db/db retinas (Supplementary Fig. 1), ICP-MS, a high sensitivity and well stablished method for retinal iron detection (Ugarte et al., 2012; Pamphlett et al., 2020; Valença et al., 2021) was used to ensure that retinal ferritin levels correlated with iron levels. Unexpectedly, ICP-MS analysis did not show any difference in the iron content between db/+ and db/db retinas

(2.264±0.212 µg iron/g retina in db/+ vs. 2.162±0.071 µg iron/g retina in db/db; n=5, p=0.744) (Figure 4A), revealing that increased retinal ferritin was not accompanied with increased iron content in the diabetic retina. In agreement with these results, no differences in ferrous iron were observed between db/+ and db/db retinas (2.288±0.9011 AU in db/+, n=4 vs. 1.927±0.3402 AU in db/db, n=5; p=0.694) using the fluorescent probe FeRhoNox-1™ (Figure 4B).

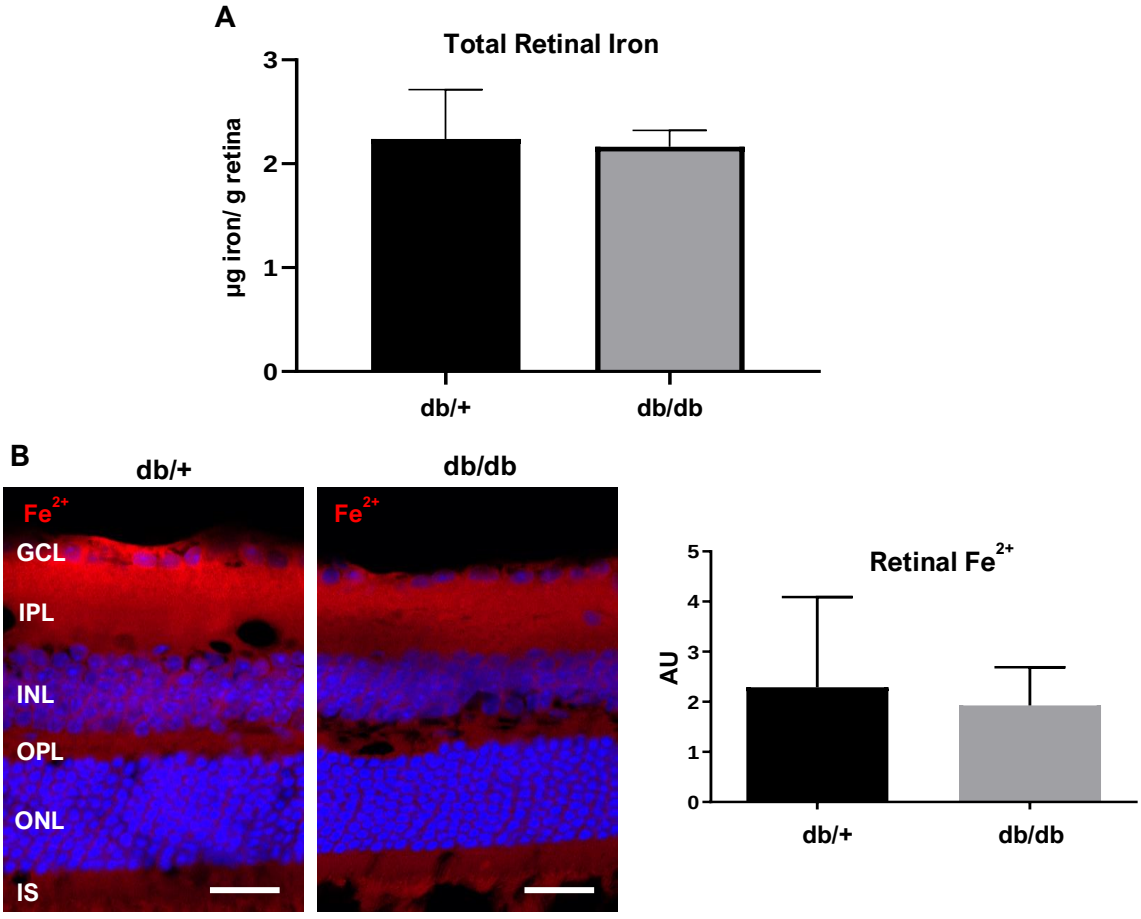

Figure 4. Iron was not increased in 20-week-old db/db mouse retinas. There were no differences between db/+ and db/db retinas in: **(A)** total iron content analyzed with ICP-MS (2.264±0.212 µg iron/g retina in db/+ vs. 2.162±0.071 µg iron/g retina in db/db; n=5, p=0.744); and **(B)** ferrous iron content analysed with fluorescent probe FeRhoNox-1™ (2.288±0.9011 AU in db/+, n=4 vs. 1.927±0.3402 AU in db/db, n=5; p=0.694). GCL: ganglion cell layer; IPL: inner plexiform layer; INL, inner nuclear layer; OPL: outer plexiform layer; ONL: outer nuclear layer; IS: inner segments of photoreceptors. Scale bar: 25 µm.

3.3. Iron import proteins were not increased in 20-week-old diabetic mouse retinas

As ferritin expression, but not iron content, was increased in the retina, we next analysed the proteins involved in iron import within the retina. Western blot showed that neither transferrin (1.013±0.071 AU in db/+ vs. 1.079±0.12 AU in db/db; n=3 p=0.665) nor transferrin receptor (1.079±0.237 AU in db/+ vs. 0.773±0.058 AU in db/db vs.; n=3,

p=0.278) were increased in diabetic retinas (Fig. 5). In addition, the receptor of circulating L-ferritin, SCARA5, expressed in retinal endothelial cells and previously proved to mediate iron import into the retina (Mendes-Jorge et al., 2014) was also not increased in diabetic retinas (0.9799±0.076 AU in db/+ vs. 1.099±0.087 AU in db/db; n=3, p=0.363) (Figure 5). Altogether, these results showed that, despite the systemic iron overload and the increase of ferritin, the iron levels and the iron import machinery were not incremented in diabetic retinas. Thus, suggesting the existence of a mechanism that protects the retina from massive iron entry.

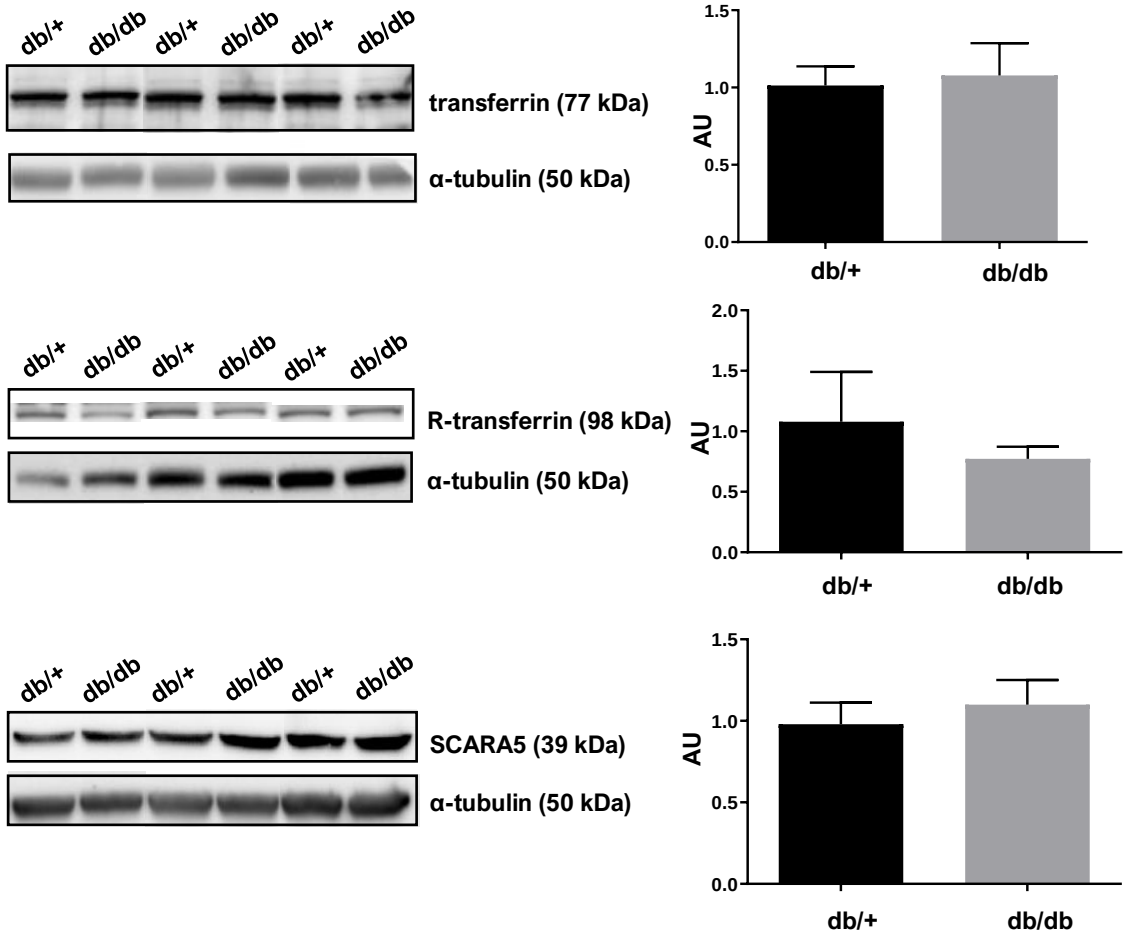

Figure 5. Iron import proteins were not increased in 20-week-old db/db mouse retinas. Western blot analysis revealed that neither transferrin (1.013±0.071 AU in db/+ vs. 1.079±0.12 AU in db/db; n=3 p=0.665) nor its receptor (1.079±0.237 AU in db/+ vs. 0.773±0.058 AU in db/db vs.; n=3, p=0.278) were increased in db/db mouse retinas. SCARA5, the receptor of L-ferritin, was also not increased in db/db mouse retinas (0.9799±0.076 AU in db/+ vs. 1.099±0.087 AU in db/db; n=3, p=0.363). α-tubulin was used as a loading control.

3.4. BRB breakdown signs were not observed in 20-week-old diabetic mice

The db/db mice develop complete BRB breakdown at 15 months of age (Cheung et al., 2005), although other studies have found retinal oedema earlier (Li et al., 2010; Kim et al., 2014; Xiong et al., 2017). To assess BRB integrity in 20-week-old diabetic mice, we first analysed eye fundus with scanning laser ophthalmoscope (SLO), which revealed that injected fluorescein remained inside the vessels and none of db/+ nor db/db mice presented vascular leakage (n=16) (Figure 6A). In addition, serum albumin detected by immunohistochemistry was confined to the vessel lumen, indicating the absence of retinal oedema in 20-week-old diabetic mice (Figure 6B). VEGF, which increases vascular permeability in diabetic retinopathy (Boyer et al., 2013), was also analysed by western blot and no statistical differences were found between db/+ and db/db retinas (1.003±0.142 AU in db/+ vs. 0.8553±0.183 AU in db/db; n=3, p=0.559) (Figure 6C). Furthermore, the comparison of retinal thickness between db/+ and db/db mice confirmed that diabetic retinas did not present oedema (183.38±2.102 µm in db/+, n=12 vs. 187.12±4.696 µm in db/db; n=6; p=0.41) (Figure 7).

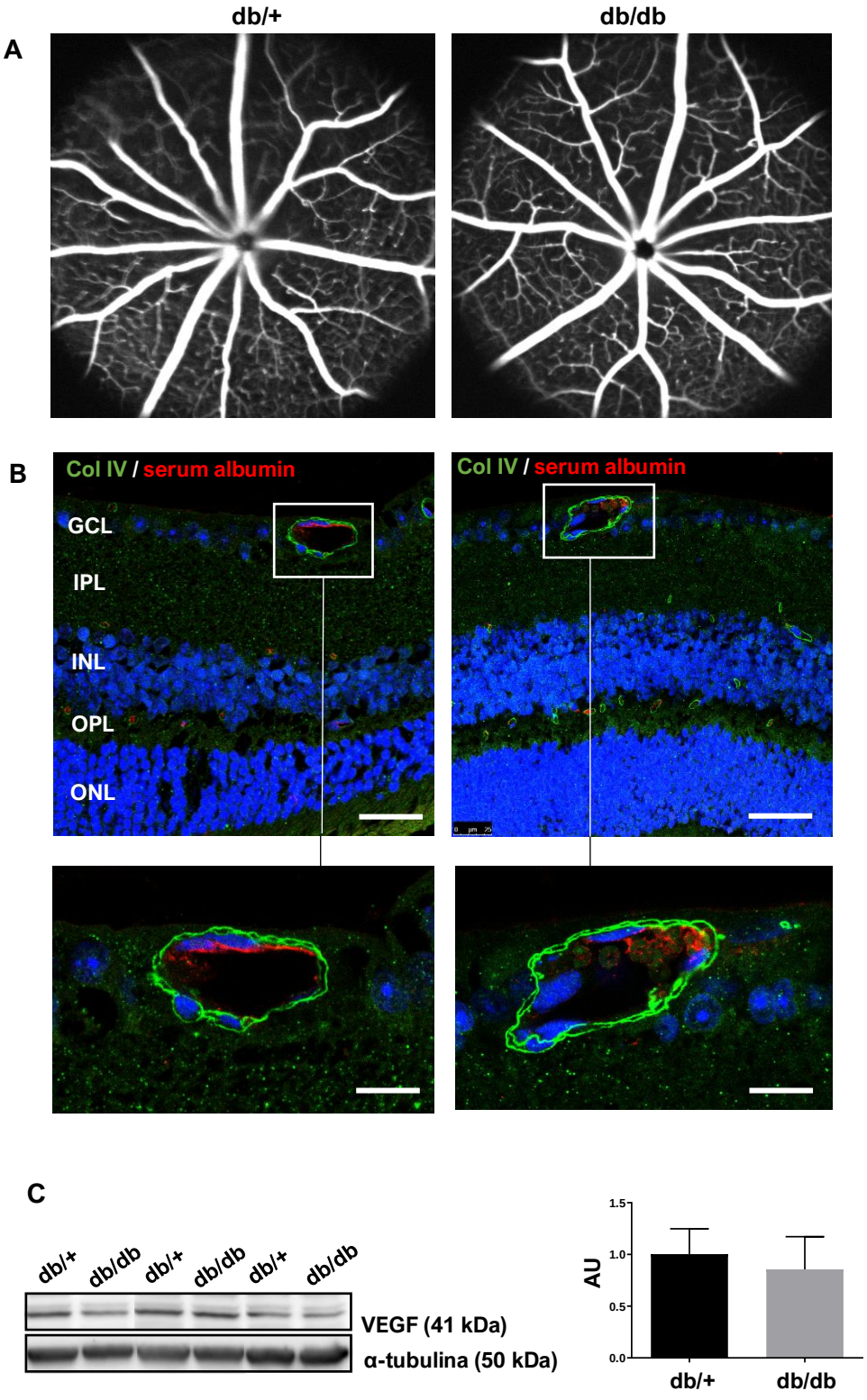

Figure 6. No signs of BRB breakdown were found in 20-week-old db/db mouse retinas. (A) Analysis of the eye fundus by SLO showed that injected fluorescein remained inside the retinal blood vessels in db/db mice showing no vascular leakage (n=16). **(B)** To assess retinal vessels leakage microscopically, immunohistochemistry against serum albumin and collagen IV, a marker for blood basement membrane, was performed. The results showed that serum albumin was restricted inside the vessel lumen in db/db mice. **(C)** Western blot analysis of VEGF expression, which induces vascular permeability, showed no statistical differences between db/+ and db/db retinas (1.003±0.142 AU in db/+ vs. 0.8553±0.183 AU in db/db; n=3, p=0.559). α-tubulin was used as a loading control. GCL: ganglion cell layer; IPL: inner plexiform layer; INL, inner nuclear layer; OPL: outer plexiform layer; ONL: outer nuclear layer. Scale bar: 29.41 µm (inset: 11.49 µm).

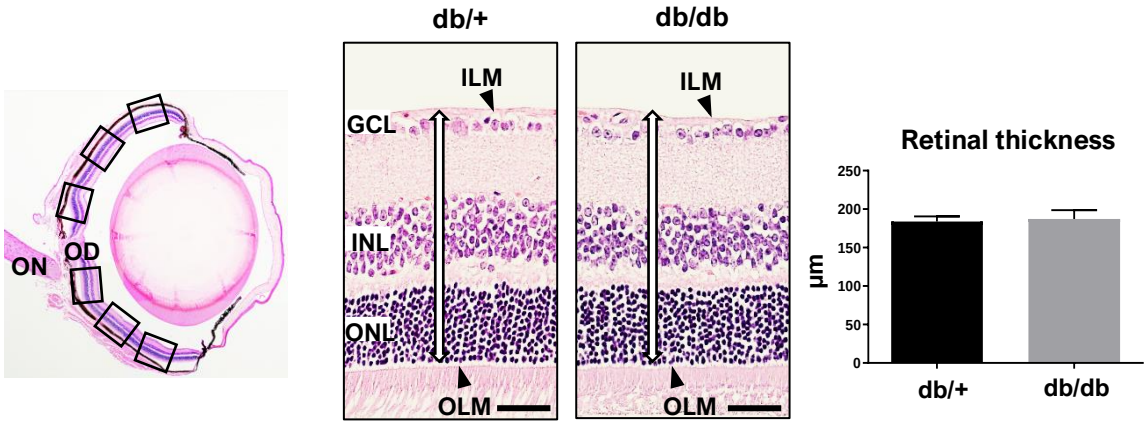

Figure 7. No differences in retinal thickness were found in 20-week-old db/db mouse retinas. To assess retinal oedema, paraffined sections stained with H/E were measured from the internal limiting membrane to the outer limiting membrane (arrowheads) in six different areas (at 100 µm, 500 µm, and 1000 µm on each side of the optic nerve head) and no differences between db/+ and db/db were found (183.38±2.102 µm in db/+, n=12 vs. 187.12±4.696 µm in db/db; n=6; p=0.41). OD: optic disc; ON: optic nerve; GCL: ganglion cell layer; INL: inner nuclear layer; ONL: outer nuclear layer; ILM: internal limiting membrane; OLM: outer nuclear membrane. Scale bar: 41.15 µm.

Next, to evaluate tight junctions, the key player in the maintenance of BRB integrity (Campbell and Humphries, 2013), ultrathin sections of the retina were analysed by transmission electron microscopy. Endothelial tight junctions in db/db retinas appeared morphologically normal, without any open space between membranes of neighbouring endothelial cells and with the characteristic electron density produced by the tight junction proteins (Figure 8A). Additionally, one of the most important tight junction proteins, claudin-5 (Tian et al., 2014), was analysed by western blot. No differences in claudin-5 expression were observed when comparing db/+ with db/db retinas (0.989±0.134 AU in db/+ vs. 1.058±0.243 AU in db/db; n=3, p=0.818) (Figure 8B). Altogether, these results showed that BRB was intact in 20-week-old diabetic mice and that could be preventing the entrance of high amounts of circulating iron into the retina.

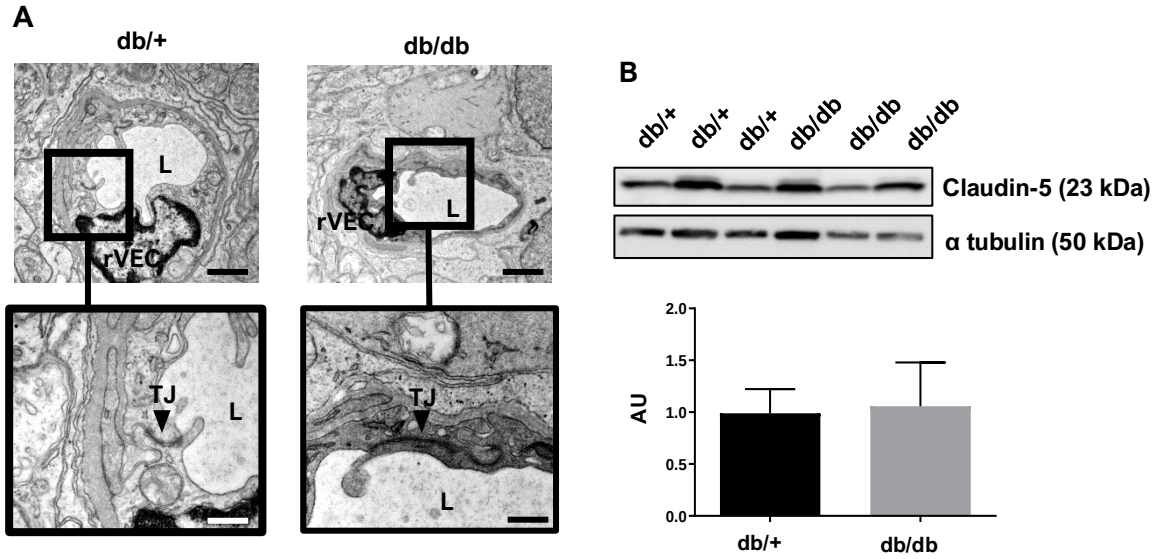

Figure 8. Retinal tight junctions were not altered in 20-week-old db/db mice. (A) Transmission electron microscopy analysis revealed a normal ultrastructure and electron density of tight junctions (arrows) in db/db retinal vessels. **(B)** Western blot analysis did not show changes in the expression of the tight junction protein claudin-5 in db/db mice retinas (0.989±0.134 AU in db/+ vs. 1.058±0.243 AU in db/db; n=3, p=0.818). α-tubulin was used as a loading control. rVEC: endothelial cell; L: vessel lumen; TJ: tight junction. Scale bar: 200 nm (inset: 217 nm).

3.5. BRB protected retina from iron entrance during systemic iron overload

To assess the BRB role in the protection of the retina during iron overload, we injected 1g/kg of iron dextran intraperitoneally to C57BL/6J WT mice. Saline solution was injected to a control group. At 4 hours post-injection, iron accumulation in the spleen was quantified with Perls stain, which demonstrated that iron dextran injected mice presented systemic iron overload (0.8051±0.46 AU in the group injected with saline solution vs. 2.281±0.13 AU in the group injected with iron dextran; n=3, p=0.037) (Figure 9). In contrast, Perls stain performed in the retina of iron dextran injected mice only detected iron inside the blood vessels and not in the parenchyma (Figure 10A). ICP-MS confirmed that no statistical differences were found in iron content in the retinal parenchyma between groups (1.768±0.521 µg iron/g retina in saline solution injected mice, n=5, vs. 2.755±1.4 µg iron/g retina in the iron dextran injected mice n=4., p=0.905) (Figure 10B). Altogether, these results supported the hypothesis that the BRB has a protective effect in preventing retinal iron overload.

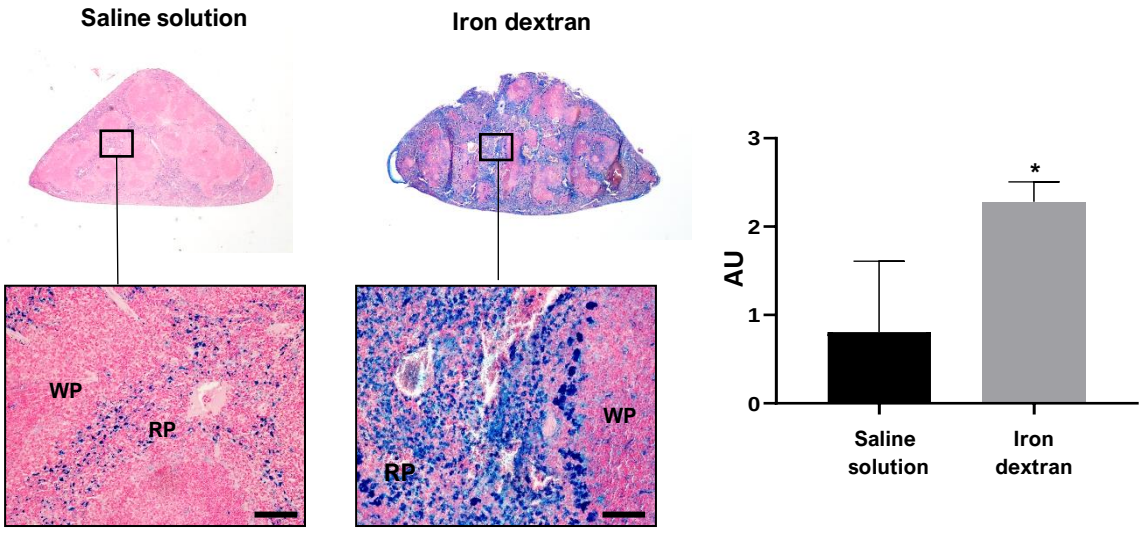

Figure 9. Intraperitoneal injection of iron dextran induced acute systemic iron overload in WT mice. At 4 hours post injection, Perls stain was performed in the mouse spleen showing an increase in iron accumulation in the red pulp of mice injected with iron dextran (0.8051±0.46 AU in the group injected with saline solution vs. 2.281±0.13 AU in the group injected with iron dextran; n=3, p=0.037). RP: red pulp; WP: white pulp. Scale bar: 82 µm.

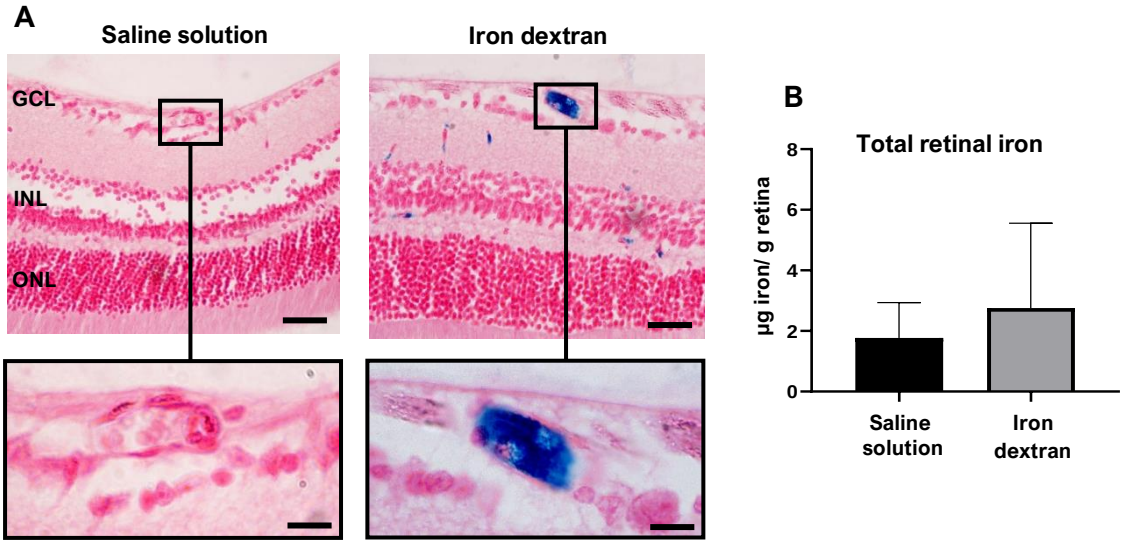

Figure 10. Systemic iron overload induced by iron dextran did not cause retinal iron overload. (A) At 4 hours post iron dextran injection, Perls stain performed in mouse retinas revealed iron exclusively inside the blood vessels, but not in the retinal parenchyma. **(B)** After a vascular washout to remove intravascular iron dextran, ICP-MS was used to quantify iron (1.768±0.521 µg iron/g retina in saline solution injected mice, n=5, vs. 2.755±1.4 µg iron/g retina in the iron dextran injected mice n=4., p=0.905). GCL: ganglion cell layer; INL, inner nuclear layer; ONL: outer nuclear layer. Scale Bar: 36.49 µm (inset: 10 µm).

Finally, to confirm our hypothesis, BRB was experimentally broken by cryopexy, a well stablished method to produce BRB breakdown (Derevjanik et al., 2002). Cryopexy was performed in the right eye of iron dextran injected mice, while the left eye served as a

control. BRB breakdown was confirmed by immunohistochemistry against serum albumin, which already showed vascular leakage 15 minutes after cryopexy (Figure 11A). Additionally, Perls stain also showed iron leaking from blood vessels in eyes with cryopexy (Figure 11B). One hour after cryopexy, ICP-MS was used to quantify total iron content in the retinal parenchyma. The results showed that iron was significatively increased in cryopexed retinas (2.755±1.4 µg iron/g retina in control eyes, n=4, vs. 12.052±1.764 µg iron/g retina with cryopexy, n=6; p=0.005) (Figure 11C), confirming that massive iron entry only occurs when BRB is compromised

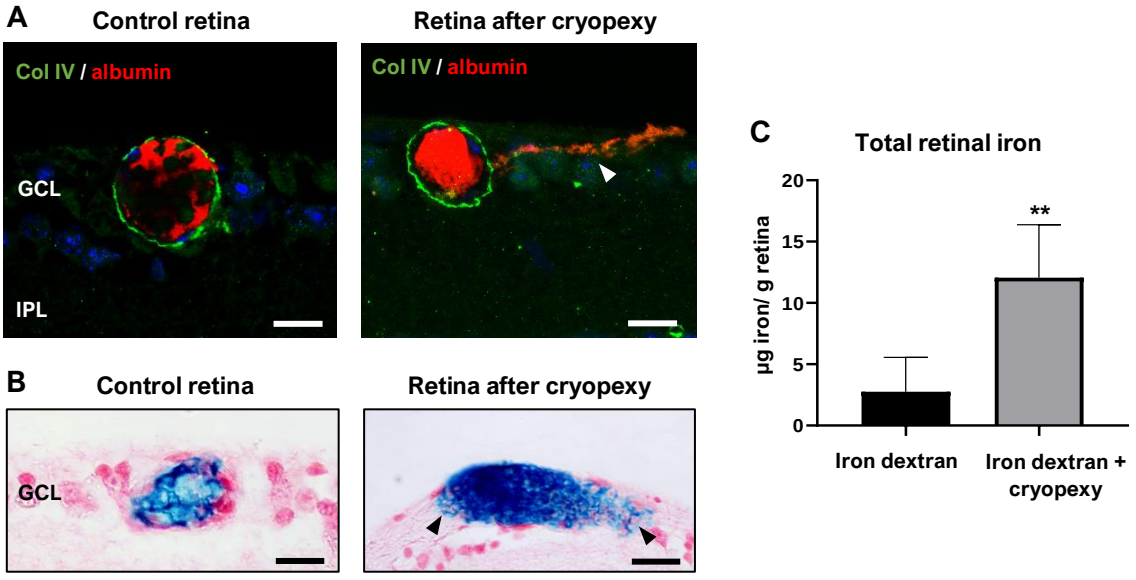

Figure 11. BRB breakdown induced by cryopexy caused retinal iron overload in mice injected with iron dextran. (A) Immunohistochemistry against serum albumin and collagen IV showed vascular leakage (arrowhead), demonstrating BRB breakdown in retinas from cryopexed eyes. **(B)** Perls stain in paraffin sections showed iron leakage (arrowheads) into the retinal parenchyma in cryopexed eyes. **(C)** ICP-MS was used to quantify iron content in the retinal parenchyma, showing, as expected, an increase in retinal iron in cryopexed eyes (2.755±1.4 µg iron/g retina in control eyes, n=4, vs. 12.052±1.764 µg iron/g retina with cryopexy, n=6; p=0.005). GCL: ganglion cell layer; IPL: inner plexiform layer. Scale bar: 12.5 µm (A), 13.7 µm and 22.72 µm (B, left and right).

3.6 Ferritin expression in the retina was also increased during experimental systemic iron overload without retinal iron overload

To understand why ferritin expression was increased while iron content remained at normal levels in diabetic retinas, and to determine whether this was a specific finding that occurred in diabetic retinopathy, retinal ferritin expression four hours after iron dextran injection in WT mice, was assessed by western blot. The results showed a 1.8-fold increased L-ferritin expression in the retinas of iron dextran injected mice (0.595±0.136 AU in the saline solution injected mice vs. 1.040±0.071 AU in the iron dextran injected mice; n=4, p=0.0272) (Figure 12). Thus, our study revealed that

systemic iron overload causes an increase in retinal L-ferritin expression without BRB breakdown and retinal parenchyma iron increase.

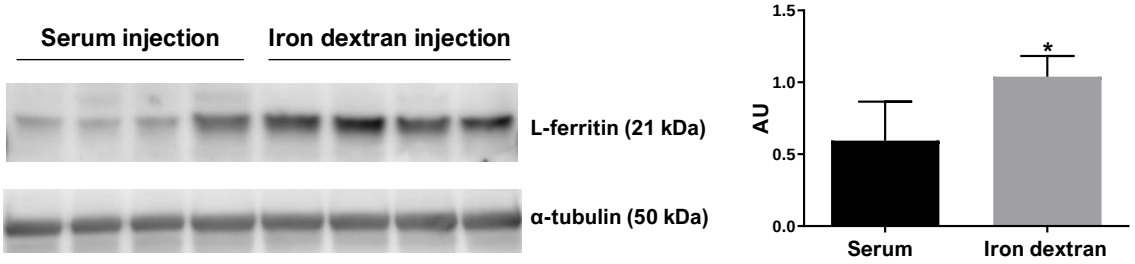

Figure 12. Ferritin expression was increased in iron dextran injected mouse retinas. Western blot analysis revealed a significant 1.8-fold increase in L-ferritin expression in the retinas of mouse injected with iron dextran before BRB breakdown (0.595±0.136 AU in the saline solution injected mice vs. 1.040±0.071 AU in the iron dextran injected mice; n=4, p=0.0272). α-tubulin was used as a loading control.

4. DISCUSSION

Previous reports have described the association between iron overload and diabetic retinopathy (Ciudin et al., 2010; Gnana-Prakasam et al., 2016). Our results showed that 20-week-old db/db mice had systemic iron overload and increased ferritin expression in the retina, which fully agree with the results observed by Chaudhary et al. in 2018. However, unexpectedly, analysis of retinal iron by ICP-MS did not show higher iron content in the retina of diabetic mice. Most importantly, the content of ferrous iron, which is responsible of oxidative damage in the retina (Shu et al., 2020), was also not increased in diabetic retinas. In addition, no changes were found in retinal iron import machinery of db/db mice, which supports the fact that retinal iron content was not increased.

Classical methods for iron detection, such as Prussian blue stain, are not sensitive enough to detect iron in the retina. There are high precision techniques to locate and quantify iron in the retina, such as particle-induced X-ray emission (PIXE) and synchrotron X-ray fluorescence (SXRF) (Ugarte et al., 2012b, 2014), although these have a very limited access. ICP-MS is also a high sensitivity method for iron detection, and it is more available, but it does not provide information about the iron location within the retinal layers. Thus, the *in situ* detection of retinal iron can be challenging. For this reason, and since ferritin expression changes proportionally to iron levels in systemic tissues (Daru et al., 2017), most studies use ferritin expression as an indirect indicator for iron content (Hahn et al., 2004; Zhao et al., 2014; Chaudhary et al., 2018; Shu et al., 2019), justifying that an increase of ferritin expression in the retina is equivalent to retinal iron overload. Nevertheless, our results point out that ferritin expression might not be always a reliable marker to estimate iron content in the retina as it has been used so far.

We have shown that in diabetic mice with systemic iron overload, the retina remains protected from iron entry, at least until the age of 20 weeks, but how is the retina protected? In a recent study of long-term iron overload induced by iron dextran injections in mice (Shu et al., 2019), BRB was proposed to prevent the retina from iron entry, so we next analysed BRB status in db/db mice. BRB breakdown is a hallmark of diabetic retinopathy (Zhang et al., 2014) and there are several studies that find signs of vascular leakage in db/db retinas at different ages (Cheung et al., 2005; Li et al., 2010; Kim et al., 2014; Xiong et al., 2017). In our study, diabetic mice did not present any sign of BRB breakdown, including vascular leakage, VEGF overexpression, endothelial tight junction alterations, or retinal oedema, confirming an early stage of diabetic retinopathy in 20-week-old db/db mice. However, we can assume that, eventually, db/db mice will develop BRB breakdown and iron will enter in the retina producing iron overload, as happened when we experimentally broke the BRB by cryopexy in iron dextran injected mice. Altogether, the results obtained demonstrated that in the retina a massive entrance of iron only occurs when BRB is compromised. This mechanism has been recently demonstrated in the brain of aging mice with systemic iron overload, where, after blood brain barrier breakdown, the brain becomes unprotected and suffers iron overload (Mezzanotte et al., 2021).

Another unexpected finding was the overexpression of ferritin in the db/db mouse retinas despite physiological levels of iron content. Why is retinal ferritin increased without iron increase? Ferritin levels are post-transcriptionally regulated by the so-called IRPs, which bind to ferritin mRNA and avoid its expression. When intracellular iron is high, IRPs lose the capacity to bind to ferritin mRNA and, thus, ferritin levels increase (Hentze and Kühn, 1996). As for the retina, this mechanism has been described using a model of IRP deficiency, in which ferritin expression in the retina was increased (Paul Hahn et al., 2004a). Surprisingly, retinas from db/db and iron dextran injected mice, which had increased ferritin expression, did not present a higher iron content that could trigger IRP depletion and ferritin increase. This could suggest the existence of a signalling mechanism between the retina and the exterior. The retina could be detecting systemic iron overload and activating ferritin synthesis as a compensatory response in front a potential BRB breakdown, given that a single ferritin complex can harbour up to 4500 molecules of iron and act as a natural iron chelator (Aisen et al., 2001).

Apart from sequestering deleterious free iron, ferritin is also overexpressed in chronic inflammatory diseases such as type 2 diabetes mellitus (Ferńandez-Real et al., 2015). Ferritin induces anti-inflammatory cytokines and works as an immunomodulator, although this applies specially to H-ferritin (Kernan and Carcillo, 2017). Nevertheless,

the fact that increased ferritin was present in both diabetic and iron dextran injected mice retinas and that both models had systemic iron overload, suggest that ferritin expression in the retina might be regulated by systemic iron excess.

Finally, monitoring iron in patients with type 2 diabetes is a common practise in the follow up of the disease (Manikandan et al., 2015; Saha and Murgod, 2019). Our findings suggests that systemic iron overload appears prior to retinal iron overload, meaning that an early detection and treatment with iron chelators could stop the passage of iron into the retina and prevent iron-induced retinal damage.

5. CONCLUSIONS

Our results demonstrated for the first time that, in the retina, ferritin expression cannot always be extrapolated to iron content. In our experiment, db/db mice suffered from iron overload and increased retinal ferritin expression but, unexpectedly, no changes were found in iron content nor iron import machinery in the retina. In addition, BRB integrity was evaluated and no signs of BRB breakdown were found in 20-week-old db/db mice, suggesting that db/db mice were in the early stages of diabetic retinopathy. In addition, iron overload induced by an injection of iron dextran confirmed that retinal iron only increased when BRB was compromised, even though retinal ferritin expression was already increased. Overall, we hypothesized that the retina might be protected by, at least, two different autonomous mechanisms in front of systemic iron overload in diabetic retinopathy. The first limiting factor for iron entry would be the regulation at the BRB, and the second would be the increase of ferritin expression prior to BRB breakdown and retinal iron increase.

Funding

This work was supported by the Instituto de Salud Carlos III, Ministerio de Ciencia e Innovación, Spain (grant number PI16/00719) and Fondo Europeo de Desarrollo Regional (FEDER).

Acknowledgements

The authors truly thank Lorena Noya, Verónica Melgarejo, and Ángel Vázquez for their technical assistance.

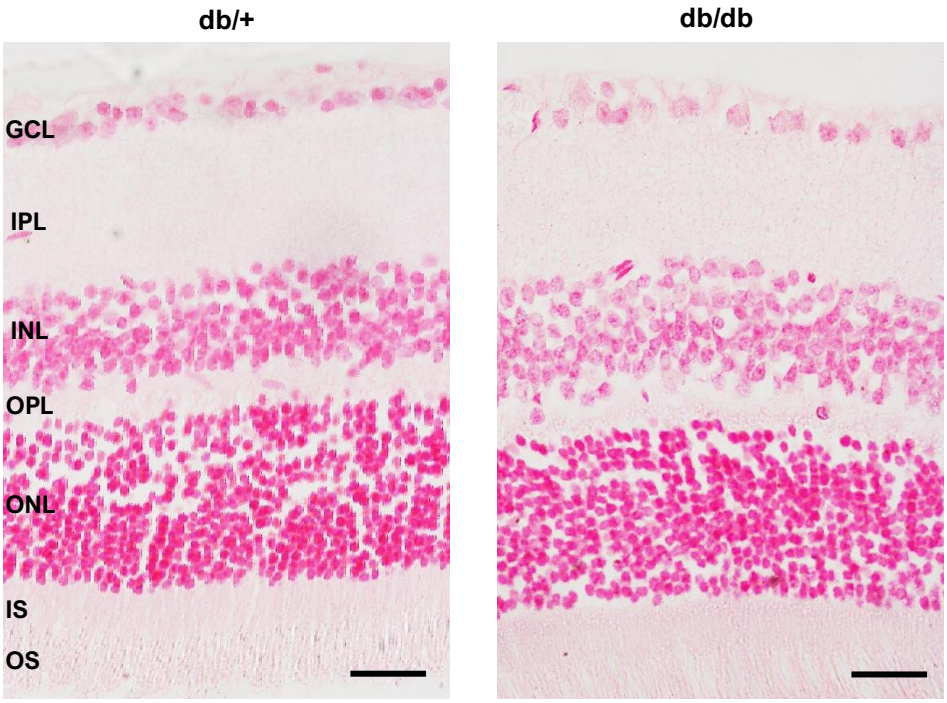

Supplementary Figure. Pearls stain failed to detect iron in the retinal parenchyma in 20-week-old db/db mouse. Perls stain was not sensible enough to stain iron in the retinal parenchyma and no blue pigmentation was observed in db/db mouse. GCL: ganglion cell layer; IPL: inner plexiform layer; INL, inner nuclear layer; OPL: outer plexiform layer; ONL: outer nuclear layer; IS: inner segments. Scale Bar: 25 µm.

CHAPTER II

DECREASED ENDOSTATIN IN DB/DB RETINAS IS ASSOCIATED WITH OPTIC DISC INTRAVITREAL VASCULARIZATION

Authors: Aina Bonet[1,2], Andreia Valença[3,4], Luísa Mendes-Jorge[4,5], Alba Casellas[1,6,7], Alfonso Rodríguez-Baeza[8], Víctor Nacher[1,2,7], David Ramos[1,4], Judit Pampalona[1], Rafael Simó[7,9], Jesús Ruberte[1,2,7].

[1]Center of Animal Biotechnology and Gene Therapy (CBATEG), Universitat Autònoma de Barcelona, Bellaterra, Spain.

[2]Department of Animal Health and Anatomy, Faculty of Veterinary Medicine, Universitat Autònoma de Barcelona, Bellaterra, Spain.

[3]Faculty of Veterinary Medicine, Universidade Lusófona de Humanidades e Tecnologias, Lisbon, Portugal.

[4]Centre for Interdisciplinary Research in Animal Health (CIISA), Faculty of Veterinary Medicine, Universidade de Lisboa, Lisbon, Portugal.

[5]Department of Morphology and Function, Faculty of Veterinary Medicine, Universidade de Lisboa, Lisbon, Portugal.

[6]Department of Biochemistry and Molecular Biology, Faculty of Veterinary Medicine, Universitat Autònoma de Barcelona, Bellaterra, Spain.

[7]Centro de Investigación Biomédica en Red de Diabetes y Enfermedades Metabólicas Asociadas (CIBERDEM), Instituto de Salud Carlos III, Madrid, Spain,

[8]Department of Morphological Sciences, Faculty of Medicine, Universitat Autònoma de Barcelona, Bellaterra, Spain.

[9]Diabetes and Metabolism Research Unit, Vall d'Hebron Research Institute, Universitat Autònoma de Barcelona, Barcelona, Spain.

[*]Corresponding author. CBATEG - Center of Animal Biotechnology and Gene Therapy, Autonomous University of Barcelona, C/ de la Vall Morona, 08193, Bellaterra (Cerdanyola del Vallès), Spain.

Declarations of interest: **A. Bonet**, None; **A. Valença**, None; **L. Mendes-Jorge**, None; **A. Casellas**, None; **A. Rodríguez-Baeza**, None; **V. Nacher**, None; **D. Ramos**, None; J. Pampalona, None; **R. Simó**, None; **J. Ruberte**, None.

This paper has been published in Experimental Eye Research (2021 Nov)

doi: 10.1016/j.exer.2021.108801

Abstract

Endostatin, a naturally cleaved fragment of type XVIII collagen with antiangiogenic activity, has been involved in the regulation of neovascularization during diabetic retinopathy. Here, the intracellular distribution of endostatin in healthy mouse and human neuroretinas has been analyzed. In addition, to study the effect of experimental hyperglycemia on retinal endostatin, the db/db mouse model has been used. Endostatin protein expression in mouse and human retinas was studied by immunofluorescence and Western blot and compared with db/db mice. Eye fundus angiography, histology, and immunofluorescence were used to visualize mouse retinal and intravitreal vessels.

For the first time, our results revealed the presence of endostatin in neurons of mouse and human retinas. Endostatin was mainly expressed in bipolar cells and photoreceptors, in contrast to the optic disc, where endostatin expression was undetectable. Diabetic mice showed a reduction of endostatin in their retinas associated with the appearance of intravitreal vessels at the optic disc in 50% of db/db mice. Intravitreal vessels showed GFAP a positive neuroglia sheath, basement membrane thickening by collagen IV deposition, and presence of MMP-2 and MMP-9 in the vascular wall. All together, these results point that decreased retinal endostatin during experimental diabetes is associated with optic disc intravitreal vascularization. Based on their phenotype, these intravitreal vessels could be neovessels. However, it cannot be ruled out the possibility that they may also represent persistent hyaloid vessels.

Key words: endostatin, intravitreal vessels, diabetic retinopathy, db/db mice.

1. INTRODUCTION

Endostatin was first discovered in the laboratory of Judah Folkman in 1997 and described as an inhibitor of angiogenesis in murine hemangioendothelioma cells (O'Reilly et al., 1997). It is a 20 kDa fragment activated by proteolytic cleavage of the C-terminal region of collagen XVIII by cathepsin L, elastases, and MMPs (Ferreras et al., 2000). Several mechanisms by which endostatin can inhibit endothelial cell proliferation, migration, and invasion have been proposed. Endostatin binds VEGF receptor KDR/Flk-1 and, thereby, interferes with VEGF signalling leading to the inhibition of proliferation and migration of endothelial cells (Kim et al., 2002). Endostatin can also promote ß-catenin degradation, inducing cell cycle arrest through inhibition of the cyclin-D1 promoter (Hanai et al., 2002). Furthermore, antimigratory effect of endostatin can also be mediated through its binding with a5ß1 integrin (Wickström et al., 2002) and the inhibition of MMP-2 activity (Kim et al., 2000). MMP-2 regulates angiogenesis by degrading collagens, laminins, and glycosaminoglycans in the blood basement membrane allowing the sprout of new vessels (Noda et al., 2003; Rodrigues et al., 2013) In mouse and human neuroretinas, endostatin has only been immunolocalized at the internal limiting membrane (Takahashi et al., 2003; Bhutto et al., 2004; Ohlmann et al., 2004; Ramesh et al., 2004; May et al., 2006; Määttä et al., 2007) and at the wall of retinal vessels, including hyaloid vessels (Bhutto et al., 2004; Ohlmann et al., 2004; May et al., 2006; Määttä et al., 2007). It is believed that this staining pattern is due to cross-reactivity between endostatin and its precursor, collagen XVIII, (Takahashi et al., 2003) which is a very well-known component of basement membranes (Karsdal, 2019). Endostatin is not expressed in neuroectodermal cells during development,(Miosge et al., 2003), however, adult neurons containing endostatin have been found in physiological conditions in human cortex (Deininger et al., 2002). Likewise, increased neuronal deposition of endostatin is found during Alzheimer's disease (Deininger et al., 2002) and cerebral ischemia (Hou et al., 2010). To date, no studies about intraneuronal endostatin in the retina have been reported.

Proliferative diabetic retinopathy is still a leading cause of visual impairment in the working-age population in developed countries (Nawaz et al., 2019). It is characterized by proliferation of fibrovascular tissue formed by the extension of retinal angiogenesis into the vitreous cavity, which ultimately leads to vitreous traction and retinal detachment (Boulton et al., 1988). Prevailing evidence suggests that changes in the relative balance between inducers and inhibitors of angiogenesis may activate the angiogenic switch in the diabetic retina (Simo et al., 2006). The inhibitor of angiogenesis endostatin has been involved in the regulation of neovascularization during diabetic retinopathy. The

concentration of endostatin in the vitreous fluid of patients with diabetic retinopathy significantly correlates with the severity of the disease. It has been shown that eyes with low levels of endostatin and high levels of VEGF in the vitreous have a significantly greater risk of progression to the proliferative phase of diabetic retinopathy (Noma et al., 2002; Funatsu et al., 2003;) Furthermore, it has been observed that endostatin in age-related macular degeneration is highly decreased in angiogenic areas of the choroid (Bhutto et al., 2004).

In this study, our results revealed for the first time the presence of intracellular endostatin in neurons of mouse and human retinas. Endostatin distribution was homogeneous throughout the neuroretina except for the optic disc where endostatin was undetectable. Diabetic mice showed a reduction of endostatin in their neuroretinas that was associated with the appearance of intravitreal vessels protruding from the optic disc. Intravitreal vessels phenotype showed similarities to the human diabetic papillovitreal neovessels, suggesting that neovascularization may occur at the optic disc in diabetic mice. However, it cannot be ruled out that the intravitreal vessels in db/db mice may represent persistent hyaloid vessels.

2. MATERIALS AND METHODS

2.1. Human Eyes

Human eyes were obtained from voluntary donations to the Faculty of Medicine of the UAB, following the Catalan law (Decret 297/1997) about human samples for research purposes. The procedure was approved by the Ethics Committee in Animal and Human Experimentation of the UAB and carried out in accordance with The Code of Ethics of the World Medical Association (Declaration of Helsinki) for experiments involving humans. Two eyes from two different donors were used in this study. Only biological data (sex, age, brief clinical history, and cause of death) were provided. None of them suffered from diabetes mellitus. Eyes were fixed in a solution of paraformaldehyde 4% with picric acid in 0.01 M PBS for 24 hours. After several washes in PBS, the eyes were partially dehydrated, and maintained in a solution of 70% alcohol at 4ºC. For immunohistochemical analysis, 3 µm paraffin retinal sections were used.

2.2. Mice

A total of 14 male diabetic db/db (BKS.Cg-Dock7^{m} +/+ Lepr^{db}/J) and 14 non-diabetic db/+ (BKS.Cg-Dock7^{m} + Lepr^{db}/+) control mice aged 8 and 12 weeks were used in this study. Mice were maintained under controlled conditions (20ºC temperature, 60% humidity and 12 hours light/dark cycles) and provided with free access to water and food (2018S TEKLAD Global, Harlan Teklad, Madison, WI, USA).

All mice were euthanized with an overdose of isoflurane inhalation followed by cervical dislocation. Animal care and experimental procedures were performed according to the ARVO Statement for the Use of Animals in Ophthalmic and Vision Research and Animal care ARRIVE guidelines and were approved by the Ethics Committee in Animal and Human Experimentation of the Universitat Autònoma de Barcelona (UAB) (FUE-2018-00717286).

2.3. Glycemia measurement

Blood was collected from the tail vein every week to monitor glycemia using a glucometer (Bayer, Leverkusen, Germany). Mice were analyzed in non-fasted conditions and were considered diabetic when glycemia exceeded 250 mg/dl in two consecutive measurements. The last measurement was performed before euthanasia. db/db mice develop obesity and hyperglycemia at 4-8 weeks of age, becoming a widely accepted model of diabetes type II (Robinson et al., 2012). In this regard, significant statistical differences were found in 8-week-old mice body weight (25.533 ± 0.383 g in db/+ vs. 36.067 ± 1.144 g in db/db; $p<0.0001$; n=6) and glycemia (150.167 ± 9.026 mg/dl in db/+ vs. 436.167 ± 14.597 mg/dl in db/db; $p<0.0001$; n=6) and also in 12-week-old mice body weight (25.65 ± 0.6462 g in db/+ vs. 43.73 ± 0.5474 g in db/db; $p<0.0001$; n=8) and glycemia (138.5 ± 3.674 mg/dl in db/+ vs. 563.0 ± 19.80 mg/dl in db/db; $p<0.0001$; n=8). These data confirmed that db/db mice used during this study were diabetic.

2.4. Immunohistochemistry

Human and mouse eyes embedded in paraffin were sectioned (3 µm) along the eye axis, deparaffinized, and rehydrated. For antigen retrieval, a solution of citrate was used to unmask the epitopes of the retinal sections. After several washes in phosphate buffered saline (PBS), retinal sections were incubated overnight at 4ºC with the following primary antibodies: rabbit anti-endostatin (Invitrogen, Carlsbad, CA, USA, PA1-601) at 1:100 dilution, obtained by immunizing a rabbit with two peptides corresponding to amino acids 129-142 from mouse and human endostatin; goat anti-mouse collagen IV (Merck Millipore, Billerica, MA, USA) at 1:20 dilution; mouse anti-mouse PKCα (Sigma-Aldrich,

St Louis, MO, USA) at 1:100 dilution; goat anti-mouse cone arrestin (Santa Cruz Biotechnology, Heidelberg, Germany) at 1:100 dilution; rabbit anti-mouse GFAP (DAKO, Glostrup, Denmark) at 1:1000 dilution; rabbit anti-mouse MMP-2 (Abcam, Cambridge, UK) at 1:500 dilution; rabbit anti-mouse MMP-9 (Proteintech, Rosemont, IL, USA) at 1:100 dilution. All primary antibody solutions were diluted with donkey serum (Sigma-Aldrich) at 1:10 dilution as a blocking agent to prevent secondary antibody unspecific binding. After washing the sections in PBS, they were incubated 2 hours at room temperature with specific fluorochrome-conjugated secondary antibodies diluted at 1:100: donkey anti-goat Alexa 488 (Life Technology, Carlsbad, Ca, USA); goat anti-rabbit 488, rabbit anti-goat Alexa 568, and goat anti-rabbit 568 (Invitrogen). Hoechst (Sigma-Aldrich) diluted in PBS (1:100 dilution) was used for nuclear counterstaining. Slides were mounted in Fluoromount (Sigma-Aldrich) medium for further analysis using a laser scanning confocal microscope (TCS SP2 or TCS SP5; Leica Microsystems GmbH, Heidelberg, Germany). Immunohistochemistry negative control was done by omission of the primary antibody in a sequential tissue section. To verify anti-endostatin antibody specificity, blocking peptide assay, Fc receptor (FcR) blocking, and isotype control assay were performed on eye paraffined sections. For blocking peptide assay, the neutralization of the primary anti-endostatin antibody was done in a previous incubation step of 1 hour before immunohistochemistry by adding 10-times excess of recombinant mouse endostatin (R&D Systems, MN, Minneapolis), in contrast to the control incubated with the anti-endostatin antibody alone. For FcR blocking, paraffin sections were incubated with Mouse Seroblock FcR (Bio-Rad Laboratories, Hercules, CA, USA) at 1:100 dilution during one hour before the start of the immunohistochemistry process in order to prevent non-specific binding of the Fc fragment from the Endostatin's IgG to the mouse Fc receptors FcRγIII and FcR&gamma:II. For isotype control assay, we used an antibody matching the host and IgG isotype of anti-endostatin antibody that targets an antigen absent in the retina. Anti-endostatin antibody's host is rabbit, which has only one subclass of IgG isotype (Weber et al., 2017). Thus, we used a rabbit antibody against collagen I (abcam), which is highly expressed in cornea and absent in the retina (Ruberte et al., 2017). To assess retinal morphology and location of intravitreal vessels, eye paraffin sections were stained with Hematoxylin/Eosin and were observed with a light microscope (Nikon Eclipse E800).

2.5. Western blot analysis

For protein extraction, mouse eyes were enucleated, and each retina was immediately dissected in PBS and homogenized in RIPA lysis buffer (25 mM Tris base, pH 8.2, 150 mM NaCl, 0.5% NP-40, 0.1% SDS, 0.5% sodium deoxycholate), containing protease

inhibitor cocktail tablets (Complete Mini, Roche, Basel, Switzerland). After vortex, retinas were centrifuged at 8000 g for 10 min. BCA assay reagent (Sigma-Aldrich) was used for each sample to determine total protein concentration.

For immunoblotting, 50 mg of protein of each sample were individually resuspended in 50% sample loading buffer (140 mM Tris base, pH 6.7, 6.8% SDS, 33% glycerol, 0.004% bromophenol) and 5% β-mercaptoethanol (Sigma-Aldrich) and heated at 95°C for 5 minutes. Afterwards, 12 µl of each sample were loaded in a 12% pre-cast SDS-PAGE gel (Bio-Rad) for electrophoresis followed by protein transfer to a PVFD membrane (Merck Millipore). PVDF membranes were blocked with 2% BSA in TBSTfor 1 hour at room temperature and incubated with rabbit anti-mouse endostatin antibody (Invitrogen) at 1:100 dilution overnight at 4ºC. After washing in TBST, the membrane was incubated with secondary antibody horseradish peroxidase-conjugated goat anti-rabbit (Bionova Scientific, Fremont, CA, USA) at 1:5000 dilution for 45 minutes at room temperature. Both primary and secondary antibodies were also diluted with 2% BSA in a 0.05% TBST.

Following antibodies incubation, the reagent Luminata Crescendo (Merck Millipore) was used for chemiluminescent detection. The bands revealed with Fluor-S Max imager (Bio-Rad) were analyzed with Image J software (National Institutes of Health, Bethesda, MD, USA) and rabbit anti-mouse α-tubulin (Abcam) at 1:500000 dilution was used as a loading control to normalize the levels of the protein of interest. Recombinant mouse endostatin was also run in the same gel to compare the molecular weight of retinal endostatin and the isolated peptide. A total of 3 repetitions were performed in each western blot.

2.6. Scanning laser ophthalmoscopy

Mice were anaesthetized using a ketamine (12 mg/kg) and xylazine (100 mg/kg) cocktail diluted in physiological saline solution and injected intraperitoneally. Toe pinch was performed to assure a correct anesthetic status and respiratory function was monitored during the process. Once mice were anesthetized, eye drops of anesthetic collyrium and tropicamide (Alcon, Barcelona, Spain) were administered to induce mydriasis. To prevent the eye from drying and developing cataracts, Viscofresh (Allergan, Dublin, Ireland) was continuously applied on both eyes and custom-made mouse lenses were placed on the corneas to visualize retinal blood vessels, 10 µl of 5% sodium fluorescein (Sigma-Aldrich) were injected subcutaneously in each mouse and angiography was performed with HRA2 Imaging Instrument (Heidelberg Engineering, Heidelberg, Germany). Angiography was performed in every mouse retina in both eyes and all

vascular plexi were analyzed, paying especial attention to the vessels that protruded into the vitreous from the optic disc.

2.7. Vessel density quantification

Vascular density of the entire retina and the central area was quantified using Angiotool software (Zudaire et al., 2011) in both groups. The results were represented in % of vessels area.

2.8. Statistical analyses

Statistical analyses were performed using R Statistical Software (version 4.1.0; R Foundation for Statistical Computing, Vienna, Austria). Shapiro-Wilk test and F test were performed for the evaluation of data distribution and variance homogeneity, respectively. For normal distribution and homogenous variances, the parametric method unpaired t-test was used. For data not normally distributed the Wilcoxon test was performed. Data are expressed as mean ± SEM. Difference between groups was considered significant at P-value<0.05.

3. RESULTS

3.1. Endostatin was expressed in mouse and human retinal neurons

Cross-reactivity of anti-endostatin antibodies with collagen XVIII, the endostatin precursor, is one of the challenges to immunolocalize cleaved active endostatin, since antibodies used to date in retinal studies also recognize uncleaved endostatin and mark almost exclusively blood basement membranes and the internal limiting membrane (Pehrsson et al., 2019). To try to solve this situation we used a polyclonal anti-endostatin antibody which previously had demonstrated its ability to detect endostatin intracellularly (Martín-Granado et al., 2017; Huaman et al., 2019). To confirm antibody specificity for cleaved endostatin, several assays were performed in retinal sections. First, a blocking peptide assay was used to neutralize the primary anti-endostatin antibody with recombinant mouse endostatin (Figure 1A). In addition to this, blocking Fc assay (Figure 1B) that specifically blocks mouse Fc receptors in the retina, and isotype control assay (Figure 1C) that guarantees non-specific binding of similar IgG isotypes, were performed. Furthermore, western blot analyses showed that bands of retinal endostatin and recombinant endostatin were comparable and around 20 kDa (Figure 2), the stablished molecular weight of cleaved endostatin (Marneros et al., 2004; Cristante et al., 2018). Lane 1 shows a different number of bands compared to lane 2 (Figure 2), probably due to the fact that lane 1 corresponds to native endostatin from the retinal tissue and lane 2

corresponds to recombinant endostatin. Recombinant endostatin is a purified peptide that might have not suffered the same post-translational modifications. In addition to this, mouse endostatin peptides can have deletions or extensions of few residues at the N or C-terminal (Yamaguchi et al., 1999) that could explain why native endostatin shows more bands and a slightly different weigh compared to the recombinant endostatin.

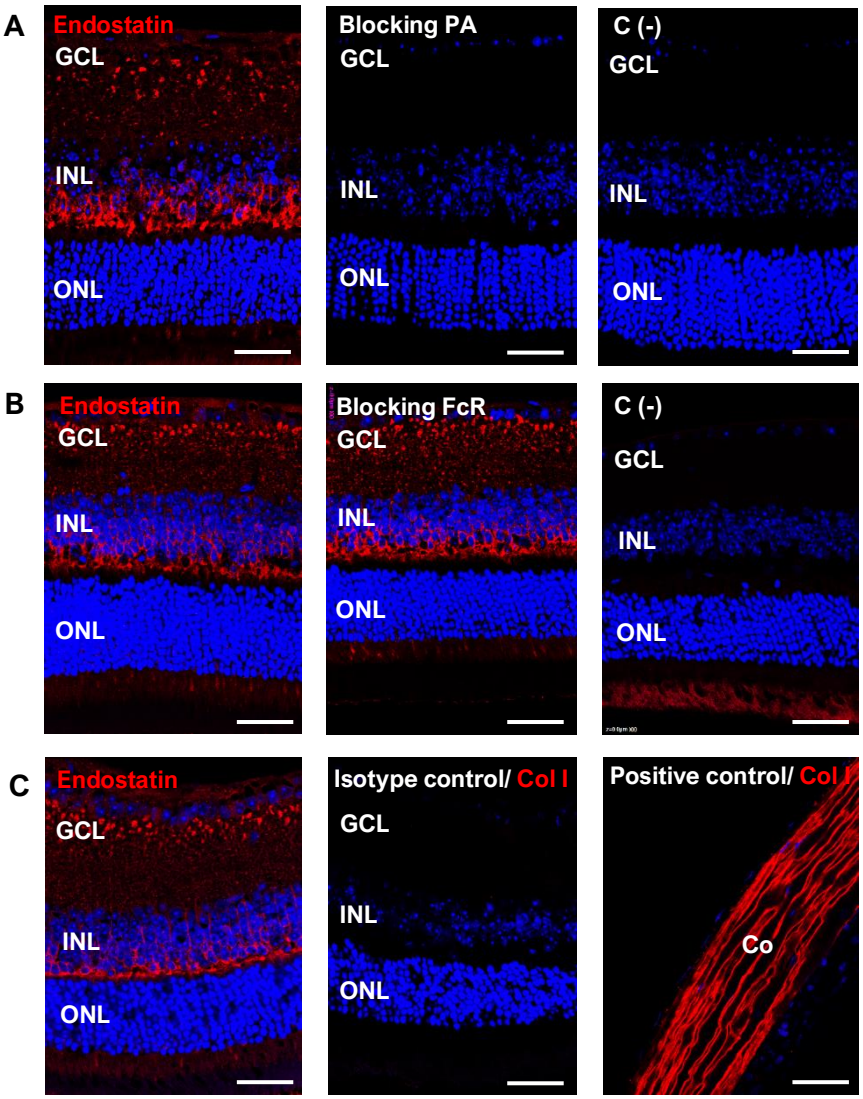

Figure 1. Endostatin staining and antibody specificity in mouse retina. **(A)** Immunofluorescence with a rabbit polyclonal anti-endostatin antibody in mice retina showed staining in the ganglion cell layer, outer plexiform layer, and in the outer segments of photoreceptors (left panel). Blocking peptide assay (Blocking PA) using recombinant mouse endostatin was performed to assess antibody specificity. Anti-endostatin antibody neutralization was complete and non-specific signal was observed in the retina (middle panel). Negative control was done by omission of the primary antibody (right panel). **(B)** FcR blocking assay confirmed the specificity of endostatin staining (left panel) when compared to retinas incubated with Mouse Seroblock FcR (middle panel). Negative control was done by omission of the primary antibody (right panel). **(C)** Isotype control assay using an anti-collagen I antibody from the same isotype and host as the anti-endostatin antibody was performed. Collagen I is absent from retina and very abundant in cornea. In comparison with the anti-endostatin antibody retinal signal (left panel), non-signal was observed in the retina when using anti-collagen I antibody (middle panel). Positive control for collagen I was performed in the cornea of the same eye in a consecutive section (right panel). Nuclei were counterstained with Hoechst. GCL: ganglion cell layer; INL: inner nuclear layer; ONL: outer nuclear layer; Co: cornea. Scale bars: 37.03 µm

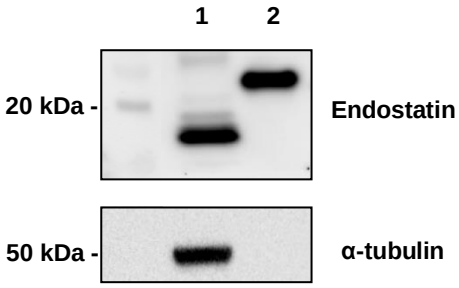

Figure 2. Western blot analysis of mouse retinal endostatin. Retinal endostatin shows a main band between 15 and 20 kD (lane 1), very close to the 21 kDa band from the recombinant endostatin (lane 2), confirming the antibody specificity for cleaved endostatin. α-tubulin was used as a loading control.

In mouse retinas, endostatin distribution was similar throughout the central and peripheral retina, but at the level of the optic disc endostatin was unobservable (Figure 3A). Endostatin signal was found inside retinal neurons, without marking neither the internal limiting membrane nor the blood vessel basement membranes (Figure 3B), which confirmed that the antibody was only detecting cleaved endostatin and not collagen XVIII.

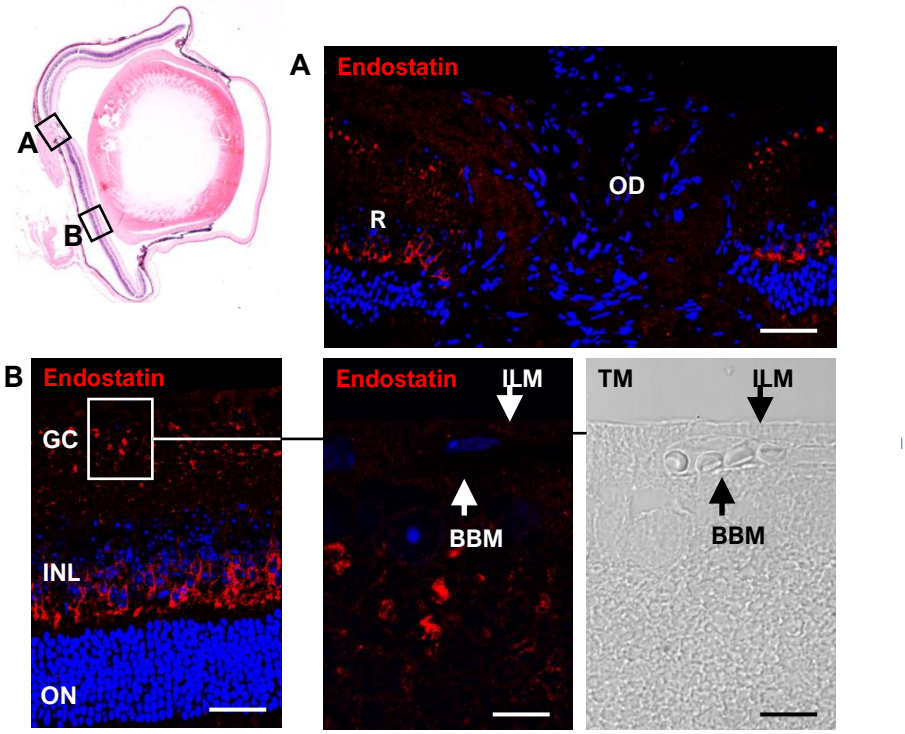

Figure 3. Endostatin in mouse neuroretina. **(A)** Immunostaining with anti-endostatin antibody revealed that endostatin is accumulated in the inner part of neuroretina, however, it was not observable at the optic disc **(B)** No endostatin signal was detected in blood vessel basement membranes or in the internal limiting membrane. Nuclei were counterstained with Hoechst. GCL: ganglion cell layer; INL: inner nuclear layer; ONL: outer nuclear layer; BBM: blood vessel basement membrane; ILM: internal limiting membrane. Scale bar: 43.48 µm (A); 33.33 µm (B).

Given that the distribution of the endostatin signal was compatible with the morphology of bipolar cells (Figure 4), dual immunostaining with anti-PKCα antibody, a specific marker of rod bipolar cells (Haverkamp et al., 2003), was performed. The result showed that endostatin was accumulated in bipolar cell axon terminals but not in the axons themselves (Figure 4A). Dendrites, including their terminals, and the perikaryon of bipolar cells also accumulated endostatin (Figure 4B). Although endostatin was mainly located at the internal neuroretina, sporadic photoreceptors also showed intracellular endostatin (Figure 5). To identify what type of photoreceptor accumulates endostatin, cone arrestin, a specific marker of cone photoreceptors (Zhu et al., 2002), was employed. Dual immunostaining with anti-cone arrestin antibody showed that endostatin was accumulated in the inner segments of cone photoreceptors. The cone synaptic terminals did not accumulate endostatin (Figure 5).

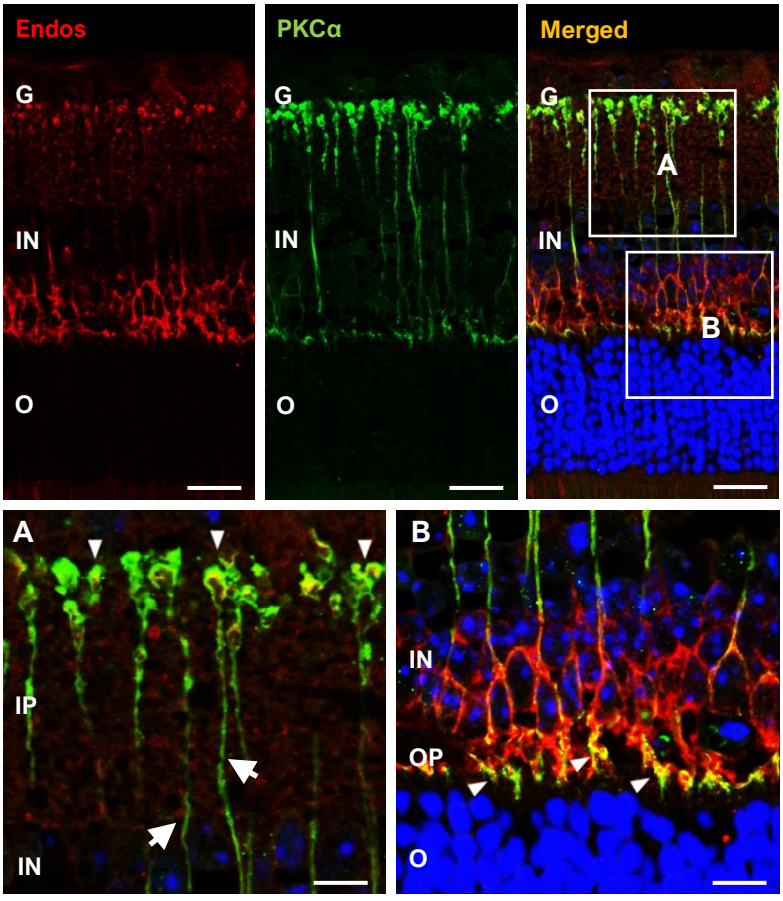

Figure 4. Endostatin was accumulated in bipolar cells of mouse retina. Double immunostaining with anti-PKCα antibody confirmed that endostatin was accumulated mainly in bipolar cells. Endostatin was found in their axon terminals (arrowheads), but not in their axons themselves (arrows) **(A)** and in the perikaryon and dendrites (arrowheads) **(B)**. Nuclei were counterstained with Hoechst. GCL: ganglion cell layer; IPL: inner plexiform layer; INL: inner nuclear layer; OPL: outer plexiform layer; ONL: outer nuclear layer. Scale bar: 25.42 μm; 9.41 μm (A); 10.17 μm (B).

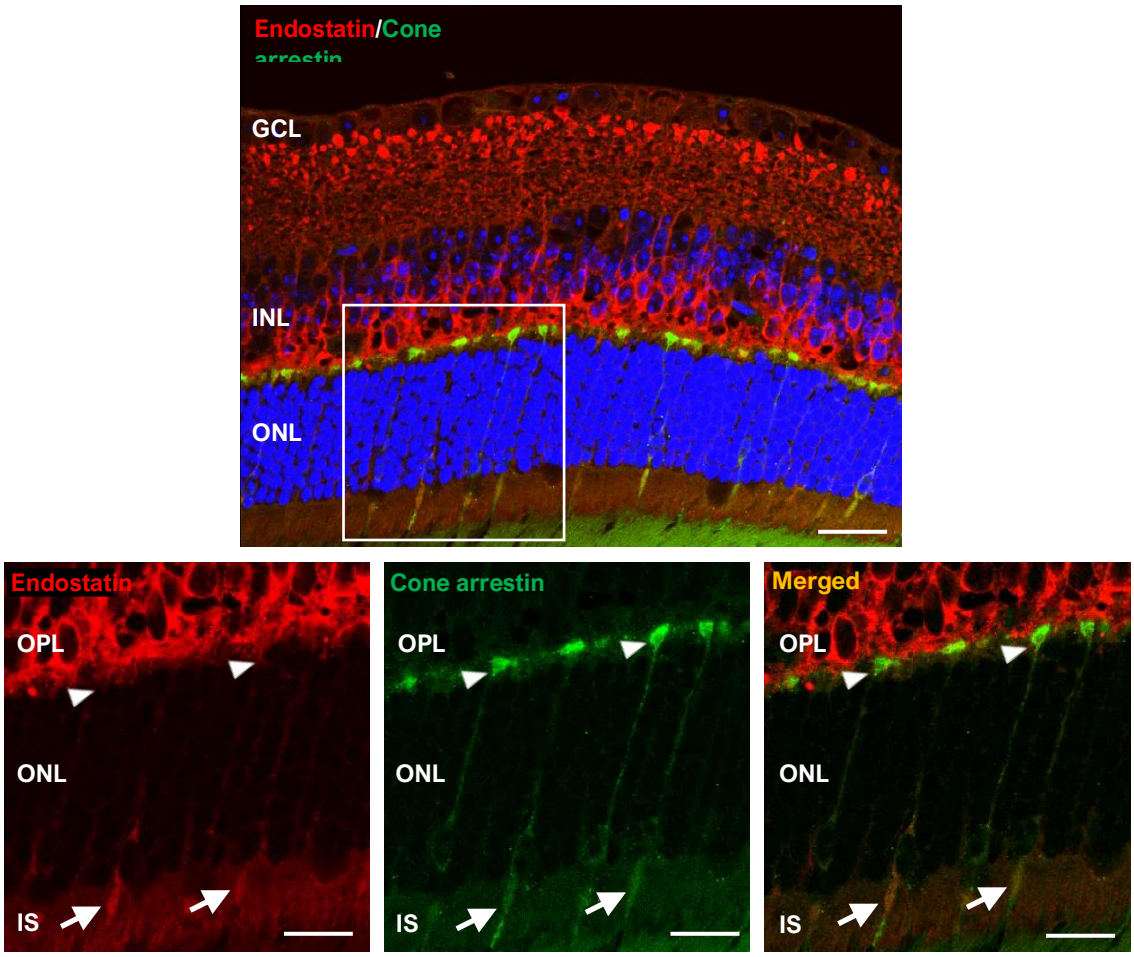

Figure 5. Endostatin was present in cone photoreceptors of mice retina. Double immunostaining with anti-cone arrestin antibody showed endostatin in the inner segments of cone photoreceptors (arrows). Cone synaptic terminals did not show endostatin expression (arrowheads). Nuclei were counterstained with Hoechst. GCL: ganglion cell layer; INL: inner nuclear layer; OPL: outer plexiform layer; ONL: outer nuclear layer; IS: inner segments of photoreceptors. Scale bar: 25.88 µm; 17.25 µm (inset).

Interestingly, the distribution pattern of endostatin in human retina was similar to the mouse retina. Endostatin was also undetectable in the human optic disc (Figure 6) and was also accumulated in bipolar cells and photoreceptors (Figure 7). However, some minor differences were found, namely a lower accumulation of endostatin in the bipolar cell axons terminals (Figure 7A), although bipolar perikaryal were stained with similar intensity (Figure 7B), and a higher number of photoreceptors with intracellular endostatin (Figure 7C). The morphology of these photoreceptors suggested that both cone and rods accumulated endostatin in the human retina (Figure 7C).

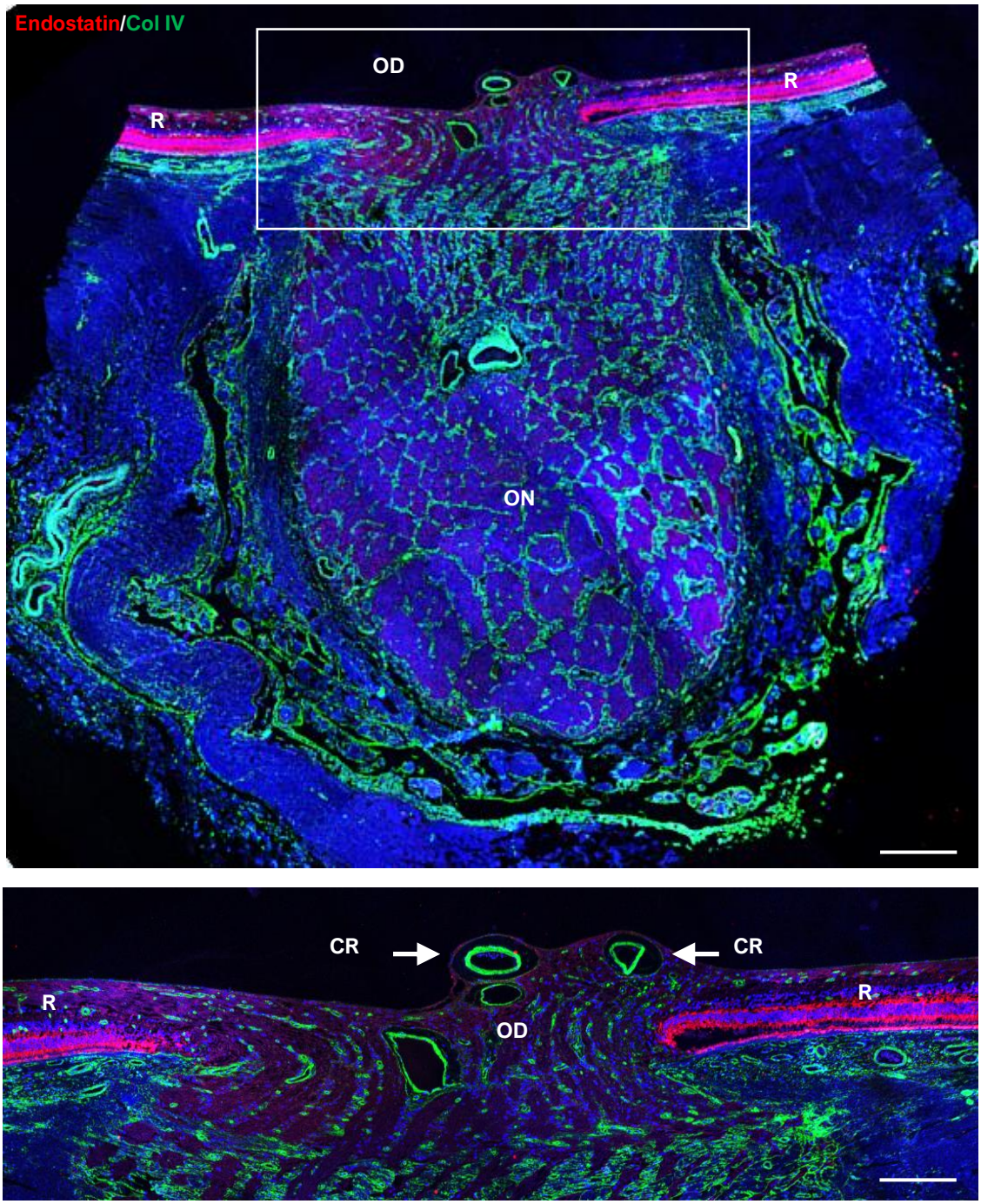

Figure 6. Human optic disc was practically devoid of endostatin. Double immunostaining with anti-endostatin and anti-collagen IV antibodies showed a markedly endostatin accumulation in the neuroretina, whereas as happens in mouse retina, endostatin was unobservable in the optic disc. The figure is a mosaic composite obtained from different captures at 63X in the laser scanning confocal microscope. OD: Optic disc; ON: Optic nerve; CR: Central retinal artery and vein; R: Retina. Scale bar: 474.92 µm; 226.15 µm (inset).

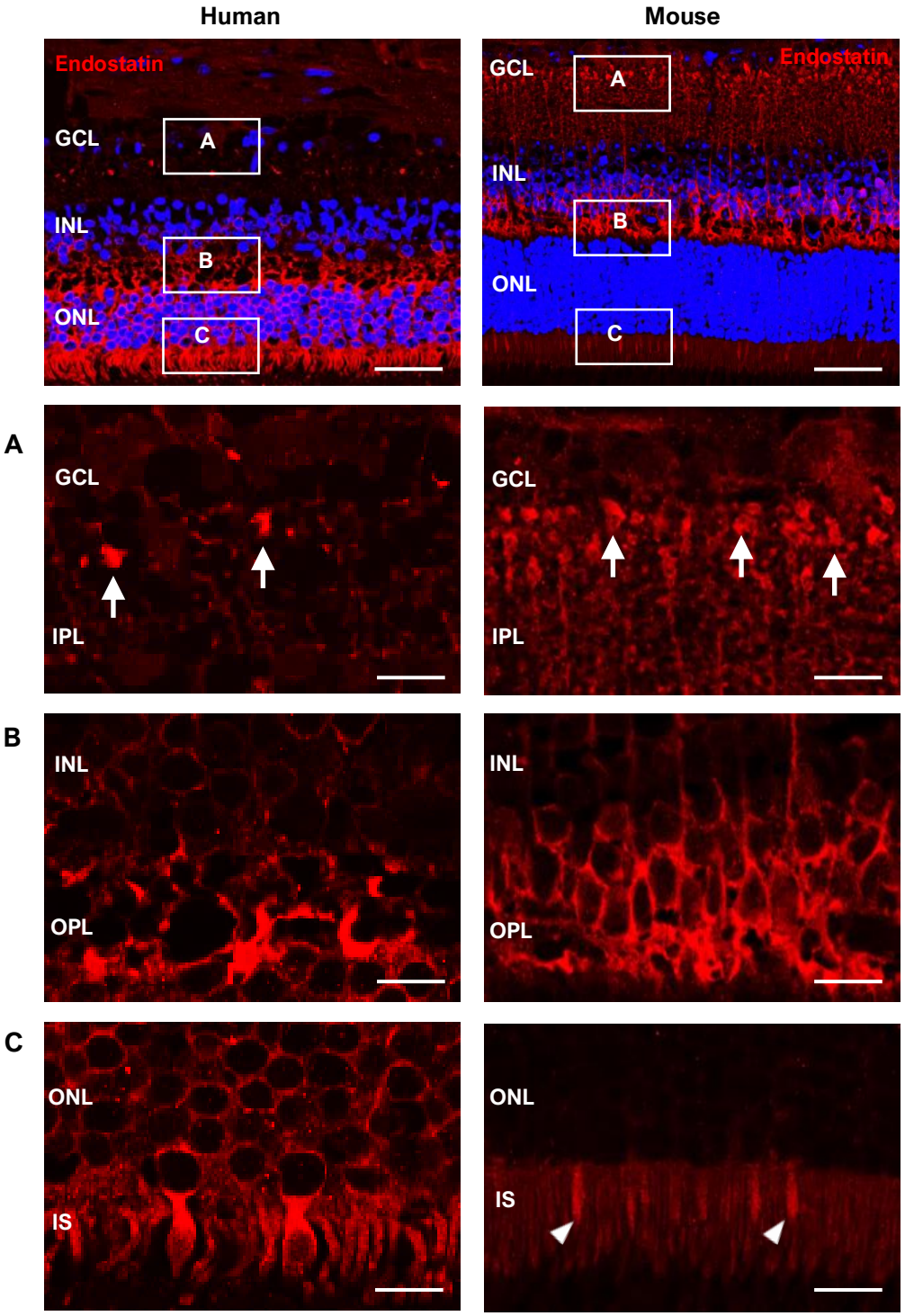

Figure 7. Comparison between human and mouse endostatin distribution in the neuroretina. Immunolabelling with anti-endostatin antibody in human and mouse retinas showed a similar, although with some differences, endostatin distribution in both species, mainly located at bipolar cells and photoreceptors. **(A)** Human bipolar terminal axons (arrows) showed lower expression of endostatin compared to mouse retina. **(B)** Bipolar cell perikaryal were stained with endostatin in both human and mice retina with a similar intensity**. (C)** In contrast with mice, where only scarce cones (arrowheads) showed endostatin accumulation in their inner segments, human retina showed a higher signal of endostatin at photoreceptors, suggesting that both cone and photoreceptors accumulated endostatin. The same anti-endostatin antibody was used on both human and mice retinal sections. GCL: ganglion cell layer; IPL: inner plexiform layer; INL, inner nuclear layer; OPL: outer plexiform layer; ONL: outer nuclear layer; IS: inner segments of photoreceptors. Scale bars: 38.3 µm; 10.64 µm (A, B, C).

3.2. Endostatin was decreased in db/db mouse retinas

Once established the presence of endostatin in mouse and human retinal neurons and given that eye concentrations of endostatin in patients with diabetic retinopathy significantly correlates with the severity of the disease (Funatsu et al., 2003), we next investigated the concentration of endostatin in the retina during experimental hyperglycemic conditions. Western blot analysis of db/db mice, a well stablished model of type 2 diabetes (Robinson et al., 2012; Bogdanov et al., 2014), showed a statistically significant decrease (0.5-fold change) of endostatin in the neuroretina of diabetic mice (1.275±0.126 AU in db/+ mice vs. 0.753±0.055 AU in db/db mice; p=0.019; n=3) (Figure 8A). In addition, in some db/db mice endostatin decrease was exacerbated in the ganglion cell layer (Figure 8B).

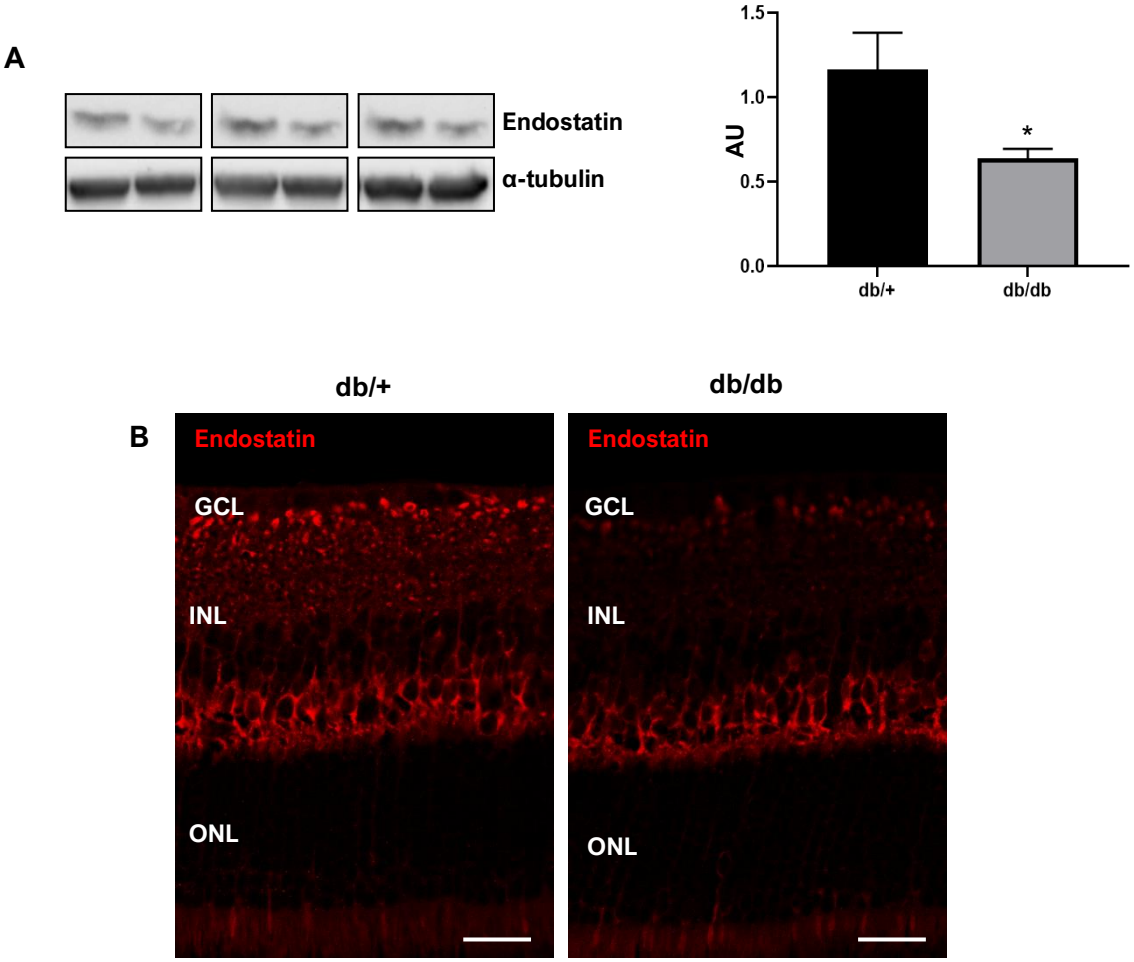

Figure 8. Endostatin was decreased in db/db mouse retinas. **(A)** Western blot analysis revealed that endostatin protein expression was 0.5-fold decreased in 12 weeks-old diabetic mouse retinas, especially in the ganglion cell layer. Statistical analysis showed significant differences in endostatin band intensity between db/+ and db/db mice (1.275 ± 0.126 AU in db/+ mice vs. 0.753 ± 0.055 AU in db/db mice; p = 0.019; n = 3). α-tubulin was used as a loading control. **(B)** Immunofluorescence representative image showing decreased endostatin expression in db/db retinas. Nuclei were counterstained with Hoechst. OD: Optic disc; CR: Central retinal vessel; R: Retina. Scale bar: 22.22 μm.

3.3. Optic disc intravitreal vascularization in db/db mouse retinas

Given that endostatin is an inhibitor of angiogenesis preventing endothelial cell proliferation, migration, and invasion (Kim et al., 2002), we next analyzed whether the decrease of endostatin in the retina of diabetic mice led to neovascularization. Retinal blood vessels were investigated using *in vivo* eye fundus fluorescein angiography (Figure 9) and the AngioTool software (Zudaire et al., 2011) was used to quantify vascular density. The results showed not significant differences in vascular density between 12-week-old db/db and db/+ mice, when the entire retinal vascular network was compared (34.82±2.32 % vessel area in db/+ retinas vs. 33.35±1.56 % vessel area in db/db retinas; p=0.652; n=5) (Figure 9A). This agrees with most of the data provided by the bibliography, which indicate that neovascularization is not a frequent finding in db/db mouse retina (Li et al., 2010; Bogdanov et al., 2014; Kim et al., 2014). To our knowledge, neovascularization in db/db mice retina has only been reported in a single study using long-standing 15-month-old mice (Cheung et al., 2005). However, when the vascular density was compared in the central part of the retina, a significant slight vascular density increase was observed in diabetic mice (52.47±1.12 % vessel area in db/+ retinas vs. 64.87±13.39 % vessel area in db/db retinas; p=0.046; n=5) (Figure 9B).

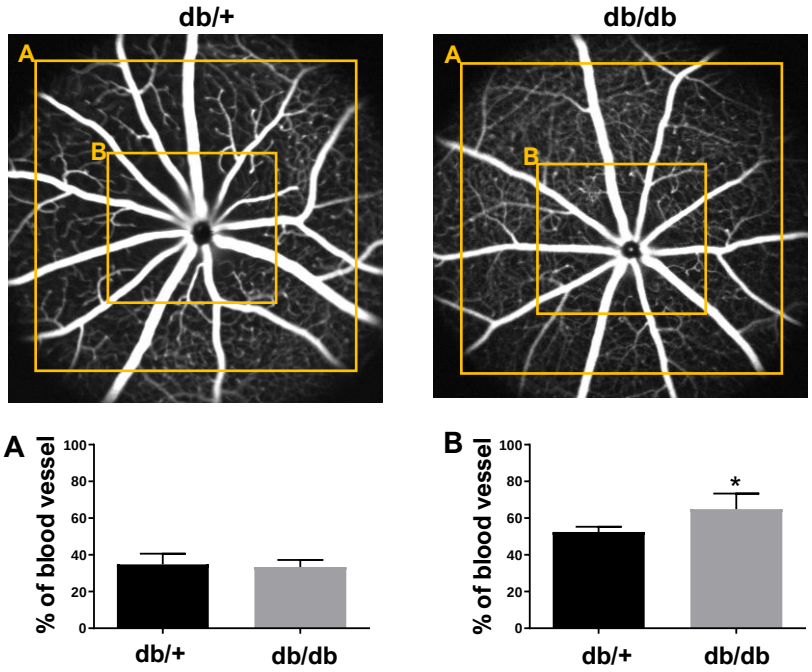

Figure 9. Vascular density in central retina was increased in db/db mice. *In vivo* fundus fluorescein angiography was performed to assess retinal vascularization. **(A)** No significant differences in vascular density were found when comparing the entire retinal vascular network (34.82 ± 2.32% vessel area in db/+ retinas vs. 33.35 ± 1.56% vessel area in db/db retinas; p = 0.652; n = 5) in 12 weeks-old mice**. (B)** However, a statistically significant increase in vascular density was found in the central part of the retina of db/db mice (52.47 ± 1.12% vessel area in db/+ retinas vs. 64.87 ± 13.39% vessel area in db/db retinas; p = 0.046; n = 5) in 12 weeks-old mice.

To confirm whether this increased vascular density in the central part of the retina was compatible with optic disc vessels protruding into the vitreous, we acquired three different focal planes of the eye fundus using SLO (Figure 10 A, B, C). Using this approach, optic disc vessels protruding the vitreous can be easily identified (Figure 10). The results obtained showed that 50% of the db/db mice (n=8) presented vessels that originated from the optic disc and invaded the vitreous. Furthermore, in comparison with db/+ mice, where only one animal presented a single small vessel contacting the vitreous, in most db/db mice several vessels, usually three, invaded the vitreous (Figure 10). This result correlated with histological analysis in paraffin eyes sections studied at the level of the optic disc, where the number of recognizable intravitreal blood vessels identified by Hematoxylin/Eosin staining was significantly increased in db/db mice (1.143± 0.261 number of intravitreal vessels in db/+ mice (n=7) vs. 2.200±0.374 number of intravitreal vessel in db/db mice (n=5); p=0.037) (Figure 11).

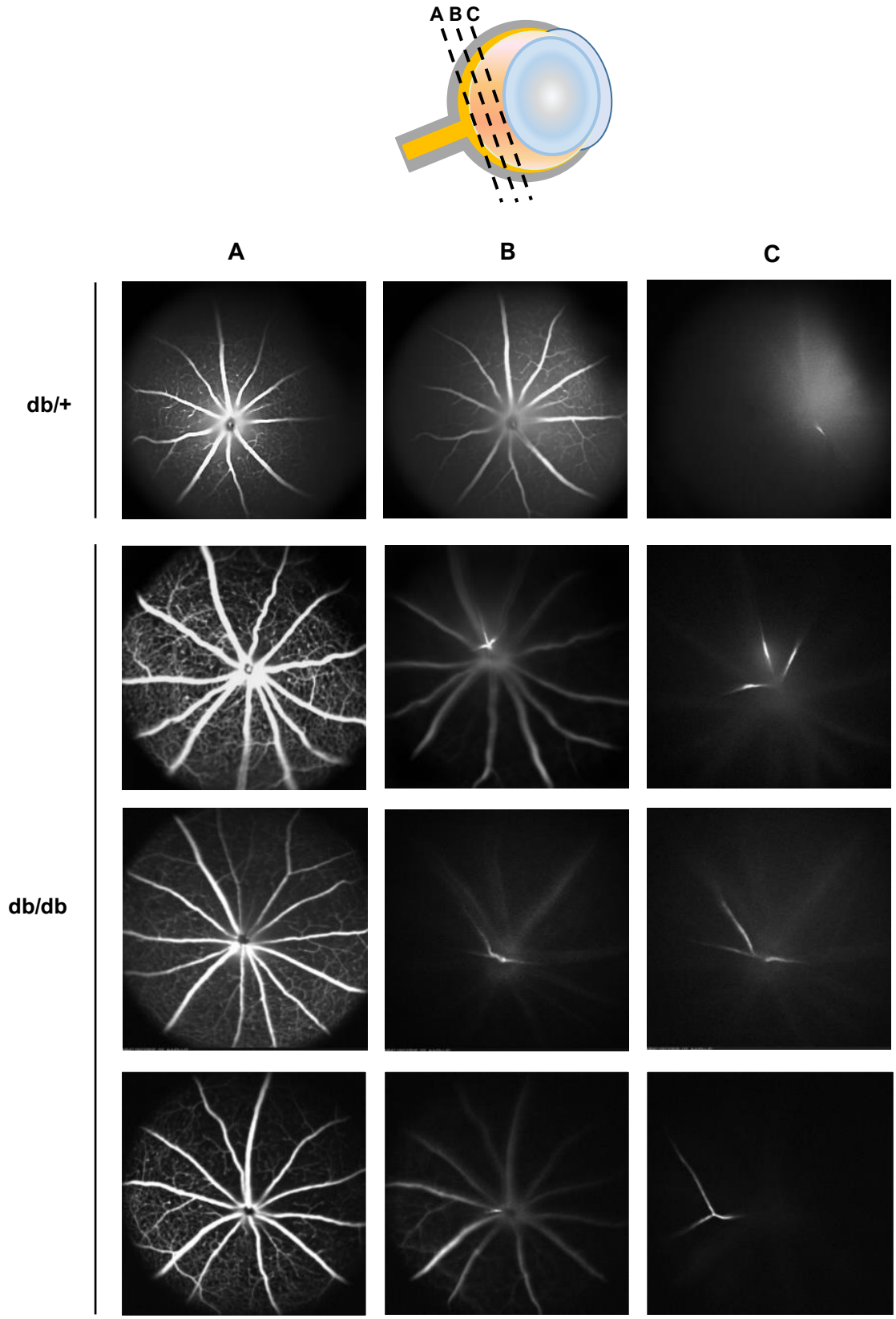

Figure 10. Intravitreal vessel angiography in db/db mouse retinas. After fluorescein injection, three consecutives focal planes of the eye fundus (A, B, and C) were performed to assess intravitreal vessels. 50% of db/db mice presented intravitreal vessels while only one db/+ presented a single tiny intravitreal vessel (n = 8). In the most part of db/db mice several vessels, usually three, invaded the vitreous from the optic disc.

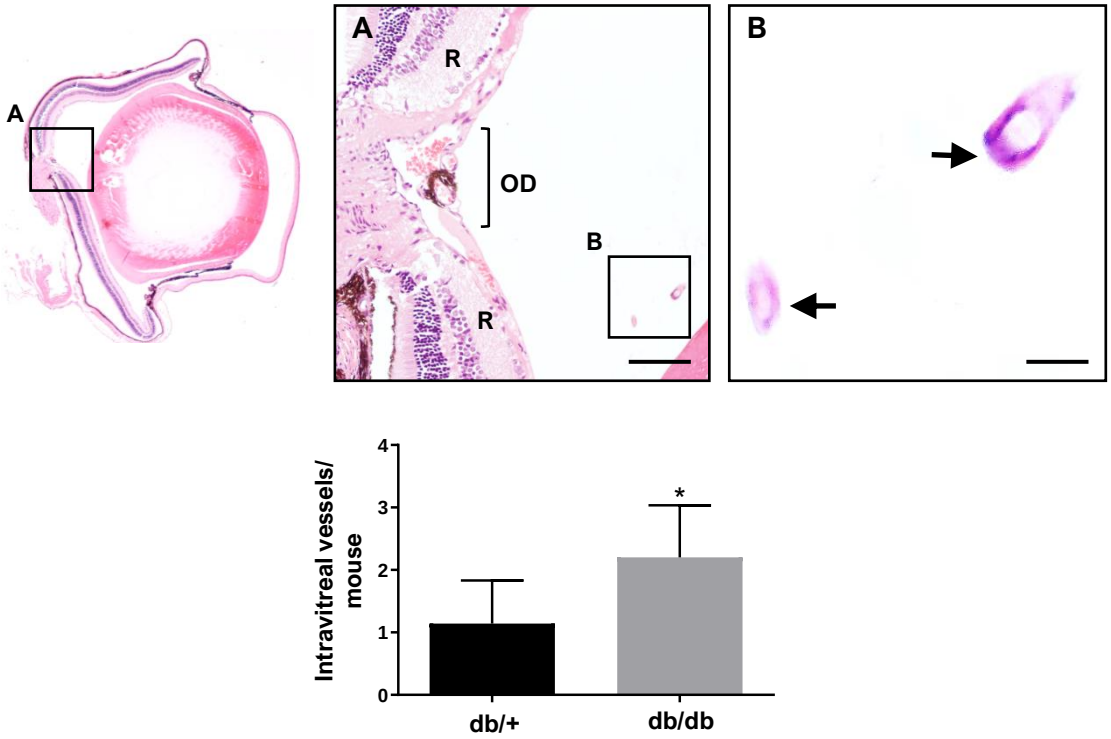

Figure 11. Intravitreal vessel histology in db/db mouse retinas. Paraffin sections of the retina sectioned along the eye axis were counterstained with Hematoxylin/Eosin. A significant increase of intravitreal vessels (arrows) in db/db mice was observed (1.143 ± 0.261 number of intravitreal vessels in db/+ mice (n = 7) vs. 2.200 ± 0.374 number of intravitreal vessel in db/db mice (n = 5); $p = 0.037$). OD: Optic disc; R: Retina. Scale bar: 76.45 µm (A); 12.23 µm (B).

3.4. Optic disc intravitreal vessel phenotype in db/db mice

Once established that 50% of 12-week-old db/db mice studied had vessels that from the optic disc penetrated the vitreous, we tried to answer the question about the nature of these vessels. Basically, two possibilities existed: (a) they were persistent hyaloid vessels or (b) they were neovessels triggered by the pro-angiogenic environment induced by the decrease of endostatin in the db/db mouse retina.

During development, the intraocular structures are nourished by the hyaloid vascular system (Saint-Geniez and D'Amore, 2004). This vascular system in mouse starts to form at embryonic day 10.5 and becomes fully developed by embryonic day 13.5 (Smith, 2002). It is widely accepted that the hyaloid vascular system in mice initiates its regression after birth and totally disappears around postnatal days 14-24 (Ito and Yoshioka, 1999; Fukai et al., 2002; Ohlmann et al., 2004; Ritter et al., 2005). In a previous study from our group, 15% of 25-week-old wild type C57BL/6J mice showed functional persistent hyaloid vessels (McLenachan et al., 2015), which matches with the presence

of a small intravitreal vessel found in one db/+ mouse (representing the 16% of the db/+ analyzed). However, 50% of db/db retinas presented intravitreal vessels, which largely exceeded the normal percentage of expected persistent hyaloid vessels in a non-diabetic mouse. In this regard, mice lacking collagen XVIII/endostatin showed ocular abnormalities including a delay in normal postnatal regression of hyaloid vessels (Fukai et al., 2002). Similarly, hyaloid vessels also persisted in collagen XVIII human mutations (Knobloch syndrome) (Sertié et al., 2000).

Although these arguments could suggest that intravitreal vessels found in db/db mouse retinas were persistent hyaloid vessels, delayed regression of hyaloid vessels in collagen XVIIII/endostatin null mice leads to abnormal disorganized vascularization of the entire retina (Fukai et al., 2002), situation that we never found in db/db mouse retinas (Figure 8). Furthermore, the morphological aspect of intravitreal vessels in db/db mice was similar to human papillovitreal neovessels during diabetic retinopathy (L'Esperance, 1998). Thus, to discriminate whether intravitreal vessels found in db/db mice were persistent hyaloid vessels or neovessels, we analyzed them by immunofluorescence in 8-week-old db/db mice. Intravitreal db/db vessels showed an incomplete lining of GFAP positive signal (Figure 12), what would indicate that db/db intravitreal vessels were partially surrounded by neuroglial cells. Similarly, it is well stated that preretinal neovessels expressed GFAP in their walls during proliferative diabetic human retinopathy (Smith et al., 1999). In contrast, published data about the presence of neuroglia surrounding persistent hyaloid vessels is contradictory. In Nuc1 spontaneous rat and in humans with persistent fetal vasculature it has been described that astrocyte sheath the persistent hyaloid artery (Zhang et al., 2005). This abnormal association of astrocytes with the hyaloid artery may impede the normal macrophage-mediated remodeling and regression of the hyaloid system (Zhang et al., 2011). However, in collagen XVIII/endostatin null mice persistent hyaloid vessels are devoid of neuroglial coverage (Hurskainen et al., 2005).

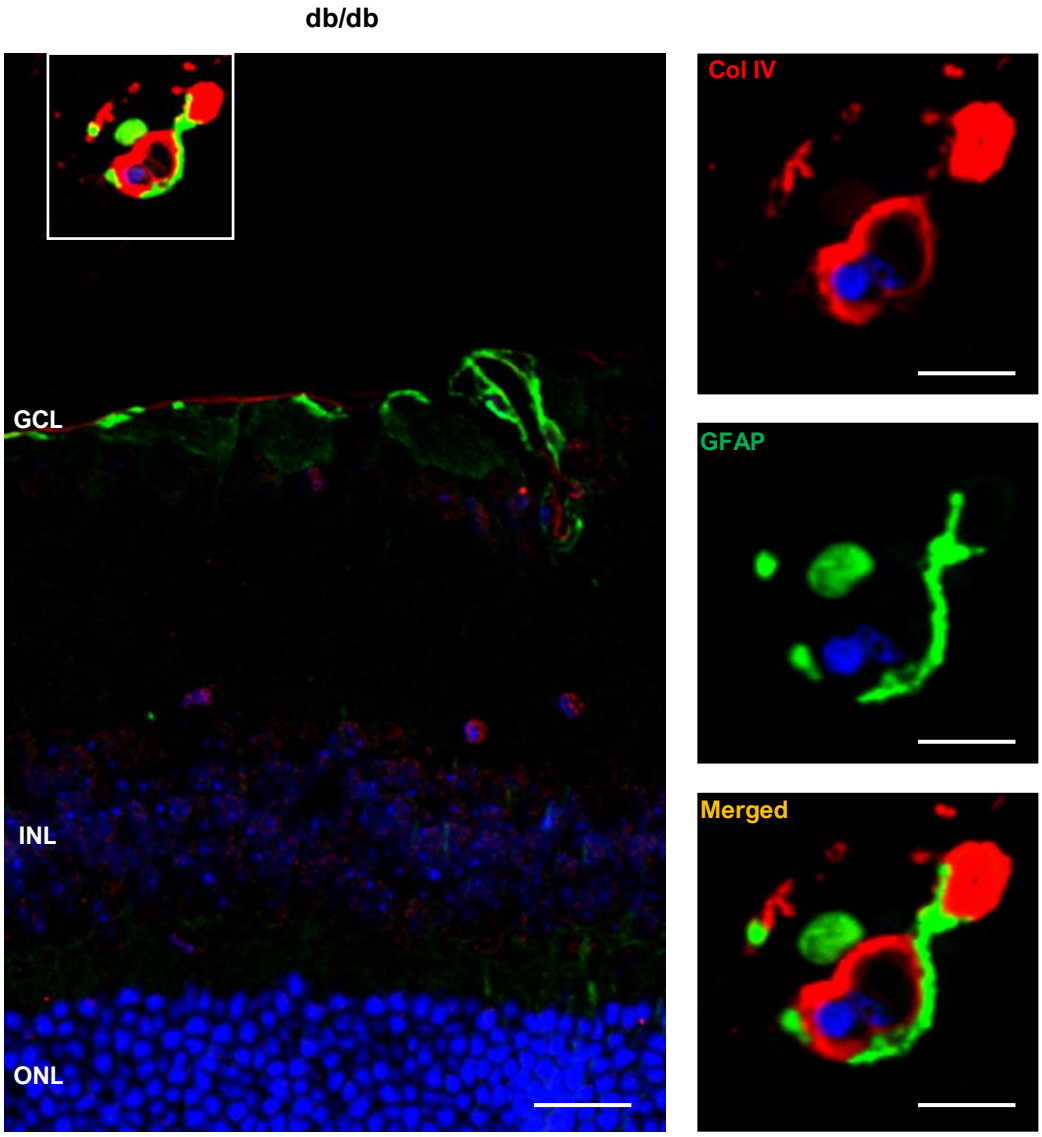

Figure 12. GFAP expression surrounding intravitreal vessels in db/db retinas. Double immunofluorescence using collagen IV and GFAP showed that intravitreal vessels in 8 weeks db/db mice were covered partially by neuroglia. Nuclei were counterstained with Hoechst. GCL: ganglion cell layer; INL: inner nuclear layer; ONL: outer nuclear layer. Scale bar: 23.82 µm; 12.54 µm (inset).

Intravitreal db/db vessels showed a thickening of their basement membrane due to increased collagen IV deposition (Figure 13A), which is the main component of the retinal vessel basement membrane (Inoue, 1989), compared to the intraretinal vessels (Figure 13B). Basement membrane thickening and increased collagen IV deposition are hallmarks of diabetic retinopathy (Roy et al., 2010). However, this is not a differential clue used to distinguish between persistent hyaloid vessels and intravitreal neovessels, because degenerating hyaloid vessels (Kishimoto et al., 2018) and persistent hyaloid vessels (Hurskainen et al., 2005) present also increased collagen IV deposition in their thicker basement membranes.

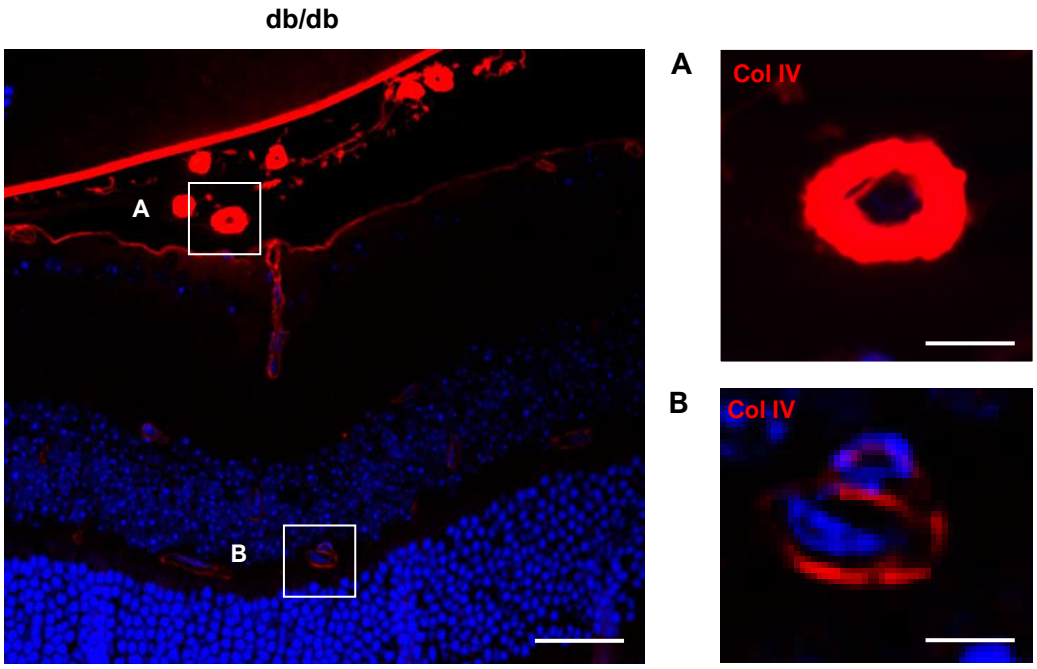

Figure 13. Thickening of intravitreal vessel basement membrane in db/db mice. Immunodetection of collagen IV in 8 weeks-old db/db mice retinas showed a thickening in the basement membrane of intravitreal vessels **(A)** compared to the intraretinal vessels **(B).** Nuclei were counterstained with Hoechst. GCL: ganglion cell layer; INL: inner nuclear layer; ONL: outer nuclear layer. Scale bar: 35.74 µm; 8.69 µm (A); 7,35 µm (B).

Degradation of extracellular matrix components is thought to be essential for the development of neovessels in proliferative diabetic retinopathy. Several species of MMPs are capable of degrading various extracellular matrix molecules and have been detected in the fibrovascular tissues in eyes with diabetic retinopathy (Roy et al., 2010). Specifically, MMP-2 and -9 have been immunohistochemically detected in the wall of intravitreal human neovessels (Noda et al., 2003). In the same way, intravitreal db/db vessels showed MMP-2 (Figure 14) and MMP-9 (Figure 15) co-localizing with collagen IV, a substrate of these MMPs (Somerville et al., 2003). Although finding both basement membrane thickening and degradation by MMPs in intravitreal db/db vessels may seem counterintuitive, it may be explained as a compensatory response to increased synthesis of basement membrane components during diabetic retinopathy (Roy et al., 2010).

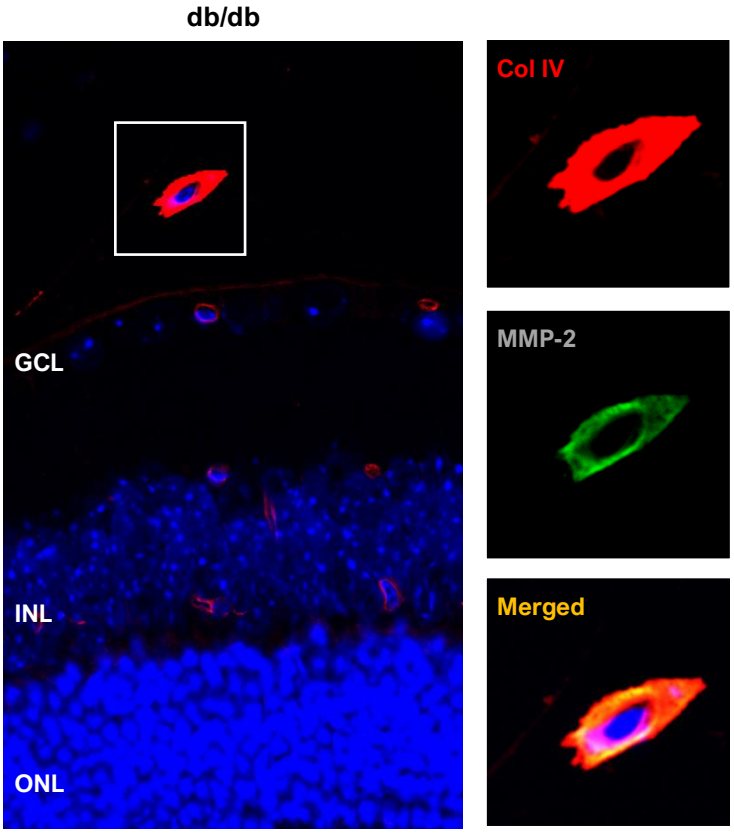

Figure 14. MMP-2 expression in the basement membrane of intravitreal vessels of db/db mice. Immunofluorescence analysis showed that collagen IV and MMP-2 co-localized in the basement membrane of 8-week-old db/db mice intravitreal vessels. Nuclei were counterstained with Hoechst. GCL: ganglion cell layer; INL: inner nuclear layer; ONL: outer nuclear layer. Scale bar: 18.49 µm; 9.24 µm (inset).

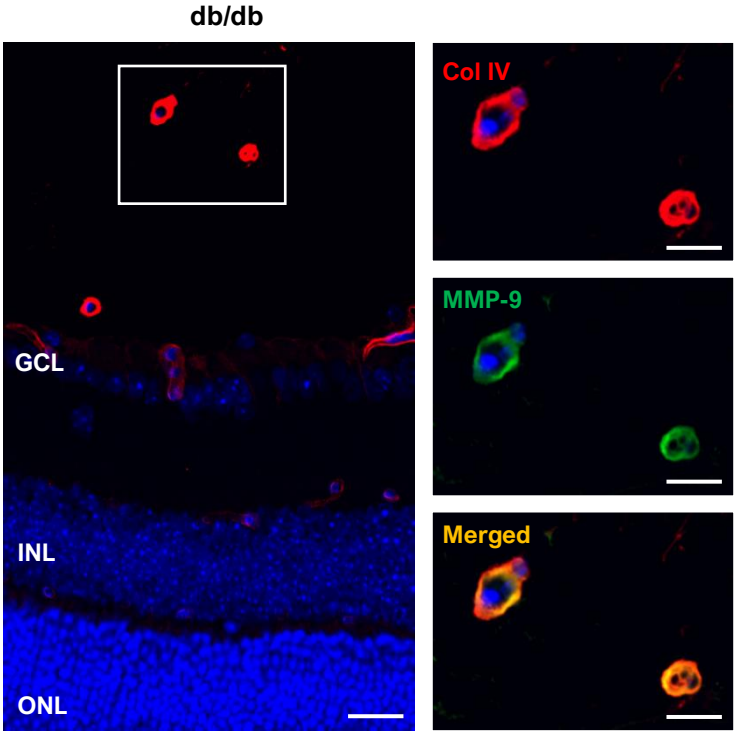

Figure 15. MMP-9 expression in the basement membrane of intravitreal vessels of db/db mice. Immunofluorescence analysis showed that collagen IV and MMP-9 co-localized in the basement membrane of 8-week-old db/db mice intravitreal vessels. Nuclei were counterstained with Hoechst. GCL: ganglion cell layer; INL: inner nuclear layer; ONL: outer nuclear layer. Scale bar: 17.82 µm 8.91 µm (inset).

4. DISCUSSION

Endostatin, the carboxyl-terminal fragment of type XVIII collagen, is a natural inhibitor of angiogenesis and its effect is being tested and proven effective in several clinical eye studies. RetinoStat, an equine infectious anemia virus-based lentiviral gene therapy vector that expresses endostatin and angiostatin, has been demonstrated to have activity against choroidal neovascularization and it was well tolerated and capable of persistent expression after subretinal delivery (Kachi et al., 2009). Furthermore, Tat PTD-Endostatin-RGD, a novel fusion protein, inhibited abnormal angiogenesis in retina via eye drops (Li et al., 2016). However, despite its therapeutic use, comprehensive research about the role of endostatin during diabetic retinopathy is scarce (Noma et al., 2002; Funatsu et al., 2003).

This study revealed for the first time the presence of intracellular endostatin in mouse and human retinal neurons. The observations made showed that endostatin was accumulated in the dendrites and axons of bipolar cells and in photoreceptors, mainly in their inner segments. The question about whether endostatin has intracellular or extracellular location is an important variable when considering likelihood of substrate/enzyme interaction. To date, endostatin in neuroretina has been only found extracellularly in basement membranes (Takahashi et al., 2003; Bhutto et al., 2004; Ramesh et al., 2004; Ohlmann et al., 2005; May et al., 2006; Määttä et al., 2007) where collagen XVIII may be cleaved by MMPs, elastases, and other extracellular proteases (Ferreras et al., 2000). However, similarly as what occurs in our study, healthy neurons containing intracellular endostatin have been found in the human cortex (Deininger et al., 2002). An explanation for this intracytoplasmic localization of endostatin could be cathepsin B, a lysosomal protease, which can generate endostatin from collagen XVIII (Im et al., 2005). Cathepsin B has been found to colocalize intracellularly with endostatin in neurons. Although intracellular localization of endostatin has been correlated with cell apoptosis (Hou et al., 2010), other studies in isolated retinal astrocytes suggested that intracellular endostatin is secreted extracellularly by exosomes (Hajrasouliha et al., 2013). Exosomes are nanometer-sized vesicles that cells can release in a controlled manner to mediate a plethora of cellular activities, including neovascularization (Klingeborn et al., 2017). Very little research on the role of exosomes in diabetic proliferative retinopathy has been done to date, although it is known that exosomes containing endostatin suppress choroidal neovascularization (Hajrasouliha et al., 2013). Investigating the role of endostatin containing exosomes from retinal neurons may identify antiangiogenic based mechanisms, which could help to develop novel therapeutic targets to control aberrant retinal neovascularization.

Diabetic db/db mice showed a reduction of endostatin in their retinas. Furthermore, in some db/db mice endostatin was especially decreased in the ganglion cell layer. However, this result is not conclusive and further studies will be necessary to clarify to what extend endostatin decrease is different among retinal layers in db/db mice. Endostatin reduction was associated with the appearance of vessels that originated from the optic disc and penetrated to the adjacent vitreous in the 50% of db/db mice. Whether these intravitreal vessels found in db/db mice were persistent hyaloid vessels at 84 postnatal day (12-week-old), when in fact they should have disappeared completely at 14-24 postnatal days (Ito and Yoshioka, 1999; Fukai et al., 2002; Ohlmann et al., 2005; Ritter et al., 2005), or neovessels induced by the pro-angiogenic environment developed by the decrease of endostatin, is a question that our study has not been fully able to answer.

The intravitreal vessel phenotype in db/db mice revealed features such as GFAP positive sheath of neuroglia and a thicker basement membrane, which are hallmarks of neovessels in diabetic retinopathy (Smith et al., 1999; Roy et al., 2010). However, they also appear in persistent hyaloid vessels (Hurskainen et al., 2005; Zhang et al., 2005). In contrast, the presence of MMP-2 and MMP-9 at the basement membrane in db/db intravitreal vessels, which is characteristic of human diabetic neovessels (Noda et al., 2003), has not been described, to our knowledge, in persistent hyaloid vessels. Since endostatin inhibits MMP-2 (Kim et al., 2000), its decrease in db/db mice retinas could explain the presence of metalloproteinase in the wall of intravitreal vessels. All together, these findings could suggest that neovascularization may occur at the optic disc in hyperglycemic db/db mice. However, it cannot be ruled out that these intravitreal vessels may also represent non-degenerated hyaloid vessels.

Finally, the human optic disc represents a preeminent site for the appearance of neovessels during proliferative diabetic retinopathy. Two situations occur during diabetic neovascularization: appearance of new blood vessels on the optic disc, which frequently lead to visual loss, and appearance of new blood vessels elsewhere on the retina, which do not pose such a serious threat to vision (Valsania et al., 1993). The almost null presence of antiangiogenic endostatin in the human optic disc, could explain why the optic disc is prone to neovascularization during human diabetic retinopathy.

5. CONCLUSIONS

For the first time, this study revealed the presence of endostatin in bipolar cells and photoreceptors, in both mouse and human retinas. Endostatin expression was inappreciable at the level of the optic disc, which could explain why this location is susceptible to neovascularization in diabetic retinopathy. Furthermore, endostatin was decreased in diabetic mouse retina. Diabetic db/db mice also presented significantly increased number of intravitreal vessels protruding from the optic disc. These intravitreal vessels showed a GFAP positive neuroglia sheath, basement membrane thickening, and expressed metalloproteinases in the vascular wall, suggesting that they could be neovessels similar to the papillovitreal neovessels observed during human diabetic retinopathy. However, we cannot ruled out the possibility that these vessels are persistent hyaloid vessels triggered by the decrease of retinal endostatin in diabetic mice.

Funding

This work was supported by the Instituto de Salud Carlos III, Ministerio de Ciencia e Innovación, Spain (grant number PI16/00719); the Fundação para a Ciência e a Tecnologia, Ministerio da Educação e Ciência, Portugal (grant numbers SFRH/BD/95330/2013 and SFRH/BPD/102573/2014); and Fond o Europeo de Desarrollo Regional (FEDER).

Acknowledgements

The authors thank Lorena Noya, Verónica Melgarejo, and Ángel Vázquez for their technical assistance.

GENERAL DISCUSSION

The role of key factors involved in the pathogenesis of DR is not totally understood (Warpeha and Chakravarthy, 2003; Tarr et al., 2013), therefore, the development of effective therapies is challenging. Moreover, current therapies of the most advanced stages of DR are invasive, short-lasting, and expensive.

One of the factors believed to exacerbate DR is iron excess (Chaudhary et al., 2018). Iron content in the retina is present in small amounts compared with other tissues, and difficult to quantify directly; thus, ferritin concentration has been classically accepted to assess iron content (Daru et al., 2017). In this regard, several studies use retinal ferritin expression to asses iron efflux in the retina, obtaining uncertain results (Hahn et al., 2004; Zhao et al., 2014; Chaudhary et al., 2018; Baumann et al., 2019; Shu et al., 2019)

In our experimental conditions, diabetic mice showed increased ferritin expression related to increased iron content in systemic tissues, such as the spleen. In the retina of these animals, ferritin was also overexpressed. However, iron content measured by the high sensitive method ICP-MS (Pamphlett et al., 2020), did not show any increase in diabetic mice retinas. This suggests that ferritin expression is not a reliable method to measure iron content in the retina and that, somehow, ferritin expression increases prior to retinal iron overload, probably as a protection mechanism. Recently, a report showed that mice intraperitoneally injected with iron dextran had minimal iron penetration in the retina, suggesting a protective role of BRB in front excessive iron entry (Shu et al., 2019). Supporting this hypothesis, our diabetic mice showed an intact BRB and the retinal iron remained at physiological concentrations despite systemic iron overload. As BRB breakdown is a hallmark of DR, we next broke the BRB experimentally in mice with systemic iron overload and demonstrated that retinal iron excess only occurs if the BRB is compromised.

Given that diabetic patients could develop systemic iron overload, control of the BRB status, which determines iron efflux into the retina, is decisive. Advanced stages of DR are characterized by BRB breakdown, thus, the use of iron chelators could be beneficial to prevent deleterious effects of iron in the retina. In this regard, iron chelators have been proved to prevent oxidative damage in the retina (Hadziahmetovic et al., 2012; Song et al., 2012; Shu and Dunaief, 2018).

The second chapter of this thesis is devoted to endostatin, which had only been detected as a part of collagen XVIII in the basement membranes and in the internal limiting membrane of the retina (Bhutto et al., 2004; May et al., 2006; Määttä et al., 2007). However, our aim was to detect active endostatin, which acts as an antiangiogenic factor when cleaved from collagen XVIII (O'Reilly et al., 1997). After extensive validation of a

selected anti-endostatin antibody, we demonstrated the presence of cleaved endostatin in bipolar cells and photoreceptors. Interestingly, endostatin was almost undetectable at the optic disc, where most of the neovascularization takes place during DR (Ishibazawa et al., 2016).

In our study, endostatin is decreased in the retina of diabetic mice. Endostatin acts blocking VEGF activity (Kim et al., 2002), thus, endostatin deficiency could cause a proangiogenic environment during DR. Supporting this hypothesis, intravitreal vessels found in diabetic mice showed an angiogenic phenotype. Nevertheless, it should be considered that in the retina, endostatin is also responsible for the regression of the hyaloid system, as proven in knockout mouse models of endostatin (Ohlmann et al., 2004; Hurskainen et al., 2005). Therefore, intravitreal vessels found in diabetic mice could also be persistent hyaloid vessels. Although the nature of intravitreal vessels remains unclear, treatment with endostatin could be beneficial to restore the angiogenic balance and prevent neovascularization during PDR, as proven in other retinopathies (Ai et al., 2020; Zhou and Xie, 2022).

CONCLUSIONS

The conclusions of this work are divided in two parts according to the main objectives:

CHAPTER I)

Main objective: to understand the mechanisms underlying retinal iron overload during DR.

Conclusion 1

Systemic iron is increased in early diabetic mice.

Conclusion 2

Ferritin expression is increased in the retina of early diabetic mice, despite no changes in retinal iron content could be observed.

Conclusion 3

Iron import proteins, such as transferrin, transferrin receptor, and Scara5, are not increased in diabetic mice retinas.

Conclusion 4

The ultrastructure and protein composition of retinal tight junctions, as well as the lack of retinal oedema and vascular leakage, indicate that BRB is intact in early diabetic mice.

Conclusion 5

During systemic iron overload, iron only increases in the retina after BRB breakdown.

CHAPTER II)

Main objective: to study the effect of endostatin expression in the development of DR.

Conclusion 6

Cleaved endostatin is expressed intracellularly in mouse and human bipolar cells and photoreceptors, and not in the basement membranes of the retina.

Conclusion 7

Endostatin expression is minor at the level of the optic disc.

Conclusion 8

Endostatin is decreased in diabetic mouse retinas inducing a proangiogenic environment.

Conclusion 9

Diabetic mouse retinas present intravitreal blood vessels at the level of the optic disc with features of neovessels, such basement membrane thickening, MMP-2 and -9 expression, and glial coverage.

Conclusion 10

Given the involvement of endostatin in the regression of hyaloid vessels, intravitreal vessels found in db/db could also be persistent hyaloid vessels.

FINAL CONCLUSIONS

Conclusion 11

As long as the BRB is intact, the diabetic retina is protected from iron overload. The increase of ferritin without retinal iron excess could be a mechanism to prevent iron toxicity after BRB breakdown.

Conclusion 12

Endostatin location and expression during diabetic retinopathy seems to be a key factor in the development of neovascularization during the proliferative phase of DR. The lack of endostatin at the level of the optic disc could explain why this location is susceptible to neovascularization during DR in humans.

BIBLIOGRAPHY

Abbaspour, N., Hurrell, R., Kelishadi, R., 2014. Review on iron and its importance for human health. J. Res. Med. Sci. 19, 164.

Abcouwer, S.F., 2013. Angiogenic Factors and Cytokines in Diabetic Retinopathy. J. Clin. Cell. Immunol. Suppl 1, 1. https://doi.org/10.4172/2155-9899

Abu El-Asrar, A.M., Mohammad, G., Nawaz, M.I., Siddiquei, M.M., Van Den Eynde, K., Mousa, A., De Hertogh, G., Opdenakker, G., 2013a. Relationship between vitreous levels of matrix metalloproteinases and vascular endothelial growth factor in proliferative diabetic retinopathy. PLoS One 8. https://doi.org/10.1371/JOURNAL.PONE.0085857

Abu El-Asrar, A.M., Nawaz, M.I., Kangave, D., Mairaj Siddiquei, M., Geboes, K., 2013b. Angiogenic and vasculogenic factors in the vitreous from patients with proliferative diabetic retinopathy. J. Diabetes Res. 2013. https://doi.org/10.1155/2013/539658

Adijanto, J., Du, J., Moffat, C., Seifert, E.L., Hurley, J.B., Philp, N.J., 2014. The retinal pigment epithelium utilizes fatty acids for ketogenesis. J. Biol. Chem. 289, 20570–20582. https://doi.org/10.1074/JBC.M114.565457

Ai, J., Ma, J., Chen, Z.Q., Sun, J.H., Yao, K., 2020. An Endostatin-lentivirus (ES-LV)-EPC gene therapy agent for suppression of neovascularization in oxygen-induced retinopathy rat model. BMC Mol. Cell Biol. 21, 1–14. https://doi.org/10.1186/S12860-020-00301-1/FIGURES/11

Aiello, L.P., Avery, R.L., Arrigg, P.G., Keyt, B.A., Jampel, H.D., Shah, S.T., Pasquale, L.R., Thieme, H., Iwamoto, M.A., Park, J.E., Nguyen, H. V., Aiello, L.M., Ferrara, N., King, G.L., 1994. Vascular Endothelial Growth Factor in Ocular Fluid of Patients with Diabetic Retinopathy and Other Retinal Disorders. N. Engl. J. Med. 331, 1480–1487. https://doi.org/10.1056/NEJM199412013312203

Aihara, M., Lindsey, J.D., Weinreb, R.N., 2003. Aqueous humor dynamics in mice. Invest. Ophthalmol. Vis. Sci. 44, 5168–5173. https://doi.org/10.1167/IOVS.03-0504

Aird, W.C., 2007. Phenotypic heterogeneity of the endothelium: I. Structure, function, and mechanisms. Circ. Res. 100, 158–173. https://doi.org/10.1161/01.RES.0000255691.76142.4A

Aisen, P., Enns, C., Wessling-Resnick, M., 2001. Chemistry and biology of eukaryotic iron metabolism. Int. J. Biochem. Cell Biol. 33, 940–959. https://doi.org/10.1016/S1357-2725(01)00063-2

Alberts B, Johnson A, Lewis J, et al., 2002. Electron transport chains and their proton pumps. Mol. Biol. cell 4th Ed. 1–10.

Ali Rahman, I.S., Li, C.R., Lai, C.M., Rakoczy, E.P., 2011. In vivo monitoring of VEGF-induced retinal damage in the Kimba mouse model of retinal neovascularization. Curr. Eye Res. 36, 654–662. https://doi.org/10.3109/02713683.2010.551172

Amano, S., Yamagishi, S.I., Inagaki, Y., Nakamura, K., Takeuchi, M., Inoue, H., Imaizumi, T., 2005. Pigment epithelium-derived factor inhibits oxidative stress-induced apoptosis and dysfunction of cultured retinal pericytes. Microvasc. Res. 69, 45–55. https://doi.org/10.1016/J.MVR.2004.11.001

Anderson, B., McIntosh, H.D., 1967. Retinal circulation. Annu. Rev. Med. https://doi.org/10.1146/annurev.me.18.020167.000311

Antonetti, D.A., Barber, A.J., Hollinger, L.A., Wolpert, E.B., Gardner, T.W., 1999. Vascular endothelial growth factor induces rapid phosphorylation of tight junction proteins occludin and zonula occluden 1. A potential mechanism for vascular permeability in diabetic retinopathy and tumors. J. Biol. Chem. 274, 23463–23467. https://doi.org/10.1074/JBC.274.33.23463

Antonetti, D.A., Barber, A.J., Khin, S., Lieth, E., Tarbell, J.M., Gardner, T.W., 1998. Vascular permeability in experimental diabetes is associated with reduced endothelial occludin content. Vascular endothelial growth factor decreases occludin in retinal endothelial cells.

Diabetes 47, 1953–1959. https://doi.org/10.2337/diabetes.47.12.1953

Argaw, A.T., Gurfein, B.T., Zhang, Y., Zameer, A., John, G.R., 2009. VEGF-mediated disruption of endothelial CLN-5 promotes blood-brain barrier breakdown. Proc. Natl. Acad. Sci. U. S. A. 106, 1977–1982. https://doi.org/10.1073/PNAS.0808698106

Arjunan, P., Gnanaprakasam, J.P., Ananth, S., Romej, M.A., Rajalakshmi, V.K., Prasad, P.D., Martin, P.M., Gurusamy, M., Thangaraju, M., Bhutia, Y.D., Ganapathy, V., 2016. Increased Retinal Expression of the Pro-Angiogenic Receptor GPR91 via BMP6 in a Mouse Model of Juvenile Hemochromatosis. Invest. Ophthalmol. Vis. Sci. 57, 1612–1619. https://doi.org/10.1167/IOVS.15-17437

Armstrong, D., Al-Awadi, F., 1991. Lipid peroxidation and retinopathy in streptozotocin-induced diabetes. Free Radic. Biol. Med. 11, 433–436. https://doi.org/10.1016/0891-5849(91)90161-U

Arosio, P., Elia, L., Poli, M., 2017. Ferritin, cellular iron storage and regulation. IUBMB Life 69, 414–422. https://doi.org/10.1002/IUB.1621

Attwell, D., Mishra, A., Hall, C.N., O'Farrell, F.M., Dalkara, T., 2016. What is a pericyte? J. Cereb. Blood Flow Metab. 36, 451. https://doi.org/10.1177/0271678X15610340

Augustine, J., Troendle, E.P., Barabas, P., McAleese, C.A., Friedel, T., Stitt, A.W., Curtis, T.M., 2021. The Role of Lipoxidation in the Pathogenesis of Diabetic Retinopathy. Front. Endocrinol. (Lausanne). 11, 1146. https://doi.org/10.3389/FENDO.2020.621938/BIBTEX

Babapoor-Farrokhran, S., Jee, K., Puchner, B., Hassan, S.J., Xin, X., Rodrigues, M., Kashiwabuchi, F., Ma, T., Hu, K., Deshpande, M., Daoud, Y., Solomon, S., Wenick, A., Lutty, G.A., Semenza, G.L., Montaner, S., Sodhi, A., 2015. Angiopoietin-like 4 is a potent angiogenic factor and a novel therapeutic target for patients with proliferative diabetic retinopathy. Proc. Natl. Acad. Sci. U. S. A. 112, E3030–E3039. https://doi.org/10.1073/PNAS.1423765112

Balda, M.S., Matter, K., 2000. Transmembrane proteins of tight junctions. Semin. Cell Dev. Biol. 11, 281–289. https://doi.org/10.1006/scdb.2000.0177

Balla, G., Jacob, H.S., Balla, J., Rosenberg, M., Nath, K., Apple, F., Eaton, J.W., Vercellotti, G.M., 1992. Ferritin: A cytoprotective antioxidant strategem of endothelium. J. Biol. Chem. 267, 18148–18153. https://doi.org/10.1016/s0021-9258(19)37165-0

Barber, A.J., Antonetti, D.A., Kern, T.S., Reiter, C.E.N., Soans, R.S., Krady, J.K., Levison, S.W., Gardner, T.W., Bronson, S.K., 2005. The Ins2Akita Mouse as a Model of Early Retinal Complications in Diabetes. Invest. Ophthalmol. Vis. Sci. 46, 2210–2218. https://doi.org/10.1167/IOVS.04-1340

Barnett, P.A., Gonzalez, R.G., Chylack, L.T., Cheng, H.M., 1986. The effect of oxidation on sorbitol pathway kinetics. Diabetes 35, 426–432. https://doi.org/10.2337/DIAB.35.4.426

Batts, K.P., 2007. Iron overload syndromes and the liver. Mod. Pathol. 2007 201 20, S31–S39. https://doi.org/10.1038/modpathol.3800715

Baumann, B.H., Shu, W., Song, Y., Simpson, E.M., Lakhal-Littleton, S., Dunaief, J.L., 2019a. Ferroportin-mediated iron export from vascular endothelial cells in retina and brain. Exp. Eye Res. 187, 107728. https://doi.org/10.1016/j.exer.2019.107728

Baumann, B.H., Shu, W., Song, Y., Sterling, J., Kozmik, Z., Lakhal-Littleton, S., Dunaief, J.L., 2019b. Liver-Specific, but Not Retina-Specific, Hepcidin Knockout Causes Retinal Iron Accumulation and Degeneration. Am. J. Pathol. 189, 1814–1830. https://doi.org/10.1016/j.ajpath.2019.05.022

Beaumont, C., Canonne-Hergaux, F., 2005. Erythrophagocytose et recyclage du fer héminique dans les conditions normales et pathologiques ; régulation par l'hepcidine. Transfus. Clin. Biol. 12, 123–130. https://doi.org/10.1016/J.TRACLI.2005.04.017

Beckman, J.A., Creager, M.A., 2016. Vascular complications of diabetes. Circ. Res.

https://doi.org/10.1161/CIRCRESAHA.115.306884

Behl, T., Kotwani, A., 2015. Possible role of endostatin in the antiangiogenic therapy of diabetic retinopathy. Life Sci. https://doi.org/10.1016/j.lfs.2015.06.017

Belhoul, K.M., Bakir, M.L., Kadhim, A.M., Dewedar, H.E.S., Eldin, M.S., Alkhaja, F.A., 2013. Prevalence of iron overload complications among patients with β-thalassemia major treated at Dubai Thalassemia Centre. Ann. Saudi Med. 33, 18. https://doi.org/10.5144/0256-4947.2013.18

Belke, D.D., Severson, D.L., 2012. Diabetes in mice with monogenic obesity: the db/db mouse and its use in the study of cardiac consequences. Methods Mol. Biol. 933, 47–57. https://doi.org/10.1007/978-1-62703-068-7_4

Beltramo, E., Lopatina, T., Mazzeo, A., Arroba, A.I., Valverde, A.M., Hernández, C., Simó, R., Porta, M., 2016. Effects of the neuroprotective drugs somatostatin and brimonidine on retinal cell models of diabetic retinopathy. Acta Diabetol. 53, 957–964. https://doi.org/10.1007/s00592-016-0895-4

Bhagat, N., Grigorian, R.A., Tutela, A., Zarbin, M.A., 2009. Diabetic Macular Edema: Pathogenesis and Treatment. Surv. Ophthalmol. 54, 1–32. https://doi.org/10.1016/J.SURVOPHTHAL.2008.10.001

Bharadwaj, A.S., Appukuttan, B., Wilmarth, P.A., Pan, Y., Stempel, A.J., Chipps, T.J., Benedetti, E.E., Zamora, D.O., Choi, D., David, L.L., Smith, J.R., 2013. Role of the retinal vascular endothelial cell in ocular disease. Prog. Retin. Eye Res. 32, 102–180. https://doi.org/10.1016/J.PRETEYERES.2012.08.004

Bhat, A.A., Uppada, S., Achkar, I.W., Hashem, S., Yadav, S.K., Shanmugakonar, M., Al-Naemi, H.A., Haris, M., Uddin, S., 2019. Tight junction proteins and signaling pathways in cancer and inflammation: A functional crosstalk. Front. Physiol. 10, 1942. https://doi.org/10.3389/FPHYS.2018.01942/BIBTEX

Bhutto, I.A., Kim, S.Y., McLeod, D.S., Merges, C., Fukai, N., Olsen, B.R., Lutty, G.A., 2004. Localization of collagen XVIII and the endostatin portion of collagen XVIII in aged human control eyes and eyes with age-related macular degeneration. Investig. Ophthalmol. Vis. Sci. 45, 1544–1552. https://doi.org/10.1167/iovs.03-0862

Birbrair, A., Zhang, T., Wang, Z.M., Messi, M.L., Mintz, A., Delbono, O., 2013. Type-1 pericytes participate in fibrous tissue deposition in aged skeletal muscle. Am. J. Physiol. Cell Physiol. 305. https://doi.org/10.1152/AJPCELL.00171.2013

Birbrair, A., Zhang, T., Wang, Z.M., Messi, M.L., Olson, J.D., Mintz, A., Delbono, O., 2014. Type-2 pericytes participate in normal and tumoral angiogenesis. Am. J. Physiol. Cell Physiol. 307. https://doi.org/10.1152/AJPCELL.00084.2014

Birnholz, J.C., Farrell, E.E., 1988. Fetal hyaloid artery: Timing of regression with US. Radiology 166, 781–783. https://doi.org/10.1148/radiology.166.3.3277246

Blinder, K.J., Dugel, P.U., Chen, S., Jumper, J.M., Walt, J.G., Hollander, D.A., Scott, L.C., 2017. Anti-VEGF treatment of diabetic macular edema in clinical practice: effectiveness and patterns of use (ECHO Study Report 1). Clin. Ophthalmol. 11, 393. https://doi.org/10.2147/OPTH.S128509

Bloodworth, J.M., Engerman, R.L., Powers, K.L., 1969. Experimental diabetic microangiopathy. I. Basement membrane statistics in the dog. Diabetes 18, 455–458. https://doi.org/10.2337/DIAB.18.7.455

Bloom, J., Czyz, C.N., 2018. Anatomy, Head and Neck, Eye Iris Sphincter Muscle, StatPearls. StatPearls Publishing.

Boehm, B.O., Lang, G., Volpert, O., Jehle, P.M., Kurkhaus, A., Rosinger, S., Lang, G.K., Bouck, N., 2003. Low content of the natural ocular anti-angiogenic agent pigment epithelium-derived factor (PEDF) in aqueous humor predicts progression of diabetic retinopathy. Diabetologia 46, 394–400. https://doi.org/10.1007/S00125-003-1040-9

Bogdanov, P., Corraliza, L., Villena, J.A., Carvalho, A.R., Garcia-Arumí, J., Ramos, D., Ruberte, J., Simó, R., Hernández, C., 2014. The db/db Mouse: A Useful Model for the Study of Diabetic Retinal Neurodegeneration. PLoS One 9. https://doi.org/10.1371/JOURNAL.PONE.0097302

Boulton, M.E., Mc Leod, D., Garner, A., 1988. Vasoproliferative retinopathies: Clinical, morphogenetic and modulatory aspects. Eye 1988 21 2, S124–S139. https://doi.org/10.1038/eye.1988.139

Boyer, D.S., Hopkins, J.J., Sorof, J., Ehrlich, J.S., 2013. Anti-vascular endothelial growth factor therapy for diabetic macular edema. Ther. Adv. Endocrinol. Metab. 4, 151–69. https://doi.org/10.1177/2042018813512360

Bressler, S.B., Qin, H., Beck, R.W., Chalam, K. V., Kim, J.E., Melia, M., Wells, J.A., 2012. Factors associated with changes in visual acuity and central subfield thickness at 1 year after treatment for diabetic macular edema with ranibizumab. Arch. Ophthalmol. (Chicago, Ill. 1960) 130, 1153–1161. https://doi.org/10.1001/ARCHOPHTHALMOL.2012.1107

Brock, J.H., Halliday, J.W., Pippard, M.J., 1995. Iron metabolism in health and disease. Edited by J. H. Brock, J. W. Halliday, M. J. Pippard, and L. W. Powell. 495 pp. London: Saunders, 1994. $79. Hepatology 21, 889–890. https://doi.org/10.1002/HEP.1840210343

Brown, D.M., Wykoff, C.C., Boyer, D., Heier, J.S., Clark, W.L., Emanuelli, A., Higgins, P.M., Singer, M., Weinreich, D.M., Yancopoulos, G.D., Berliner, A.J., Chu, K., Reed, K., Cheng, Y., Vitti, R., 2021. Evaluation of Intravitreal Aflibercept for the Treatment of Severe Nonproliferative Diabetic Retinopathy: Results From the PANORAMA Randomized Clinical Trial. JAMA Ophthalmol. 139, 946–955. https://doi.org/10.1001/JAMAOPHTHALMOL.2021.2809

Burke, S.J., Batdorf, H.M., Burk, D.H., Noland, R.C., Eder, A.E., Boulos, M.S., Karlstad, M.D., Jason Collier, J., 2017. db/ db Mice Exhibit Features of Human Type 2 Diabetes That Are Not Present in Weight-Matched C57BL/6J Mice Fed a Western Diet. J. Diabetes Res. 2017. https://doi.org/10.1155/2017/8503754

Cai, J., Jiang, W.G., Ahmed, A., Boulton, M., 2006. Vascular endothelial growth factor-induced endothelial cell proliferation is regulated by interaction between VEGFR-2, SH-PTP1 and eNOS. Microvasc. Res. 71, 20–31. https://doi.org/10.1016/J.MVR.2005.10.004

Campbell, M., Humphries, P., 2013. The blood-retina barrier tight junctions and barrier modulation. Adv. Exp. Med. Biol. 763, 70–84. https://doi.org/10.1007/978-1-4614-4711-5_3

Carrasco, E., Hernández, C., Miralles, A., Huguet, P., Farrés, J., Simó, R., 2007. Lower somatostatin expression is an early event in diabetic retinopathy and is associated with retinal neurodegeneration. Diabetes Care 30, 2902–2908. https://doi.org/10.2337/dc07-0332

Carter-Dawson, L.D., Lavail, M.M., 1979. Rods and cones in the mouse retina. I. Structural analysis using light and electron microscopy. J. Comp. Neurol. 188, 245–262. https://doi.org/10.1002/CNE.901880204

Chaffee, E.L., Bovie, W.T., Hampson, A., 1923. The Electrical Response of the Retina Under Stimulation by Light. J. Opt. Soc. Am. 7, 1. https://doi.org/10.1364/josa.7.000001

Charkoudian, L.K., Dentchev, T., Lukinova, N., Wolkow, N., Dunaief, J.L., Franz, K.J., 2008. Iron prochelator BSIH protects retinal pigment epithelial cells against cell death induced by hydrogen peroxide. J. Inorg. Biochem. 102, 2130–2135. https://doi.org/10.1016/J.JINORGBIO.2008.08.001

Chaudhary, K., Promsote, W., Ananth, S., Veeranan-Karmegam, R., Tawfik, A., Arjunan, P., Martin, P., Smith, S.B., Thangaraju, M., Kisselev, O., Ganapathy, V., Gnana-Prakasam, J.P., 2018. Iron Overload Accelerates the Progression of Diabetic Retinopathy in Association with Increased Retinal Renin Expression. Sci. Rep. 8, 3025. https://doi.org/10.1038/s41598-018-21276-2

Chavakis, T., Keiper, T., Matz-Westphal, R., Hersemeyer, K., Sachs, U.J., Nawroth, P.P.,

Preissner, K.T., Santoso, S., 2004. The junctional adhesion molecule-C promotes neutrophil transendothelial migration in vitro and in vivo. J. Biol. Chem. 279, 55602–55608. https://doi.org/10.1074/JBC.M404676200

Chen, B. hua, Jiang, D. yong, Tang, L. sheng, 2006. Advanced glycation end-products induce apoptosis involving the signaling pathways of oxidative stress in bovine retinal pericytes. Life Sci. 79, 1040–1048. https://doi.org/10.1016/J.LFS.2006.03.020

Chen, T.T., Li, L., Chung, D.H., Allen, C.D.C., Torti, S. V., Torti, F.M., Cyster, J.G., Chen, C.Y., Brodsky, F.M., Niemi, E.C., Nakamura, M.C., Seaman, W.E., Daws, M.R., 2005. TIM-2 is expressed on B cells and in liver and kidney and is a receptor for H-ferritin endocytosis. J. Exp. Med. 202, 955–965. https://doi.org/10.1084/JEM.20042433

Cheung, A.K.H., Fung, M.K.L., Lo, A.C.Y., Lam, T.T.L., Kwok, F.S., Chung, S.S.M., Chung, S.K., 2005. Aldose reductase deficiency prevents diabetes-induced blood-retinal barrier breakdown, apoptosis, and glial reactivation in the retina of db/db mice. Diabetes 54, 3119–3125. https://doi.org/10.2337/diabetes.54.11.3119

Chevion, M., 1988a. A site-specific mechanism for free radical induced biological damage: the essential role of redox-active transition metals. Free Radic. Biol. Med. 5, 27–37. https://doi.org/10.1016/0891-5849(88)90059-7

Chevion, M., 1988b. A site-specific mechanism for free radical induced biological damage: the essential role of redox-active transition metals. Free Radic. Biol. Med. 5, 27–37. https://doi.org/10.1016/0891-5849(88)90059-7

Ciudin, A., Hernández, C., Simó, R., 2010. Iron Overload in Diabetic Retinopathy: A Cause or a Consequence of Impaired Mechanisms? Exp. Diabetes Res. 2010. https://doi.org/10.1155/2010/714108

Cogan, D.G., Toussaint, D., Kuwabara, T., 1961. Retinal vascular patterns. IV. Diabetic retinopathy. Arch. Ophthalmol. (Chicago, Ill. 1960) 66, 366–378. https://doi.org/10.1001/ARCHOPHT.1961.00960010368014

Connolly, S.E., Hores, T.A., Smith, L.E.H., D'Amore, P.A., 1988. Characterization of vascular development in the mouse retina. Microvasc. Res. 36, 275–290. https://doi.org/10.1016/0026-2862(88)90028-3

Coorey, N.J., Shen, W., Chung, S.H., Zhu, L., Gillies, M.C., 2021. The role of glia in retinal vascular disease. https://doi.org/10.1111/j.1444-0938.2012.00741.x 95, 266–281. https://doi.org/10.1111/J.1444-0938.2012.00741.X

Cristante, E., Liyanage, S.E., Sampson, R.D., Kalargyrou, A., De Rossi, G., Rizzi, M., Hoke, J., Ribeiro, J., Maswood, R.N., Duran, Y., Matsuki, T., Aghaizu, N.D., Luhmann, U.F., Smith, A.J., Ali, R.R., Bainbridge, J.W.B., 2018. Late neuroprogenitors contribute to normal retinal vascular development in a Hif2a-dependent manner. Development 145. https://doi.org/10.1242/dev.157511

Curcio, C.A., Sloan, K.R., Kalina, R.E., Hendrickson, A.E., 1990. Human photoreceptor topography. J. Comp. Neurol. 292, 497–523. https://doi.org/10.1002/CNE.902920402

Dagher, Z., Gerhardinger, C., Vaz, J., Goodridge, M., Tecilazich, F., Lorenzi, M., 2017. The Increased Transforming Growth Factor-β Signaling Induced by Diabetes Protects Retinal Vessels. Am. J. Pathol. 187, 627. https://doi.org/10.1016/J.AJPATH.2016.11.007

Danilova, I., Medvedeva, S., Shmakova, S., Chereshneva, M., Sarapultsev, A., Sarapultsev, P., 2018. Pathological changes in the cellular structures of retina and choroidea in the early stages of alloxan-induced diabetes. World J. Diabetes 9, 239. https://doi.org/10.4239/WJD.V9.I12.239

Daru, J., Colman, K., Stanworth, S.J., De La Salle, B., Wood, E.M., Pasricha, S.R., 2017. Serum ferritin as an indicator of iron status: what do we need to know? Am. J. Clin. Nutr. 106, 1634S-1639S. https://doi.org/10.3945/AJCN.117.155960

Das, A., McLamore, A., Song, W., McGuire, P.G., 1999. Retinal Neovascularization Is

Suppressed With a Matrix Metalloproteinase Inhibitor. Arch. Ophthalmol. 117, 498–503. https://doi.org/10.1001/ARCHOPHT.117.4.498

Dautry Varsat, A., Ciechanover, A., Lodish, H.F., 1983. pH and the recycling of transferrin during receptor-mediated endocytosis. Proc. Natl. Acad. Sci. U. S. A. 80, 2258. https://doi.org/10.1073/PNAS.80.8.2258

de la Maza, M.S., Tauber, J., Foster, C.S., 2012. Structural Considerations of the Sclera, in: The Sclera. Springer, Boston, MA, pp. 1–30. https://doi.org/10.1007/978-1-4419-6502-8_1

Deininger, M.H., Fimmen, B.A., Thal, D.R., Schluesener, H.J., Meyermann, R., 2002. Aberrant neuronal and paracellular deposition of endostatin in brains of patients with Alzheimer's disease. J. Neurosci. 22, 10621–10626. https://doi.org/10.1523/jneurosci.22-24-10621.2002

DelMonte, D.W., Kim, T., 2011. Anatomy and physiology of the cornea. J. Cataract Refract. Surg. 37, 588–598. https://doi.org/10.1016/j.jcrs.2010.12.037

Derbyshire, E.R., Marletta, M.A., 2012. Structure and regulation of soluble guanylate cyclase. Annu. Rev. Biochem. 81, 533–559. https://doi.org/10.1146/ANNUREV-BIOCHEM-050410-100030

Derevjanik, N.L., Vinores, S.A., Xiao, W.H., Mori, K., Turon, T., Hudish, T., Dong, S., Campochiaro, P.A., 2002. Quantitative assessment of the integrity of the blood-retinal barrier in mice. Investig. Ophthalmol. Vis. Sci. 43, 2462–2467.

Díaz-Coránguez, M., Liu, X., Antonetti, D.A., 2019. Tight Junctions in Cell Proliferation. Int. J. Mol. Sci. 20, 5972. https://doi.org/10.3390/IJMS20235972

Díaz-Coránguez, M., Ramos, C., Antonetti, D.A., 2017. The inner Blood-Retinal Barrier: Cellular Basis and Development. Vision Res. 139, 123. https://doi.org/10.1016/J.VISRES.2017.05.009

Dorrell, M.I., Aguilar, E., Friedlander, M., 2002. Retinal vascular development is mediated by endothelial filopodia, a preexisting astrocytic template and specific R-cadherin adhesion. Investig. Ophthalmol. Vis. Sci. 43, 3500–3510.

Du, L., Zhao, Z., Cui, A., Zhu, Y., Zhang, L., Liu, J., Shi, S., Fu, C., Han, X., Gao, W., Song, T., Xie, L., Wang, L., Sun, S., Guo, R., Ma, G., 2018. Increased Iron Deposition on Brain Quantitative Susceptibility Mapping Correlates with Decreased Cognitive Function in Alzheimer's Disease. ACS Chem. Neurosci. 9, 1849–1857. https://doi.org/10.1021/ACSCHEMNEURO.8B00194

du Sert, N.P., Ahluwalia, A., Alam, S., Avey, M.T., Baker, M., Browne, W.J., Clark, A., Cuthill, I.C., Dirnagl, U., Emerson, M., Garner, P., Holgate, S.T., Howells, D.W., Hurst, V., Karp, N.A., Lazic, S.E., Lidster, K., MacCallum, C.J., Macleod, M., Pearl, E.J., Petersen, O.H., Rawle, F., Reynolds, P., Rooney, K., Sena, E.S., Silberberg, S.D., Steckler, T., Würbel, H., 2020. Reporting animal research: Explanation and elaboration for the arrive guidelines 2.0. PLoS Biol. 18. https://doi.org/10.1371/JOURNAL.PBIO.3000411

Duh, E.J., Sun, J.K., Stitt, A.W., 2017. Diabetic retinopathy: current understanding, mechanisms, and treatment strategies. JCI Insight 2. https://doi.org/10.1172/jci.insight.93751

Dunaief, J.L., Hahn, P., Rouault, T., Harris, Z.L., 2004. Retinal iron metabolism and its possible role in AMD pathogenesis. Invest. Ophthalmol. Vis. Sci. 45, 2291–2291.

Ehrlich, R., Harris, A., Wentz, S.M., Moore, N.A., Siesky, B.A., 2016. Anatomy and regulation of the optic nerve blood flow. Curated Ref. Collect. Neurosci. Biobehav. Psychol. 73–82. https://doi.org/10.1016/B978-0-12-809324-5.01301-8

Essner, E., Lin, W.L., 1988. Immunocytochemical localization of laminin, type IV collagen and fibronectin in rat retinal vessels. Exp. Eye Res. 47, 317–327. https://doi.org/10.1016/0014-4835(88)90014-0

Faruqi, A., Mukkamalla, S.K.R., 2020. Iron Binding Capacity, in: Definitions. Qeios.

https://doi.org/10.32388/R7RR6W

Feng, S., Cen, J., Huang, Y., Shen, H., Yao, L., Wang, Y., Chen, Z., 2011. Matrix metalloproteinase-2 and -9 secreted by leukemic cells increase the permeability of blood-brain barrier by disrupting tight junction proteins. PLoS One 6. https://doi.org/10.1371/JOURNAL.PONE.0020599

Ferńandez-Real, J.M., Mcclain, D., Review, M.M., 2015. Mechanisms Linking Glucose Homeostasis and Iron Metabolism Toward the Onset and Progression of Type 2 Diabetes. Diabetes Care 38, 2169–2176. https://doi.org/10.2337/DC14-3082

Ferreras, M., Felbor, U., Lenhard, T., Olsen, B.R., Delaissé, J.M., 2000. Generation and degradation of human endostatin proteins by various proteinases. FEBS Lett. 486, 247–251. https://doi.org/10.1016/S0014-5793(00)02249-3

Fisher, J., Devraj, K., Ingram, J., Slagle-Webb, B., Madhankumar, A.B., Liu, X., Klinger, M., Simpson, I.A., Connor, J.R., 2007. Ferritin: a novel mechanism for delivery of iron to the brain and other organs. Am. J. Physiol. Physiol. 293, C641–C649. https://doi.org/10.1152/ajpcell.00599.2006

Fonseca-Nunes, A., Jakszyn, P., Agudo, A., 2014. Iron and cancer risk--a systematic review and meta-analysis of the epidemiological evidence. Cancer Epidemiol. Biomarkers Prev. 23, 12–31. https://doi.org/10.1158/1055-9965.EPI-13-0733

Frambach, D.A., Marmor, M.F., 1982. The rate and route of fluid resorption from the subretinal space of the rabbit. Investig. Ophthalmol. Vis. Sci. 22, 292–302.

Freyberger, H., Bröcker, M., Yakut, H., Hammer, J., Effert, R., Schifferdecker, E., Schatz, H., Derwahl, M., 2000. Increased levels of platelet-derived growth factor in vitreous fluid of patients with proliferative diabetic retinopathy. Exp. Clin. Endocrinol. Diabetes 108, 106–109. https://doi.org/10.1055/S-2000-5803/ID/16

Fruttiger, M., 2007. Development of the retinal vasculature. Angiogenesis 10, 77–88. https://doi.org/10.1007/s10456-007-9065-1

Fruttiger, M., 2002. Development of the mouse retinal vasculature: Angiogenesis versus vasculogenesis. Investig. Ophthalmol. Vis. Sci. 43, 522–527.

Fu, Z., Gong, Y., Liegl, R., Hellstrom, A., Talukdar, S., Smith, L.E.H., 2017. FGF21 Administration Suppresses Retinal and Choroidal Neovascularization in Mice. CellReports 18, 1606–1613. https://doi.org/10.1016/j.celrep.2017.01.014

Fukai, N., Eklund, L., Marneros, A.G., Oh, S.P., Keene, D.R., Tamarkin, L., Niemelä, M., Ilves, M., Li, E., Pihlajaniemi, T., Olsen, B.R., 2002. Lack of collagen XVIII/endostatin results in eye abnormalities. EMBO J. 21, 1535–44. https://doi.org/10.1093/emboj/21.7.1535

Funatsu, H., Yamashita, H., Noma, H., Mochizuki, H., Mimura, T., Ikeda, T., Hori, S., 2003. Outcome of vitreous surgery and the balance between vascular endothelial growth factor and endostatin. Investig. Ophthalmol. Vis. Sci. 44, 1042–1047. https://doi.org/10.1167/iovs.02-0374

Furuse, M., Hirase, T., Itoh, M., Nagafuchi, A., Yonemura, S., Tsukita, S., Tsukita, S., 1993. Occludin: a novel integral membrane protein localizing at tight junctions. J. Cell Biol. 123, 1777. https://doi.org/10.1083/JCB.123.6.1777

Ganz, T., Nemeth, E., 2006. Iron imports. IV. Hepcidin and regulation of body iron metabolism. Am. J. Physiol. - Gastrointest. Liver Physiol. 290, 199–203. https://doi.org/10.1152/AJPGI.00412.2005/ASSET/IMAGES/LARGE/ZH30020643340004.JPEG

Gao, G., Li, J., Zhang, Y., Chang, Y.Z., 2019. Cellular Iron Metabolism and Regulation. Adv. Exp. Med. Biol. 1173, 21–32. https://doi.org/10.1007/978-981-13-9589-5_2

Gardiner, T.A., Archer, D.B., 1986. Endocytosis in the retinal and choroidal microcirculation. Br. J. Ophthalmol. 70, 361–372. https://doi.org/10.1136/BJO.70.5.361

Garner, A., 1993. Histopathology of diabetic retinopathy in man. Eye 1993 72 7, 250–253. https://doi.org/10.1038/eye.1993.58

Gastinger, M.J., Singh, R.S.J., Barber, A.J., 2006. Loss of cholinergic and dopaminergic amacrine cells in streptozotocin- diabetic rat and Ins2Akita-diabetic mouse retinas. Investig. Ophthalmol. Vis. Sci. 47, 3143–3150. https://doi.org/10.1167/iovs.05-1376

Gerhardt, H., Golding, M., Fruttiger, M., Ruhrberg, C., Lundkvist, A., Abramsson, A., Jeltsch, M., Mitchell, C., Alitalo, K., Shima, D., Betsholtz, C., 2003. VEGF guides angiogenic sprouting utilizing endothelial tip cell filopodia. J. Cell Biol. 161, 1163–1177. https://doi.org/10.1083/JCB.200302047

Ghosh, K.K., Bujan, S., Haverkamp, S., Feigenspan, A., Wässle, H., 2004. Types of bipolar cells in the mouse retina. J. Comp. Neurol. 469, 70–82. https://doi.org/10.1002/CNE.10985

Gnana-Prakasam, J.P., Ananth, S., Prasad, P.D., Zhang, M., Atherton, S.S., Martin, P.M., Smith, S.B., Ganapathy, V., 2011. Expression and iron-dependent regulation of succinate receptor GPR91 in retinal pigment epithelium. Invest. Ophthalmol. Vis. Sci. 52, 3751–3758. https://doi.org/10.1167/IOVS.10-6722

Gnana-Prakasam, J.P., Chaudhary, K., Promsote, W., Smith, S.B., Ganapathy, V., Martin, P.M., Saul, A., 2016. Retinal Iron Overload during Diabetic Retinopathy Accelerates Ganglion Cell Death. Invest. Ophthalmol. Vis. Sci. 57, 751–751.

Gnana-Prakasam, J.P., Martin, P.M., Mysona, B.A., Roon, P., Smith, S.B., Ganapathy, V., 2008. Hepcidin expression in mouse retina and its regulation via lipopolysaccharide/Toll-like receptor-4 pathway independent of Hfe. Biochem. J. 411, 79–88. https://doi.org/10.1042/BJ20071377

Goebel, W., Kretzchmar-Gross, T., 2002. Retinal thickness in diabetic retinopathy: a study using optical coherence tomography (OCT). Retina 22, 759–767. https://doi.org/10.1097/00006982-200212000-00012

Gonzales, A.L., Klug, N.R., Moshkforoush, A., Lee, J.C., Lee, F.K., Shui, B., Tsoukias, N.M., Kotlikoff, M.I., Hill-Eubanks, D., Nelson, M.T., 2020. Contractile pericytes determine the direction of blood flow at capillary junctions. Proc. Natl. Acad. Sci. U. S. A. 117, 27022–27033. https://doi.org/10.1073/PNAS.1922755117/VIDEO-3

Gray, N.K., Hentze, M.W., 1994. Iron regulatory protein prevents binding of the 43S translation pre-initiation complex to ferritin and eALAS mRNAs. EMBO J. 13, 3882–3891. https://doi.org/10.1002/j.1460-2075.1994.tb06699.x

Guaraldo, M., Santambrogio, P., Rovelli, E., Di Savino, A., Saglio, G., Cittaro, D., Roetto, A., Levi, S., 2016. Characterization of human mitochondrial ferritin promoter: identification of transcription factors and evidences of epigenetic control. Sci. Reports 2016 61 6, 1–11. https://doi.org/10.1038/srep33432

Gulec, S., Anderson, G.J., Collins, J.F., 2014a. Mechanistic and regulatory aspects of intestinal iron absorption. Am. J. Physiol. - Gastrointest. Liver Physiol. 307, G397. https://doi.org/10.1152/AJPGI.00348.2013

Gulec, S., Anderson, G.J., Collins, J.F., 2014b. Mechanistic and regulatory aspects of intestinal iron absorption. Am. J. Physiol. - Gastrointest. Liver Physiol. 307, G397. https://doi.org/10.1152/AJPGI.00348.2013

Hadziahmetovic, M., Pajic, M., Grieco, S., Song, Y., Song, D., Li, Y., Cwanger, A., Iacovelli, J., Chu, S., Ying, G., Connelly, J., Spino, M., Dunaief, J.L., 2012. The Oral Iron Chelator Deferiprone Protects Against Retinal Degeneration Induced through Diverse Mechanisms. Transl. Vis. Sci. Technol. 1, 2. https://doi.org/10.1167/TVST.1.3.2

Hadziahmetovic, M., Song, Y., Ponnuru, P., Iacovelli, J., Hunter, A., Haddad, N., Beard, J., Connor, J.R., Vaulont, S., Dunaief, J.L., 2011. Age-dependent retinal iron accumulation and degeneration in hepcidin knockout mice. Invest. Ophthalmol. Vis. Sci. 52, 109–118. https://doi.org/10.1167/IOVS.10-6113

Hahn, P., Chen, L., Beard, J.L., Harris, Z.L., Dunaief, J.L., 2004. Disruption of Ceruloplasmin and Hephaestin in mice causes retinal iron overload and retinal degeneration with features of age–related macular degeneration. Invest. Ophthalmol. Vis. Sci. 45, 2292–2292.

Hahn, Paul, Dentchev, T., Qian, Y., Rouault, T., Harris, Z.L., Dunaief, J.L., 2004a. Immunolocalization and regulation of iron handling proteins ferritin and ferroportin in the retina. Mol. Vis. 10, 598–607.

Hahn, Paul, Qian, Y., Dentchev, T., Chen, L., Beard, J., Harris, Z.L., Dunaief, J.L., 2004b. Disruption of ceruloplasmin and hephaestin in mice causes retinal iron overload and retinal degeneration with features of age-related macular degeneration. Proc. Natl. Acad. Sci. 101, 13850–13855. https://doi.org/10.1073/PNAS.0405146101

Hajitou, A., Grignet, C., Devy, L., Berndt, S., Blacher, S., Deroanne, C.F., Bajou, K., Fong, T., Chiang, Y., Foidart, J.M., Noël, A., 2002. The antitumoral effect of endostatin and angiostatin is associated with a down-regulation of vascular endothelial growth factor expression in tumor cells. FASEB J. 16, 1802–1804. https://doi.org/10.1096/FJ.02-0109FJE

Hajrasouliha, A.R., Jiang, G., Lu, Q., Lu, H., Kaplan, H.J., Zhang, H.G., Shao, H., 2013. Exosomes from retinal astrocytes contain antiangiogenic components that inhibit laser-induced choroidal neovascularization. J. Biol. Chem. 288, 28058–28067. https://doi.org/10.1074/jbc.M113.470765

Haller, H., 1997. Endothelial function. General considerations, in: Drugs. pp. 1–10. https://doi.org/10.2165/00003495-199700531-00003

Hamanaka, T., Akabane, N., Yajima, T., Takahashi, T., Tanabe, A., 2001. Retinal ischemia and angle neovascularization in proliferative diabetic retinopathy. Am. J. Ophthalmol. 132, 648–658. https://doi.org/10.1016/S0002-9394(01)01108-4

Hammes, H.P., 2005. Pericytes and the pathogenesis of diabetic retinopathy. Horm. Metab. Res. 37, 39–43. https://doi.org/10.1055/S-2005-861361/ID/28

Han, J., Seaman, W.E., Di, X., Wang, W., Willingham, M., Torti, F.M., Torti, S. V., 2011. Iron Uptake Mediated by Binding of H-Ferritin to the TIM-2 Receptor in Mouse Cells. PLoS One 6, e23800. https://doi.org/10.1371/journal.pone.0023800

Hanai, J.I., Dhanabal, M., Ananth Karumanchi, S., Albanese, C., Waterman, M., Chan, B., Ramchandran, R., Pestell, R., Sukhatme, V.P., 2002. Endostatin causes G 1 arrest of endothelial cells through inhibition of cyclin D1. J. Biol. Chem. 277, 16464–16469. https://doi.org/10.1074/jbc.M112274200

Harrison, P.M., Arosio, P., 1996. The ferritins: Molecular properties, iron storage function and cellular regulation. Biochim. Biophys. Acta - Bioenerg. https://doi.org/10.1016/0005-2728(96)00022-9

Haverkamp, S., Ghosh, K.K., Hirano, A.A., Wässle, H., 2003. Immunocytochemical description of five bipolar cell types of the mouse retina. J. Comp. Neurol. 455, 463–476. https://doi.org/10.1002/cne.10491

Hentze, M.W., Kühn, L.C., 1996. Molecular control of vertebrate iron metabolism: mRNA-based regulatory circuits operated by iron, nitric oxide, and oxidative stress. Proc. Natl. Acad. Sci. U. S. A. 93, 8175. https://doi.org/10.1073/PNAS.93.16.8175

Hernández, C., Simó-Servat, O., Simó, R., 2014. Somatostatin and diabetic retinopathy: current concepts and new therapeutic perspectives. Endocrine 46, 209–214. https://doi.org/10.1007/S12020-014-0232-Z

Hicks, K., O'Neil, R.G., Dubinsky, W.S., Brown, R.C., 2010. TRPC-mediated actin-myosin contraction is critical for BBB disruption following hypoxic stress. Am. J. Physiol. Cell Physiol. 298. https://doi.org/10.1152/AJPCELL.00458.2009

Holländer, H., Makarov, F., Dreher, Z., van Driel, D., Chan-Ling, T., Stone, J., 1991. Structure of the macroglia of the retina: Sharing and division of labour between astrocytes and Müller cells. J. Comp. Neurol. 313, 587–603. https://doi.org/10.1002/CNE.903130405

Hou, Q., Ling, L., Wang, F., Xing, S., Pei, Z., Zeng, J., 2010. Endostatin expression in neurons during the early stage of cerebral ischemia is associated with neuronal apoptotic cell death in adult hypertensive rat model of stroke. Brain Res. 1311, 182–188. https://doi.org/10.1016/j.brainres.2009.11.033

Huaman, J., Naidoo, M., Zang, X., Ogunwobi, O.O., 2019. Fibronectin Regulation of Integrin B1 and SLUG in Circulating Tumor Cells. Cells 8, 618. https://doi.org/10.3390/cells8060618

Huang, H.-W., Yang, C.-M., Yang, C.-H., Fibroblast Growth Factor, C., Santiago, R., Boia, R., 2021. Fibroblast Growth Factor Type 1 Ameliorates High-Glucose-Induced Oxidative Stress and Neuroinflammation in Retinal Pigment Epithelial Cells and a Streptozotocin-Induced Diabetic Rat Model. Int. J. Mol. Sci. 2021, Vol. 22, Page 7233 22, 7233. https://doi.org/10.3390/IJMS22137233

Hughes, J.M., Groot, A.J., Van Groep, P. Der, Sersansie, R., Vooijs, M., Van Diest, P.J., Van Noorden, C.J.F., Schlingemann, R.O., Klaassen, I., 2010. Active HIF-1 in the Normal Human Retina. J. Histochem. Cytochem. 58, 247. https://doi.org/10.1369/JHC.2009.953786

Hunt, R.C., Davis, A.A., 1992. Release of iron by human retinal pigment epithelial cells. J. Cell. Physiol. 152, 102–110. https://doi.org/10.1002/JCP.1041520114

Hunt, R.C., Dewey, A., Davis, A.A., 1989. Transferrin receptors on the surfaces of retinal pigment epithelial cells are associated with the cytoskeleton. J. Cell Sci. 92 (Pt 4). https://doi.org/10.1242/JCS.92.4.655

Hurskainen, M., Eklund, L., Hägg, P.O., Fruttiger, M., Sormunen, R., Ilves, M., Pihlajaniemi, T., 2005. Abnormal maturation of the retinal vasculature in type XVIII collagen/endostatin deficient mice and changes in retinal glial cells due to lack of collagen types XV and XVIII. FASEB J. 19, 1564–1566. https://doi.org/10.1096/fj.04-3101fje

IDF, 2021. IDF Diabetes Atlas | Tenth Edition [WWW Document]. Int. Diabetes Fed. URL https://diabetesatlas.org/ (accessed 2.18.22).

Igarashi, T., Miyake, K., Kato, K., Watanabe, A., Ishizaki, M., Ohara, K., Shimada, T., 2003. Lentivirus-mediated expression of angiostatin efficiently inhibits neovascularization in a murine proliferative retinopathy model. Gene Ther. 2003 103 10, 219–226. https://doi.org/10.1038/sj.gt.3301878

Im, E., Venkatakrishnan, A., Kazlauskas, A., 2005. Cathepsin B regulates the intrinsic angiogenic threshold of endothelial cells. Mol. Biol. Cell 16, 3488–3500. https://doi.org/10.1091/mbc.E04-11-1029

Imamura, T., Hirayama, T., Tsuruma, K., Shimazawa, M., Nagasawa, H., Hara, H., 2014. Hydroxyl radicals cause fluctuation in intracellular ferrous ion levels upon light exposure during photoreceptor cell death. Exp. Eye Res. 129, 24–30. https://doi.org/10.1016/J.EXER.2014.10.019

Inoue, S., 1989. Ultrastructure of Basement Membranes. Int. Rev. Cytol. 117, 57–98. https://doi.org/10.1016/S0074-7696(08)61334-0

Ishibazawa, A., Nagaoka, T., Yokota, H., Takahashi, A., Omae, T., Song, Y.S., Takahashi, T., Yoshida, A., 2016. Characteristics of Retinal Neovascularization in Proliferative Diabetic Retinopathy Imaged by Optical Coherence Tomography Angiography. Invest. Ophthalmol. Vis. Sci. 57, 6247–6255. https://doi.org/10.1167/IOVS.16-20210

Ishii, H., Koya, D., King, G.L., 1998. Protein kinase C activation and its role in the development of vascular complications in diabetes mellitus. J. Mol. Med. (Berl). 76, 21–31. https://doi.org/10.1007/S001090050187

Ito, M., Yoshioka, M., 1999. Regression of the hyaloid vessels and pupillary membrane of the mouse. Anat. Embryol. (Berl). 200, 403–411. https://doi.org/10.1007/S004290050289

Jeon, C.J., Strettoi, E., Masland, R.H., 1998. The Major Cell Populations of the Mouse Retina. J. Neurosci. 18, 8936–8946. https://doi.org/10.1523/JNEUROSCI.18-21-08936.1998

Jonas, J.B., Schneider, U., Naumann, G.O.H., 1992. Count and density of human retinal photoreceptors. Graefes Arch. Clin. Exp. Ophthalmol. 230, 505–510. https://doi.org/10.1007/BF00181769

Kachi, S., Binley, K., Yokoi, K., Umeda, N., Akiyama, H., Muramatu, D., Iqball, S., Kan, O., Naylor, S., Campochiaro, P.A., 2009. Equine infectious anemia viral vector-mediated codelivery of endostatin and angiostatin driven by retinal pigmented epithelium-specific VMD2 promoter inhibits choroidal neovascularization. Hum. Gene Ther. 20, 31–39. https://doi.org/10.1089/hum.2008.046

Kanda, A., Dong, Y., Noda, K., Saito, W., Ishida, S., 2017. Advanced glycation endproducts link inflammatory cues to upregulation of galectin-1 in diabetic retinopathy. Sci. Reports 2017 71 7, 1–15. https://doi.org/10.1038/s41598-017-16499-8

Kant, S., Seth, G., Anthony, K., 2009. Vascular endothelial growth factor-A (VEGF-A) in vitreous fluid of patients with proliferative diabetic retinopathy. Ann. Ophthalmol. (Skokie). 41, 170–173.

Karnovsky, M.J., 1967. The ultrastructural basis of capillary permeability studied with peroxidase as a tracer. J. Cell Biol. 35, 213–236. https://doi.org/10.1083/JCB.35.1.213

Karsdal, M.A., 2019. Biochemistry of collagens, laminins and elastin: Structure, function and biomarkers, Biochemistry of Collagens, Laminins and Elastin: Structure, Function and Biomarkers. https://doi.org/10.1016/C2018-0-00074-2

Kaskan, P.M., Franco, E.C.S., Yamada, E.S., De Lima Silveira, L.C., Darlington, R.B., Finlay, B.L., 2005. Peripheral variability and central constancy in mammalian visual system evolution. Proc. R. Soc. B Biol. Sci. 272, 91–100. https://doi.org/10.1098/RSPB.2004.2925

Kaštelan, S., Orešković, I., Bišćan, F., Kaštelan, H., Gverović Antunica, A., 2020. Inflammatory and angiogenic biomarkers in diabetic retinopathy. Biochem. Medica 30, 1–15. https://doi.org/10.11613/BM.2020.030502

Kaul, K., Tarr, J.M., Ahmad, S.I., Kohner, E.M., Chibber, R., 2012. Introduction to diabetes mellitus. Adv. Exp. Med. Biol. 771, 1–11. https://doi.org/10.1007/978-1-4614-5441-0_1

Kernan, K.F., Carcillo, J.A., 2017. Hyperferritinemia and inflammation. Int. Immunol. 29, 401. https://doi.org/10.1093/INTIMM/DXX031

Kiagiadaki, F., Savvaki, M., Thermos, K., 2010. Activation of somatostatin receptor (sst5) protects the rat retina from AMPA-induced neurotoxicity. Neuropharmacology 58, 297–303. https://doi.org/10.1016/j.neuropharm.2009.06.028

Kim, J., Kim, C.-S., Lee, I.S., Lee, Y.M., Sohn, E., Jo, K., Kim, J.H., Kim, J.S., 2014. Extract of Litsea japonica ameliorates blood–retinal barrier breakdown in db/db mice. Endocrine 46, 462–469. https://doi.org/10.1007/s12020-013-0085-x

Kim, Y.M., Jang, J.W., Lee, O.H., Yeon, J., Choi, E.Y., Kim, K.W., Lee, S.T., Kwon, Y.G., 2000. Endostatin inhibits endothelial and tumor cellular invasion by blocking the activation and catalytic activity of matrix metalloproteinase 2. Cancer Res. 60, 5410–5413.

Kim, Young Mi, Hwang, S., Kim, Young Myoeng, Pyun, B.J., Kim, T.Y., Lee, S.T., Gho, Y.S., Kwon, Y.G., 2002. Endostatin blocks vascular endothelial growth factor-mediated signaling via direct interaction with KDR/Flk-1. J. Biol. Chem. 277, 27872–27879. https://doi.org/10.1074/JBC.M202771200

Kimura, K., Orita, T., Kobayashi, Y., Matsuyama, S., Fujimoto, K., Yamauchi, K., 2017. Concentration of acute phase factors in vitreous fluid in diabetic macular edema. Jpn. J. Ophthalmol. 61, 479–483. https://doi.org/10.1007/S10384-017-0525-X

Kinnunen, K., Korpisalo, P., Rissanen, T.T., Heikura, T., Viita, H., Uusitalo, H., Ylä-Herttuala, S., 2006. Overexpression of VEGF-A induces neovascularization and increased vascular leakage in rabbit eye after intravitreal adenoviral gene transfer. Acta Physiol. (Oxf). 187, 447–457. https://doi.org/10.1111/J.1748-1716.2006.01588.X

Kishimoto, A., Kimura, S., Nio-Kobayashi, J., Takahashi-Iwanaga, H., Park, A.M., Iwanaga, T., 2018. Histochemical characteristics of regressing vessels in the hyaloid vascular system of neonatal mice: Novel implication for vascular atrophy. Exp. Eye Res. 172, 1–9. https://doi.org/10.1016/j.exer.2018.03.024

Klaassen, I., Van Noorden, C.J.F., Schlingemann, R.O., 2013. Molecular basis of the inner blood-retinal barrier and its breakdown in diabetic macular edema and other pathological conditions. Prog. Retin. Eye Res. 34, 19–48. https://doi.org/10.1016/J.PRETEYERES.2013.02.001

Klingeborn, M., Dismuke, W.M., Bowes Rickman, C., Stamer, W.D., 2017. Roles of exosomes in the normal and diseased eye. Prog. Retin. Eye Res. https://doi.org/10.1016/j.preteyeres.2017.04.004

Knowland, D., Arac, A., Sekiguchi, K.J., Hsu, M., Lutz, S.E., Perrino, J., Steinberg, G.K., Barres, B.A., Nimmerjahn, A., Agalliu, D., 2014. Stepwise recruitment of transcellular and paracellular pathways underlies blood-brain barrier breakdown in stroke. Neuron 82, 603–617. https://doi.org/10.1016/J.NEURON.2014.03.003

Knutson, M.D., 2017. Iron transport proteins: Gateways of cellular and systemic iron homeostasis. J. Biol. Chem. 292, 12735. https://doi.org/10.1074/JBC.R117.786632

Kohgo, Y., Ikuta, K., Ohtake, T., Torimoto, Y., Kato, J., 2008. Body iron metabolism and pathophysiology of iron overload. Int. J. Hematol. 88, 7. https://doi.org/10.1007/S12185-008-0120-5

Köhler, K., Zahraoui, A., 2005. Tight junction: a co-ordinator of cell signalling and membrane trafficking. Biol. Cell 97, 659–665. https://doi.org/10.1042/BC20040147

Kokona, D., Mastrodimou, N., Pediaditakis, I., Charalampopoulos, I., Schmid, H.A., Thermos, K., 2012. Pasireotide (SOM230) protects the retina in animal models of ischemia induced retinopathies. Exp. Eye Res. 103, 90–98. https://doi.org/10.1016/J.EXER.2012.08.005

Kolb, H., 1995. Glial Cells of the Retina, Webvision: The Organization of the Retina and Visual System. University of Utah Health Sciences Center.

Kolb, H., Ralph, N., Eduardo, F., 1995. Webvision: The Organization of the Retina and Visual System [Internet]. Salt Lake City Univ. Utah Heal. Sci. Cent. 1995.

Kolnagou, A., Michaelides, Y., Kontoghiorghe, C.N., Kontoghiorghes, G.J., 2013. The importance of spleen, spleen iron, and splenectomy for determining total body iron load, ferrikinetics, and iron toxicity in thalassemia major patients. Toxicol. Mech. Methods 23, 34–41. https://doi.org/10.3109/15376516.2012.735278

Konerirajapuram, N.S., Coral, K., Punitham, R., Sharma, T., Kasinathan, N., Sivaramakrishnan, R., 2004. Trace elements iron, copper and zinc in vitreous of patients with various vitreoretinal diseases. Indian J. Ophthalmol. 52, 145–8.

Koto, T., Takubo, K., Ishida, S., Shinoda, H., Inoue, M., Tsubota, K., Okada, Y., Ikeda, E., 2007. Hypoxia disrupts the barrier function of neural blood vessels through changes in the expression of claudin-5 in endothelial cells. Am. J. Pathol. 170, 1389–1397. https://doi.org/10.2353/AJPATH.2007.060693

Kowluru, R.A., 2010. Role of Matrix Metalloproteinase-9 in the Development of Diabetic Retinopathy and Its Regulation by H-Ras. Invest. Ophthalmol. Vis. Sci. 51, 4320–4326. https://doi.org/10.1167/IOVS.09-4851

Kowluru, R.A., Chan, P.S., 2007. Oxidative Stress and Diabetic Retinopathy. Exp. Diabetes Res. 2007, 12. https://doi.org/10.1155/2007/43603

Kowluru, R.A., Mohammad, G., Dos Santos, J.M., Zhong, Q., 2011. Abrogation of MMP-9 Gene Protects Against the Development of Retinopathy in Diabetic Mice by Preventing Mitochondrial Damage. Diabetes 60, 3023. https://doi.org/10.2337/DB11-0816

Kumar, S., West, D.C., Ager, A., 1987. Heterogeneity in endothelial cells from large vessels and

microvessels. Differentiation. 36, 57–70. https://doi.org/10.1111/J.1432-0436.1987.TB00181.X

Kusuhara, S., Fukushima, Y., Ogura, S., Inoue, N., Uemura, A., 2018. Pathophysiology of Diabetic Retinopathy: The Old and the New. Diabetes Metab. J. 42, 364–376. https://doi.org/10.4093/DMJ.2018.0182

L'Esperance, F.A., 1998. The natural history and classification of diabetic retinopathy, in: Diabetic Renal-Retinal Syndrome. Springer Netherlands, pp. 117–150. https://doi.org/10.1007/978-94-011-4962-4_9

Lane, D.J.R., Bae, D.H., Merlot, A.M., Sahni, S., Richardson, D.R., 2015. Duodenal Cytochrome b (DCYTB) in Iron Metabolism: An Update on Function and Regulation. Nutr. 2015, Vol. 7, Pages 2274-2296 7, 2274–2296. https://doi.org/10.3390/NU7042274

Larsson, L.I., Nuija, E., 2001. Increased permeability of the blood-aqueous barrier after panretinal photocoagulation for proliferative diabetic retinopathy. Acta Ophthalmol. Scand. 79, 414–416. https://doi.org/10.1034/j.1600-0420.2001.079004414.x

Lattanzio, R., Cicinelli, M.V., Bandello, F., 2017. Intravitreal Steroids in Diabetic Macular Edema. Dev. Ophthalmol. 60, 78–90. https://doi.org/10.1159/000459691

Lechner, J., O'Leary, O.E., Stitt, A.W., 2017. The pathology associated with diabetic retinopathy. Vision Res. 139, 7–14. https://doi.org/10.1016/j.visres.2017.04.003

Lee, A.Y.W., Chung, S.S.M., 1999. Contributions of polyol pathway to oxidative stress in diabetic cataract. FASEB J. 13, 23–30. https://doi.org/10.1096/fasebj.13.1.23

Lee Ann, R.A., 2012. Clinical Anatomy and Physiology of the Visual System, Clinical Anatomy and Physiology of the Visual System. Elsevier Inc. https://doi.org/10.1016/C2009-0-56108-9

Lee, I.G., Chae, S.L., Kim, J.C., 2005. Involvement of circulating endothelial progenitor cells and vasculogenic factors in the pathogenesis of diabetic retinopathy. Eye 2006 205 20, 546–552. https://doi.org/10.1038/sj.eye.6701920

Lee, S.E., Ma, W., Rattigan, E.M., Aleshin, A., Chen, L., Johnson, L.L., D'Agati, V.D., Schmidt, A.M., Barile, G.R., 2010. Ultrastructural Features of Retinal Capillary Basement Membrane Thickening in Diabetic Swine. Ultrastruct. Pathol. 34, 35. https://doi.org/10.3109/01913120903308583

Lefevere, E., Van Hove, I., Sergeys, J., Steel, D.H.W., Schlingemann, R., Moons, L., Klaassen, I., 2021. PDGF as an Important Initiator for Neurite Outgrowth Associated with Fibrovascular Membranes in Proliferative Diabetic Retinopathy. https://doi.org/10.1080/02713683.2021.1966479

Léger, H., Santana, E., Beltran, W.A., Luca, F.C., 2019. Preparation of Mouse Retinal Cryo-sections for Immunohistochemistry. JoVE (Journal Vis. Exp. 2019, e59683. https://doi.org/10.3791/59683

Leiter, E.H., 2009. Selecting the "right" mouse model for metabolic syndrome and type 2 diabetes research. Methods Mol. Biol. 560, 1–17. https://doi.org/10.1007/978-1-59745-448-3_1

Lem, J., Krasnoperova, N. V., Calvert, P.D., Kosaras, B., Cameron, D.A., Nicolò, M., Makino, C.L., Sidman, R.L., 1999. Morphological, physiological, and biochemical changes in rhodopsin knockout mice. Proc. Natl. Acad. Sci. U. S. A. 96, 736–741. https://doi.org/10.1073/PNAS.96.2.736

Lenzen, S., 2008. The mechanisms of alloxan- and streptozotocin-induced diabetes. Diabetologia 51, 216–226. https://doi.org/10.1007/S00125-007-0886-7

Levi, S., Santambrogio, P., Cozzi, A., Rovida, E., Corsi, B., Tamborini, E., Spada, S., Albertini, A., Arosio, P., 1994. The Role of the L-Chain in Ferritin Iron Incorporation. J. Mol. Biol. 238, 649–654. https://doi.org/10.1006/jmbi.1994.1325

Levi, S., Yewdall, S.J., Harrison, P.M., Santambrogio, P., Cozzi, A., Rovida, E., Albertini, A.,

Arosio, P., 1992. Evidence that H- and L-chains have co-operative roles in the iron-uptake mechanism of human ferritin. Biochem. J. 288, 591–596. https://doi.org/10.1042/bj2880591

Lewis, G.P., Fisher, S.K., 2003. Up-regulation of glial fibrillary acidic protein in response to retinal injury: its potential role in glial remodeling and a comparison to vimentin expression. Int. Rev. Cytol. 230, 263–290. https://doi.org/10.1016/S0074-7696(03)30005-1

Li, J., Wang, J.J., Yu, Q., Chen, K., Mahadev, K., Zhang, S.X., 2010. Inhibition of Reactive Oxygen Species by Lovastatin Downregulates Vascular Endothelial Growth Factor Expression and Ameliorates Blood-Retinal Barrier Breakdown in db / db Mice. Diabetes 59, 1528–1538. https://doi.org/10.2337/db09-1057

Li, J.Y., Paragas, N., Ned, R.M., Qiu, A., Viltard, M., Leete, T., Drexler, I.R., Chen, X., Sanna-Cherchi, S., Mohammed, F., Williams, D., Lin, C.S., Schmidt-Ott, K.M., Andrews, N.C., Barasch, J., 2009a. Scara5 Is a Ferritin Receptor Mediating Non-Transferrin Iron Delivery. Dev. Cell 16, 35–46. https://doi.org/10.1016/j.devcel.2008.12.002

Li, J.Y., Paragas, N., Ned, R.M., Qiu, A., Viltard, M., Leete, T., Drexler, I.R., Chen, X., Sanna-Cherchi, S., Mohammed, F., Williams, D., Lin, C.S., Schmidt-Ott, K.M., Andrews, N.C., Barasch, J., 2009b. Scara5 is a ferritin receptor mediating non-transferrin iron delivery. Dev. Cell 16, 35–46. https://doi.org/10.1016/J.DEVCEL.2008.12.002

Li, Y., Li, L., Li, Z., Sheng, J., Zhang, Xinke, Feng, D., Zhang, Xu, Yin, F., Wang, A., Wang, F., 2016. Tat PTD-Endostatin-RGD: A novel protein with anti-angiogenesis effect in retina via eye drops. Biochim. Biophys. Acta - Gen. Subj. 1860, 2137–2147. https://doi.org/10.1016/j.bbagen.2016.05.031

Lieth, E., Barber, A.J., Xu, B., Dice, C., Ratz, M.J., Tanase, D., Strother, J.M., 1998. Glial reactivity and impaired glutamate metabolism in short-term experimental diabetic retinopathy. Penn State Retina Research Group. Diabetes 47, 815–820. https://doi.org/10.2337/DIABETES.47.5.815

Lin, Y., Xiao, Y.C., Zhu, H., Xu, Q.Y., Qi, L., Wang, Y. Bin, Li, X.J., Zheng, M.L., Zhong, R.S., Zhang, Y., Xu, X.D., Wu, B. Le, Xu, Z.M., Lu, X.H., 2014. Serum fibroblast growth factor 21 levels are correlated with the severity of diabetic retinopathy. J. Diabetes Res. 2014. https://doi.org/10.1155/2014/929756

Liu, F., Koval, M., Ranganathan, S., Fanayan, S., Hancock, W.S., Lundberg, E.K., Beavis, R.C., Lane, L., Duek, P., McQuade, L., Kelleher, N.L., Baker, M.S., 2016. Systems Proteomics View of the Endogenous Human Claudin Protein Family. J. Proteome Res. 15, 339–359. https://doi.org/10.1021/ACS.JPROTEOME.5B00769

Liu, G., Chen, L., Cai, Q., Wu, H., Chen, Z., Zhang, X., Lu, P., 2018. Streptozotocin-induced diabetic mice exhibit reduced experimental choroidal neovascularization but not corneal neovascularization. Mol. Med. Rep. 18, 4388–4398. https://doi.org/10.3892/MMR.2018.9445/HTML

Liu, J., Li, Q., Yang, Y., Ma, L., 2020. Iron metabolism and type 2 diabetes mellitus: A meta-analysis and systematic review. J. Diabetes Investig. 11, 946–955. https://doi.org/10.1111/JDI.13216

Liu, Y., Leo, L.F., McGregor, C., Grivitishvili, A., Barnstable, C.J., Tombran-Tink, J., 2012. Pigment epithelium-derived factor (PEDF) peptide eye drops reduce inflammation, cell death and vascular leakage in diabetic retinopathy in Ins2(Akita) mice. Mol. Med. 18, 1387–1401. https://doi.org/10.2119/MOLMED.2012.00008/FIGURES/12

Lopes de Faria, J.M., Russ, H., Costa, V.P., 2002. Retinal nerve fibre layer loss in patients with type 1 diabetes mellitus without retinopathy. Br. J. Ophthalmol. 86, 725. https://doi.org/10.1136/BJO.86.7.725

Loukovaara, S., Robciuc, A., Holopainen, J.M., Lehti, K., Pessi, T., Liinamaa, J., Kukkonen, K.T., Jauhiainen, M., Koli, K., Keski-Oja, J., Immonen, I., 2013. Ang-2 upregulation correlates with increased levels of MMP-9, VEGF, EPO and TGFβ1 in diabetic eyes undergoing vitrectomy. Acta Ophthalmol. 91, 531–539. https://doi.org/10.1111/J.1755-3768.2012.02473.X

Luo, Y., Xiao, W., Zhu, X., Mao, Y., Liu, X., Chen, X., Huang, J., Tang, S., Rizzolo, L.J., 2011. Differential Expression of Claudins in Retinas during Normal Development and the Angiogenesis of Oxygen-Induced Retinopathy. Invest. Ophthalmol. Vis. Sci. 52, 7556–7564. https://doi.org/10.1167/IOVS.11-7185

Määttä, M., Heljasvaara, R., Pihlajaniemi, T., Uusitalo, M., 2007. Collagen XVIII/endostatin shows a ubiquitous distribution in human ocular tissues and endostatin-containing fragments accumulate in ocular fluid samples, in: Graefe's Archive for Clinical and Experimental Ophthalmology. pp. 74–81. https://doi.org/10.1007/s00417-006-0281-y

Manikandan, A., Ganesh, M., Silambanan, S., 2015. RESEARCH ARTICLE STUDY OF IRON STATUS IN TYPE 2 DIABETES MELLITUS. Int. J. Clin. Biochem. Res. 2, 77–82.

Marneros, A.G., Keene, D.R., Hansen, U., Fukai, N., Moulton, K., Goletz, P.L., Moiseyev, G., Pawlyk, B.S., Halfter, W., Dong, S., Shibata, M., Li, T., Crouch, R.K., Bruckner, P., Olsen, B.R., 2004. Collagen XVIII/endostatin is essential for vision and retinal pigment epithelial function. EMBO J. 23, 89–99. https://doi.org/10.1038/sj.emboj.7600014

Martín-Granado, V., Ortiz-Rivero, S., Carmona, R., Herrero, S.G., Barrera, M., San-Segundo, L., Sequera, C., Perdiguero, P., Lozano, F., Martín-Herrero, F., González-Porras, J.R., Muñoz-Chápuli, R., Porras, A., Guerrero, C., 2017. C3G promotes a selective release of angiogenic factors from activated mouse platelets to regulate angiogenesis and tumor metastasis. Oncotarget 8, 110994–111011. https://doi.org/10.18632/oncotarget.22339

Martìn-Padura, I., Lostaglio, S., Schneemann, M., Williams, L., Romano, M., Fruscella, P., Panzeri, C., Stoppacciaro, A., Ruco, L., Villa, A., Simmons, D., Dejana, E., 1998. Junctional adhesion molecule, a novel member of the immunoglobulin superfamily that distributes at intercellular junctions and modulates monocyte transmigration. J. Cell Biol. 142, 117–127. https://doi.org/10.1083/JCB.142.1.117

Masland, R.H., 2011. Cell Populations of the Retina: The Proctor Lecture. Invest. Ophthalmol. Vis. Sci. 52, 4581–4591. https://doi.org/10.1167/IOVS.10-7083

May, C.A., Ohlmann, A. V., Hammes, H., Spandau, U.H.M., 2006. Proteins with an endostatin-like domain in a mouse model of oxygen-induced retinopathy. Exp. Eye Res. 82, 341–348. https://doi.org/10.1016/j.exer.2005.07.005

Mayle, K.M., Le, A.M., Kamei, D.T., 2012. The Intracellular Trafficking Pathway of Transferrin. Biochim. Biophys. Acta 1820, 264. https://doi.org/10.1016/J.BBAGEN.2011.09.009

McCarthy, R.C., Kosman, D.J., 2015. Mechanisms and regulation of iron trafficking across the capillary endothelial cells of the blood-brain barrier. Front. Mol. Neurosci. 8, 31. https://doi.org/10.3389/FNMOL.2015.00031/BIBTEX

McDonald, H.R., Schatz, H., 1985. Visual loss following panretinal photocoagulation for proliferative diabetic retinopathy. Ophthalmology 92, 388–393. https://doi.org/10.1016/S0161-6420(85)34016-2

McGahan, M.C., Harned, J., Mukunnemkeril, M., Goralska, M., Fleisher, L., Ferrell, J.B., 2005. Iron alters glutamate secretion by regulating cytosolic aconitase activity. Am. J. Physiol. Cell Physiol. 288. https://doi.org/10.1152/AJPCELL.00444.2004

McLenachan, S., Magno, A.L., Ramos, D., Catita, J., McMenamin, P.G., Chen, F.K., Rakoczy, E.P., Ruberte, J., 2015. Angiography reveals novel features of the retinal vasculature in healthy and diabetic mice. Exp. Eye Res. 138, 6–21. https://doi.org/10.1016/j.exer.2015.06.023

Mendes-Jorge, L., Ramos, D., Valença, A., López-Luppo, M., Pires, V.M.R., Catita, J., Nacher, V., Navarro, M., Carretero, A., Rodriguez-Baeza, A., Ruberte, J., 2014. L-Ferritin Binding to Scara5: A New Iron Traffic Pathway Potentially Implicated in Retinopathy. PLoS One 9, e106974. https://doi.org/10.1371/journal.pone.0106974

Meneghini, R., 1997. Iron Homeostasis, Oxidative Stress, and DNA Damage. Free Radic. Biol. Med. 23, 783–792. https://doi.org/10.1016/S0891-5849(97)00016-6

Meneses, P.I., Hajjar, K.A., Berns, K.I., Duvoisin, R.M., 2001. Recombinant angiostatin prevents retinal neovascularization in a murine proliferative retinopathy model. Gene Ther. 2001 88 8, 646–648. https://doi.org/10.1038/sj.gt.3301423

Mezzanotte, M., Ammirata, G., Boido, M., Stanga, S., Roetto, A., 2021. BBB damage in aging causes brain iron deposits via astrocyte-neuron crosstalk and Hepc/Fpn1 pathway. bioRxiv 2021.07.01.450665. https://doi.org/10.1101/2021.07.01.450665

Milic, S., Mikolasevic, I., Orlic, L., Devcic, E., Starcevic-Cizmarevic, N., Stimac, D., Kapovic, M., Ristic, S., 2016. The Role of Iron and Iron Overload in Chronic Liver Disease. Med. Sci. Monit. 22, 2144. https://doi.org/10.12659/MSM.896494

Miller, D.D., Berner, L.A., 1989. Is solubility in vitro a reliable predictor of iron bioavailability? Biol. Trace Elem. Res. 19, 11–24. https://doi.org/10.1007/BF02925446

Miller, H., Miller, B., Zonis, S., Nir, I., 1984. Diabetic neovascularization: permeability and ultrastructure. Invest. Ophthalmol. Vis. Sci. 25, 1338–1342.

Miller, J.L., 2013. Iron deficiency anemia: A common and curable disease. Cold Spring Harb. Perspect. Med. 3. https://doi.org/10.1101/cshperspect.a011866

Miosge, N., Simniok, T., Sprysch, P., Herken, R., 2003. The collagen type XVIII endostatin domain is co-localized with perlecan in basement membranes in vivo. J. Histochem. Cytochem. 51, 285–296. https://doi.org/10.1177/002215540305100303

Misra, G., Bhatter, S.K., Kumar, A., Gupta, V., Khan, M.Y., 2016. Iron Profile and Glycaemic Control in Patients with Type 2 Diabetes Mellitus. Med. Sci. 4, 22. https://doi.org/10.3390/MEDSCI4040022

Mohammad, G., Kowluru, R.A., 2011. Novel Role of Mitochondrial Matrix Metalloproteinase-2 in the Development of Diabetic Retinopathy. Invest. Ophthalmol. Vis. Sci. 52, 3832. https://doi.org/10.1167/IOVS.10-6368

Moiseyev, G., Takahashi, Y., Chen, Y., Gentleman, S., Redmond, T.M., Crouch, R.K., Ma, J.X., 2006a. RPE65 is an iron(II)-dependent isomerohydrolase in the retinoid visual cycle. J. Biol. Chem. 281, 2835–2840. https://doi.org/10.1074/JBC.M508903200

Moiseyev, G., Takahashi, Y., Chen, Y., Gentleman, S., Redmond, T.M., Crouch, R.K., Ma, J.X., 2006b. RPE65 is an iron(II)-dependent isomerohydrolase in the retinoid visual cycle. J. Biol. Chem. 281, 2835–2840. https://doi.org/10.1074/JBC.M508903200

Moore, T.C.B., Moore, J.E., Kaji, Y., Frizzell, N., Usui, T., Poulaki, V., Campbell, I.L., Stitt, A.W., Gardiner, T.A., Archer, D.B., Adamis, A.P., 2003. The Role of Advanced Glycation End Products in Retinal Microvascular Leukostasis. Invest. Ophthalmol. Vis. Sci. 44, 4457–4464. https://doi.org/10.1167/IOVS.02-1063

Moos, T., Trinder, D., Morgan, E.H., 2002. Effect of iron status on DMT1 expression in duodenal enterocytes from β2-microglobulin knockout mice. Am. J. Physiol. - Gastrointest. Liver Physiol. 283. https://doi.org/10.1152/AJPGI.00346.2001/ASSET/IMAGES/LARGE/H30920958007.JPEG

Morgan, J.W., ANDERSt, E., Cu, M., Ga Ge, Z., 1980. Chemical composition of Earth, Venus, and Mercury. Proc. Natl. Acad. Sci. 77, 6973–6977. https://doi.org/10.1073/PNAS.77.12.6973

Muir, A., Hopfer, U., 1985. Regional specificity of iron uptake by small intestinal brush-border membranes from normal and iron-deficient mice. Am. J. Physiol. - Gastrointest. Liver Physiol. 11. https://doi.org/10.1152/ajpgi.1985.248.3.g376

Munro, H.N., 1990. Iron regulation of ferritin gene expression. J. Cell. Biochem. 44, 107–115. https://doi.org/10.1002/jcb.240440205

Murakami, T., Felinski, E.A., Antonetti, D.A., 2009. Occludin phosphorylation and ubiquitination regulate tight junction trafficking and vascular endothelial growth factor-induced permeability. J. Biol. Chem. 284, 21036–21046. https://doi.org/10.1074/JBC.M109.016766

Murakami, T., Frey, T., Lin, C., Antonetti, D.A., 2012. Protein kinase Cβ phosphorylates occludin regulating tight junction trafficking in vascular endothelial growth factor - Induced permeability in vivo. Diabetes 61, 1573–1583. https://doi.org/10.2337/db11-1367

Murphy, C.J., Oudit, G.Y., 2010. Iron-overload cardiomyopathy: pathophysiology, diagnosis, and treatment. J. Card. Fail. 16, 888–900. https://doi.org/10.1016/J.CARDFAIL.2010.05.009

Mustafi, D., Engel, A.H., Palczewski, K., 2009. Structure of cone photoreceptors. Prog. Retin. Eye Res. 28, 289–302. https://doi.org/10.1016/J.PRETEYERES.2009.05.003

Musumeci, M., Maccari, S., Massimi, A., Stati, T., Sestili, P., Corritore, E., Pastorelli, A., Stacchini, P., Marano, G., Catalano, L., 2014. Iron excretion in iron dextran-overloaded mice. Blood Transfus. 12, 485. https://doi.org/10.2450/2014.0288-13

Muthusamy, A., Lin, C.M., Shanmugam, S., Lindner, H.M., Abcouwer, S.F., Antonetti, D.A., 2014. Ischemia-reperfusion injury induces occludin phosphorylation/ubiquitination and retinal vascular permeability in a VEGFR-2-dependent manner. J. Cereb. Blood Flow Metab. 34, 522–531. https://doi.org/10.1038/jcbfm.2013.230

Nagineni, C.N., Kommineni, V.K., William, A., Detrick, B., Hooks, J.J., 2012. Regulation of VEGF expression in human retinal cells by cytokines: implications for the role of inflammation in age-related macular degeneration. J. Cell. Physiol. 227, 116–126. https://doi.org/10.1002/JCP.22708

Nawaz, I.M., Rezzola, S., Cancarini, A., Russo, A., Costagliola, C., Semeraro, F., Presta, M., 2019. Human vitreous in proliferative diabetic retinopathy: Characterization and translational implications. Prog. Retin. Eye Res. 72. https://doi.org/10.1016/J.PRETEYERES.2019.03.002

Naylor, A., Hopkins, A., Hudson, N., Campbell, M., 2020. Tight Junctions of the Outer Blood Retina Barrier. Int. J. Mol. Sci. 21. https://doi.org/10.3390/IJMS21010211

Nehls, V., Drenckhahn, D., 1991. Heterogeneity of microvascular pericytes for smooth muscle type alpha-actin. J. Cell Biol. 113, 147–154. https://doi.org/10.1083/jcb.113.1.147

Nguyen, N.T., Nguyen, X.M.T., Lane, J., Wang, P., 2011. Relationship between obesity and diabetes in a US adult population: findings from the National Health and Nutrition Examination Survey, 1999-2006. Obes. Surg. 21, 351–355. https://doi.org/10.1007/S11695-010-0335-4

Nitta, T., Hata, M., Gotoh, S., Seo, Y., Sasaki, H., Hashimoto, N., Furuse, M., Tsukita, S., 2003. Size-selective loosening of the blood-brain barrier in claudin-5-deficient mice. J. Cell Biol. 161, 653–660. https://doi.org/10.1083/JCB.200302070

Noda, K., Ishida, S., Inoue, M., Obata, K.I., Oguchi, Y., Okada, Y., Ikeda, E., 2003. Production and Activation of Matrix Metalloproteinase-2 in Proliferative Diabetic Retinopathy. Invest. Ophthalmol. Vis. Sci. 44, 2163–2170. https://doi.org/10.1167/IOVS.02-0662

Noma, H., Funatsu, H., Yamashita, H., Kitano, S., Mishima, H.K., Hori, S., 2002. Regulation of angiogenesis in diabetic retinopathy: Possible balance between vascular endothelial growth factor and endostatin. Arch. Ophthalmol. 120, 1075–1080. https://doi.org/10.1001/archopht.120.8.1075

O'Reilly, M.S., Boehm, T., Shing, Y., Fukai, N., Vasios, G., Lane, W.S., Flynn, E., Birkhead, J.R., Olsen, B.R., Folkman, J., 1997. Endostatin: An endogenous inhibitor of angiogenesis and tumor growth. Cell 88, 277–285. https://doi.org/10.1016/S0092-8674(00)81848-6

Ogura, S., Kurata, K., Hattori, Y., Takase, H., Ishiguro-Oonuma, T., Hwang, Y., Ahn, S., Park, I., Ikeda, W., Kusuhara, S., Fukushima, Y., Nara, H., Sakai, H., Fujiwara, T., Matsushita, J., Ema, M., Hirashima, M., Minami, T., Shibuya, M., Takakura, N., Kim, P., Miyata, T., Ogura, Y., Uemura, A., 2017. Sustained inflammation after pericyte depletion induces irreversible blood-retina barrier breakdown. JCI insight 2. https://doi.org/10.1172/JCI.INSIGHT.90905

Ohlmann, Anne V., Adamek, E., Ohlmann, Andreas, Lütjen-Drecoll, E., 2004. Norrie gene product is necessary for regression of hyaloid vessels. Investig. Ophthalmol. Vis. Sci. 45, 2384–

2390. https://doi.org/10.1167/iovs.03-1214

Ohlmann, Anne V., Ohlmann, Andreas, Welge-Lüssen, U., May, C.A., 2005. Localization of collagen XVIII and endostatin in the human eye. Curr. Eye Res. 30, 27–34. https://doi.org/10.1080/02713680490894333

Okawa, H., Sampath, A.P., Laughlin, S.B., Fain, G.L., 2008. ATP consumption by mammalian rod photoreceptors in darkness and in light. Curr. Biol. 18, 1917–1921. https://doi.org/10.1016/J.CUB.2008.10.029

Overby, D.R., Bertrand, J., Schicht, M., Paulsen, F., Daniel Stamer, W., Lütjen-Drecoll, E., 2014. The Structure of the Trabecular Meshwork, Its Connections to the Ciliary Muscle, and the Effect of Pilocarpine on Outflow Facility in Mice. Invest. Ophthalmol. Vis. Sci. 55, 3727. https://doi.org/10.1167/IOVS.13-13699

Ozaki, H., Hayashi, H., Vinores, S.A., Moromizato, Y., Campochiaro, P.A., Oshima, K., 1997. Intravitreal sustained release of VEGF causes retinal neovascularization in rabbits and breakdown of the blood-retinal barrier in rabbits and primates. Exp. Eye Res. 64, 505–517. https://doi.org/10.1006/EXER.1996.0239

Ozaki, H., Yu, A.Y., Della, N., Ozaki, K., Luna, J.D., Yamada, H., Hackett, S.F., Okamoto, N., D J Zack, G.L.S., Campochiaro, P.A., 1999. Hypoxia inducible factor-1alpha is increased in ischemic retina: temporal and spatial correlation with VEGF expression. | IOVS | ARVO Journals. Invest Ophthalmol Vis Sci 40, 182–9.

Özen, I., Boix, J., Paul, G., 2012. Perivascular mesenchymal stem cells in the adult human brain: a future target for neuroregeneration? Clin. Transl. Med. 1. https://doi.org/10.1186/2001-1326-1-30

Palm, E., 1947. ON THE OCCURRENCE IN THE RETINA OF CONDITIONS CORRESPONDING TO THE «BLOOD-BRAIN BARRIER». Acta Ophthalmol. 25, 29–35. https://doi.org/10.1111/j.1755-3768.1947.tb07542.x

Pamphlett, R., Cherepanoff, S., Too, L.K., Jew, S.K., Doble, P.A., Bishop, D.P., 2020. The distribution of toxic metals in the human retina and optic nerve head: Implications for age-related macular degeneration. PLoS One 15. https://doi.org/10.1371/JOURNAL.PONE.0241054

Paques, M., Tadayoni, R., Sercombe, R., Laurent, P., Genevois, O., Gaudric, A., Vicaut, E., 2003a. Structural and Hemodynamic Analysis of the Mouse Retinal Microcirculation. Investig. Ophthalmol. Vis. Sci. 44, 4960–4967. https://doi.org/10.1167/iovs.02-0738

Paques, M., Tadayoni, R., Sercombe, R., Laurent, P., Genevois, O., Gaudric, A., Vicaut, E., 2003b. Structural and Hemodynamic Analysis of the Mouse Retinal Microcirculation. Invest. Ophthalmol. Vis. Sci. 44, 4960–4967. https://doi.org/10.1167/IOVS.02-0738

Park, S.H., Park, J.W., Park, S.J., Kim, K.Y., Chung, J.W., Chun, M.H., Oh, S.J., 2003. Apoptotic death of photoreceptors in the streptozotocin-induced diabetic rat retina. Diabetologia 46, 1260–1268. https://doi.org/10.1007/S00125-003-1177-6

Park, S.W., Yun, J.H., Kim, Jin Hyoung, Kim, K.W., Cho, C.H., Kim, Jeong Hun, 2014. Angiopoietin 2 Induces Pericyte Apoptosis via α3β1 Integrin Signaling in Diabetic Retinopathy. Diabetes 63, 3057–3068. https://doi.org/10.2337/DB13-1942

Patel, J.I., Jenkins, L., Benjamin, L., Webber, S., 2002. Dilated pupils and loss of accommodation following diode panretinal photocoagulation with sub-tenon local anaesthetic in four cases. Eye (Lond). 16, 628–632. https://doi.org/10.1038/SJ.EYE.6700004

Paul, B.T., Manz, D.H., Torti, F.M., Torti, S. V., 2017. Mitochondria and Iron: current questions. Expert Rev. Hematol. 10, 65–79. https://doi.org/10.1080/17474086.2016.1268047

Pe'er, J., Folberg, R., Itin, A., Gnessin, H., Hemo, I., Keshet, E., 1998. Vascular endothelial growth factor upregulation in human central retinal vein occlusion. Ophthalmology 105, 412–416. https://doi.org/10.1016/S0161-6420(98)93020-2

Pehrsson, M., Bager, C.L., Karsdal, M.A., 2019. Type XVIII collagen, Second Edi. ed, Biochemistry of Collagens, Laminins and Elastin: Structure, Function and Biomarkers. Elsevier Inc. https://doi.org/10.1016/B978-0-12-817068-7.00018-5

Peichl, L., 2005. Diversity of mammalian photoreceptor properties: Adaptations to habitat and lifestyle? Anat. Rec. Part A Discov. Mol. Cell. Evol. Biol. 287A, 1001–1012. https://doi.org/10.1002/AR.A.20262

Peichl, L., Sandmann, D., Boycott, B.B., 1998. Comparative Anatomy and Function of Mammalian Horizontal Cells, in: Development and Organization of the Retina. Springer, Boston, MA, pp. 147–172. https://doi.org/10.1007/978-1-4615-5333-5_9

Perls, 1868. Nachweis von Eisenoxyd in gewissen Pigmenten. J. Prakt. Chemie 105, 281–287. https://doi.org/10.1002/prac.18681050136

Petrovič, D., 2013. Candidate genes for proliferative diabetic retinopathy. Biomed Res. Int. https://doi.org/10.1155/2013/540416

Picard, E., Daruich, A., Youale, J., Courtois, Y., Behar-Cohen, F., 2020. From Rust to Quantum Biology: The Role of Iron in Retina Physiopathology. Cells 9. https://doi.org/10.3390/CELLS9030705

Pirpamer, L., Hofer, E., Gesierich, B., De Guio, F., Freudenberger, P., Seiler, S., Duering, M., Jouvent, E., Duchesnay, E., Dichgans, M., Ropele, S., Schmidt, R., 2016. Determinants of iron accumulation in the normal aging brain. Neurobiol. Aging 43, 149–155. https://doi.org/10.1016/J.NEUROBIOLAGING.2016.04.002

Poulaki, V., Joussen, A.M., Mitsiades, N., Mitsiades, C.S., Iliaki, E.F., Adamis, A.P., 2004. Insulin-like growth factor-I plays a pathogenetic role in diabetic retinopathy. Am. J. Pathol. 165, 457–469. https://doi.org/10.1016/S0002-9440(10)63311-1

Praidou, A., Androudi, S., Brazitikos, P., Karakiulakis, G., Papakonstantinou, E., Dimitrakos, S., 2010. Angiogenic growth factors and their inhibitors in diabetic retinopathy. Curr. Diabetes Rev. 6, 304–312. https://doi.org/10.2174/157339910793360815

Przybyszewska, J., Zekanowska, E., 2014. The role of hepcidin, ferroportin, HCP1, and DMT1 protein in iron absorption in the human digestive tract. Przegląd Gastroenterol. 9, 208. https://doi.org/10.5114/PG.2014.45102

Puig, S., Ramos-Alonso, L., Romero, A.M., Martínez-Pastor, M.T., 2017. The elemental role of iron in DNA synthesis and repair. Metallomics 9, 1483–1500. https://doi.org/10.1039/C7MT00116A

Quiroz, J., Yazdanyar, A., 2021. Animal models of diabetic retinopathy. Ann. Transl. Med. 9. https://doi.org/10.21037/ATM-20-6737

Raja, K.B., Simpson, R.J., Pippard, M.J., Peters, T.J., 1988. In vivo studies on the relationship between intestinal iron (Fe3+) absorption, hypoxia and erythropoiesis in the mouse. Br. J. Haematol. 68, 373–378. https://doi.org/10.1111/J.1365-2141.1988.TB04217.X

Rakoczy, E.P., Ali Rahman, I.S., Binz, N., Li, C.R., Vagaja, N.N., De Pinho, M., Lai, C.M., 2010. Characterization of a mouse model of hyperglycemia and retinal neovascularization. Am. J. Pathol. 177, 2659–2670. https://doi.org/10.2353/AJPATH.2010.090883

Raman, P., Singal, A.K., Behl, A., 2019. Effect of Insulin-Like Growth Factor-1 on Diabetic Retinopathy in Pubertal Age Patients With Type 1 Diabetes. Asia-Pacific J. Ophthalmol. 8, 319–323. https://doi.org/10.1097/APO.0000000000000250

Ramesh, S., Bonshek, R.E., Bishop, P.N., 2004. Immunolocalisation of opticin in the human eye. Br. J. Ophthalmol. 88, 697–702. https://doi.org/10.1136/bjo.2003.031989

Ramón y Cajal S. La rétine des Vertébrés. La Cellule 1893; 9: 119–257

Ramos, D., Carretero, A., Navarro, M., Mendes-Jorge, L., Nacher, V., Rodriguez-Baeza, A., Ruberte, J., 2013a. Mimicking Microvascular Alterations of Human Diabetic Retinopathy: A Challenge for the Mouse Models. Curr. Med. Chem. 20, 3200–3217.

https://doi.org/10.2174/09298673113209990028

Ramos, D., Carretero, A., Navarro, M., Mendes-Jorge, L., Rodriguez-Baeza, A., Nacher, V., Ruberte, J., 2013b. Mouse models of diabetic retinopathy. Drug Discov. Today Dis. Model. https://doi.org/10.1016/j.ddmod.2014.02.002

Ramos, David, Navarro, M., Mendes-Jorge, L., Carretero, A., López-Luppo, M., Nacher, V., Rodríguez-Baeza, A., Ruberte, J., 2013. The Use of Confocal Laser Microscopy to Analyze Mouse Retinal Blood Vessels. Confocal Laser Microsc. - Princ. Appl. Med. Biol. Food Sci. https://doi.org/10.5772/56131

Raviola, G., 1977. The structural basis of the blood-ocular barriers. Exp. Eye Res. 25, 27–63. https://doi.org/10.1016/S0014-4835(77)80009-2

Reddy, M.A., Natarajan, R., 2011. Epigenetic mechanisms in diabetic vascular complications. Cardiovasc. Res. 90, 421–429. https://doi.org/10.1093/CVR/CVR024

Remington, L.A., 2012. Retina, in: Clinical Anatomy and Physiology of the Visual System. Elsevier, pp. 61–92. https://doi.org/10.1016/B978-1-4377-1926-0.10004-9

Rezzola, S., Belleri, M., Gariano, G., Ribatti, D., Costagliola, C., Semeraro, F., Presta, M., 2014. In vitro and ex vivo retina angiogenesis assays. Angiogenesis 17, 429–442. https://doi.org/10.1007/S10456-013-9398-X/FIGURES/3

Richardson, D.R., Ponka, P., 1997. The molecular mechanisms of the metabolism and transport of iron in normal and neoplastic cells. Biochim. Biophys. Acta 1331, 1–40. https://doi.org/10.1016/S0304-4157(96)00014-7

Risau, W., 1997. Mechanisms of angiogenesis. Nature. https://doi.org/10.1038/386671a0

Ritter, M.R., Aguilar, E., Banin, E., Scheppke, L., Uusitalo-Jarvinen, H., Friedlander, M., 2005. Three-dimensional in vivo imaging of the mouse intraocular vasculature during development and disease. Investig. Ophthalmol. Vis. Sci. 46, 3021–3026. https://doi.org/10.1167/iovs.05-0153

Robinson, R., Barathi, V.A., Chaurasia, S.S., Wong, T.Y., Kern, T.S., 2012. Update on animal models of diabetic retinopathy: From molecular approaches to mice and higher mammals. DMM Dis. Model. Mech. https://doi.org/10.1242/dmm.009597

Rodrigues, M., Xin, X., Jee, K., Babapoor-Farrokhran, S., Kashiwabuchi, F., Ma, T., Bhutto, I., Hassan, S.J., Daoud, Y., Baranano, D., Solomon, S., Lutty, G., Semenza, G.L., Montaner, S., Sodhi, A., 2013. VEGF secreted by hypoxic Müller cells induces MMP-2 expression and activity in endothelial cells to promote retinal neovascularization in proliferative diabetic retinopathy. Diabetes 62, 3863–3873. https://doi.org/10.2337/DB13-0014

Rogers, B.S., Symons, R.C.A., Komeima, K., Shen, J.K., Xiao, W., Swaim, M.E., Yuan, Y.G., Kachi, S., Campochiaro, P.A., 2007. Differential sensitivity of cones to iron-mediated oxidative damage. Invest. Ophthalmol. Vis. Sci. 48, 438–445. https://doi.org/10.1167/IOVS.06-0528

Roy, S., Ha, J., Trudeau, K., Beglova, E., 2010. Vascular basement membrane thickening in diabetic retinopathy. Curr. Eye Res. https://doi.org/10.3109/02713683.2010.514659

Roy, S., Kim, D., 2021. Retinal capillary basement membrane thickening: Role in the pathogenesis of diabetic retinopathy. Prog. Retin. Eye Res. 82. https://doi.org/10.1016/J.PRETEYERES.2020.100903

Ruberte, J., Ayuso, E., Navarro, M., Carretero, A., Nacher, V., Haurigot, V., George, M., Llombart, C., Casellas, A., Costa, C., Bosch, A., Bosch, F., 2004. Increased ocular levels of IGF-1 in transgenic mice lead to diabetes-like eye disease. J. Clin. Invest. 113, 1149. https://doi.org/10.1172/JCI19478

Ruberte, J., Carretero, A., Navarro, M., 2017. Morphological Mouse Phenotyping: Anatomy, Histology and Imaging, Morphological Mouse Phenotyping: Anatomy, Histology and Imaging.

Rucker, P., Torti, F.M., Torti, S. V., 1996. Role of H and L Subunits in Mouse Ferritin ". J. Biol. Chem. 271, 33352–33357. https://doi.org/10.1074/JBC.271.52.33352

Saadane, A., Lessieur, E.M., Du, Y., Liu, H., Kern, T.S., 2020. Successful induction of diabetes in mice demonstrates no gender difference in development of early diabetic retinopathy. PLoS One 15, e0238727. https://doi.org/10.1371/JOURNAL.PONE.0238727

Saha, S., Murgod, R., 2019. Evaluation of Iron Profile in Type II Diabetes Mellitus Cases. Int. J. Biotechnol. Biochem. 15, 27–37.

Sahni, J., Patel, S.S., Dugel, P.U., Khanani, A.M., Jhaveri, C.D., Wykoff, C.C., Hershberger, V.S., Pauly-Evers, M., Sadikhov, S., Szczesny, P., Schwab, D., Nogoceke, E., Osborne, A., Weikert, R., Fauser, S., 2019. Simultaneous Inhibition of Angiopoietin-2 and Vascular Endothelial Growth Factor-A with Faricimab in Diabetic Macular Edema: BOULEVARD Phase 2 Randomized Trial. Ophthalmology 126, 1155–1170. https://doi.org/10.1016/J.OPHTHA.2019.03.023

Saint-Geniez, M., D'Amore, P.A., 2004. Development and pathology of the hyaloid, choroidal and retinal vasculature. Int. J. Dev. Biol. 48, 1045–1058. https://doi.org/10.1387/ijdb.041895ms

Sasai, H., Sairenchi, T., Iso, H., Irie, F., Otaka, E., Tanaka, K., Ota, H., Muto, T., 2010. Relationship Between Obesity and Incident Diabetes in Middle-Aged and Older Japanese Adults: The Ibaraki Prefectural Health Study. Mayo Clin. Proc. 85, 36. https://doi.org/10.4065/MCP.2009.0230

Sato, T., Shapiro, J.S., Chang, H.C., Miller, R.A., Ardehali, H., 2022. Aging is associated with increased brain iron through cortex-derived hepcidin expression. Elife 11. https://doi.org/10.7554/ELIFE.73456

Schaller, O., Constantinescu, G.M., 2007. Illustrated veterinary anatomical nomenclature 614.

Schnitzer, J., 1988. Astrocytes in the guinea pig, horse, and monkey retina: their occurrence coincides with the presence of blood vessels. Glia 1, 74–89. https://doi.org/10.1002/GLIA.440010109

Schreibelt, G., Kooij, G., Reijerkerk, A., Doorn, R., Gringhuis, S.I., Pol, S., Weksler, B.B., Romero, I.A., Couraud, P., Piontek, J., Blasig, I.E., Dijkstra, C.D., Ronken, E., Vries, H.E., 2007. Reactive oxygen species alter brain endothelial tight junction dynamics via RhoA, PI3 kinase, and PKB signaling. FASEB J. 21, 3666–3676. https://doi.org/10.1096/FJ.07-8329COM

Scott, A., Fruttiger, M., 2009. Oxygen-induced retinopathy: a model for vascular pathology in the retina. Eye 2010 243 24, 416–421. https://doi.org/10.1038/eye.2009.306

Seo, E.J., Choi, J.A., Koh, J.Y., Yoon, Y.H., 2020. Aflibercept ameliorates retinal pericyte loss and restores perfusion in streptozotocin-induced diabetic mice. BMJ Open Diabetes Res. Care 8, e001278. https://doi.org/10.1136/BMJDRC-2020-001278

Sertié, A.L., Sossi, V., Camargo, A.M.A., Zatz, M., Brahe, C., Passos-Bueno, M.R., 2000. Collagen XVIII, containing an endogenous inhibitor of angiogenesis and tumor growth, plays a critical role in the maintenance of retinal structure and in neural tube closure (Knobloch syndrome). Hum. Mol. Genet. 9, 2051–2058. https://doi.org/10.1093/HMG/9.13.2051

Sheibani, N., Sorenson, C.M., Cornelius, L.A., Frazier, W.A., 2000. Thrombospondin-1, a natural inhibitor of angiogenesis, is present in vitreous and aqueous humor and is modulated by hyperglycemia. Biochem. Biophys. Res. Commun. 267, 257–261. https://doi.org/10.1006/BBRC.1999.1903

Shen, W., Li, S., Chung, S.H., Gillies, M.C., 2010. Retinal vascular changes after glial disruption in rats. J. Neurosci. Res. 88, 1485–1499. https://doi.org/10.1002/JNR.22317

Shu, W., Baumann, B.H., Song, Y., Liu, Y., Wu, X., Dunaief, J.L., 2020. Ferrous but not ferric iron sulfate kills photoreceptors and induces photoreceptor-dependent RPE autofluorescence. Redox Biol. 34. https://doi.org/10.1016/J.REDOX.2020.101469

Shu, W., Baumann, B.H., Song, Y., Liu, Y., Wu, X., Dunaief, J.L., 2019. Iron accumulates in retinal vascular endothelial cells but has minimal retinal penetration after IP iron dextran injection in mice. Investig. Ophthalmol. Vis. Sci. 60, 4378–4387. https://doi.org/10.1167/iovs.19-28250

Shu, W., Dunaief, J.L., 2018. Potential Treatment of Retinal Diseases with Iron Chelators. Pharmaceuticals 11. https://doi.org/10.3390/PH11040112

Siah, C.W., Ombiga, J., Adams, L.A., Trinder, D., Olynyk, J.K., 2006. Normal Iron Metabolism and the Pathophysiology of Iron Overload Disorders. Clin. Biochem. Rev. 27, 5.

Sima, J., Zhang, S.X., Shao, C., Fant, J., Ma, J.X., 2004. The effect of angiostatin on vascular leakage and VEGF expression in rat retina. FEBS Lett. 564, 19–23. https://doi.org/10.1016/S0014-5793(04)00297-2

Simo, R., Carrasco, E., Garcia-Ramirez, M., Hernandez, C., 2006. Angiogenic and Antiangiogenic Factors in Proliferative Diabetic Retinopathy. Curr. Diabetes Rev. 2, 71–98. https://doi.org/10.2174/157339906775473671

Sivaprasad, S., Prevost, A.T., Vasconcelos, J.C., Riddell, A., Murphy, C., Kelly, J., Bainbridge, J., Tudor-Edwards, R., Hopkins, D., Hykin, P., Bhatnagar, A., Burton, B., Chakravarthy, U., Eleftheriadis, H., Empeslidis, T., Gale, R., George, S., Habib, M., Kelly, S., Lotery, A., McKibbin, M., Membrey, L., Menon, G., Mushtaq, B., Nicholson, L., Ramu, J., Osoba, O., Patel, J., Prakash, P., Purbrick, R., Ross, A., Stylianides, A., Talks, J., Harding, S., Peto, T., Yeo, S.T., Laidlaw, A., Amoaku, W., Hood, G., Hitman, G.A., Preece, D., Burns, P., Walker, S., Mensah, E., Karia, N., 2017. Clinical efficacy of intravitreal aflibercept versus panretinal photocoagulation for best corrected visual acuity in patients with proliferative diabetic retinopathy at 52 weeks (CLARITY): a multicentre, single-blinded, randomised, controlled, phase 2b, non-inferiority trial. Lancet (London, England) 389, 2193–2203. https://doi.org/10.1016/S0140-6736(17)31193-5

Smith, G., McLeod, D., Foreman, D., Boulton, M., 1999. Immunolocalisation of the VEGF receptors FLT-1, KDR, and FLT-4 in diabetic retinopathy. Br. J. Ophthalmol. 83, 486–494. https://doi.org/10.1136/bjo.83.4.486

Smith, M.A., Harris, P.L.R., Sayre, L.M., Perry, G., 1997. Iron accumulation in Alzheimer disease is a source of redox-generated free radicals. Proc. Natl. Acad. Sci. U. S. A. 94, 9866–9868. https://doi.org/10.1073/PNAS.94.18.9866

Smith, R.S. (Richard S., 2002. Systematic evaluation of the mouse eye : anatomy, pathology, and biomethods. CRC Press.

Soliman, S.M., Adam, Z.A.A., Abd allah, U.K.M., 2010. Light and electron microscopic structure of goat's retina. J. Vet. Med. Res. 20, 52–62. https://doi.org/10.21608/jvmr.2020.77580

Somerville, R.P.T., Oblander, S.A., Apte, S.S., 2003. Matrix metalloproteinases: Old dogs with new tricks. Genome Biol. https://doi.org/10.1186/gb-2003-4-6-216

Song, D., Dunaief, J.L., 2013. Retinal iron homeostasis in health and disease. Front. Aging Neurosci. 5, 24. https://doi.org/10.3389/FNAGI.2013.00024/BIBTEX

Song, D., Song, Y., Hadziahmetovic, M., Zhong, Y., Dunaief, J.L., 2012. Systemic administration of the iron chelator deferiprone protects against light-induced photoreceptor degeneration in the mouse retina. Free Radic. Biol. Med. 53, 64. https://doi.org/10.1016/J.FREERADBIOMED.2012.04.020

Sorenson, C.M., Wang, S., Gendron, R., Paradis, H., Sheibani, N., 2013. Thrombospondin-1 Deficiency Exacerbates the Pathogenesis of Diabetic Retinopathy. J. Diabetes Metab. Suppl 12. https://doi.org/10.4172/2155-6156.S12-005

Speiser, P., Gittelsohn, A.M., Patz, A., 1968. Studies on Diabetic Retinopathy: III. Influence of Diabetes on Intramural Pericytes. Arch. Ophthalmol. 80, 332–337. https://doi.org/10.1001/ARCHOPHT.1968.00980050334007

Spranger, J., Osterhoff, M., Reimann, M., Möhlig, M., Ristow, M., Francis, M.K., Cristofalo, V.,

Hammes, H.P., Smith, G., Boulton, M., Pfeiffer, A.F.H., 2001. Loss of the antiangiogenic pigment epithelium-derived factor in patients with angiogenic eye disease. Diabetes 50, 2641–2645. https://doi.org/10.2337/DIABETES.50.12.2641

Sridhar, M.S., 2018. Anatomy of cornea and ocular surface. Indian J. Ophthalmol. 66, 190. https://doi.org/10.4103/IJO.IJO_646_17

Steegmann-Olmedillas, J.L., 2011. The role of iron in tumour cell proliferation. Clin. Transl. Oncol. 13, 71–76. https://doi.org/10.1007/S12094-011-0621-1

Stone, J., Dreher, Z., 1987. Relationship between astrocytes, ganglion cells and vasculature of the retina. J. Comp. Neurol. 255, 35–49. https://doi.org/10.1002/CNE.902550104

Surguladze, N., Patton, S., Cozzi, A., Fried, M.G., Connor, J.R., 2005. Characterization of nuclear ferritin and mechanism of translocation. Biochem. J. 388, 731. https://doi.org/10.1042/BJ20041853

Suriano, F., Vieira-Silva, S., Falony, G., Roumain, M., Paquot, A., Pelicaen, R., Régnier, M., Delzenne, N.M., Raes, J., Muccioli, G.G., Van Hul, M., Cani, P.D., 2021. Novel insights into the genetically obese (ob/ob) and diabetic (db/db) mice: two sides of the same coin. Microbiome 9, 1–20. https://doi.org/10.1186/S40168-021-01097-8/FIGURES/7

Suzuki, H., Tani, K., Tamura, A., Tsukita, S., Fujiyoshi, Y., 2015. Model for the architecture of claudin-based paracellular ion channels through tight junctions. J. Mol. Biol. 427, 291–297. https://doi.org/10.1016/J.JMB.2014.10.020

Takahashi, K., Saishin, Yoshitsugu, Saishin, Yumiko, Silva, R.L., Oshima, Y., Oshima, S., Melia, M., Paszkiet, B., Zerby, D., Kadan, M.J., Liau, G., Kaleko, M., Connelly, S., Luo, T., Campochiaro, P.A., 2003. Intraocular expression of endostatin reduces VEGF-induced retinal vascular permeability, neovascularization, and retinal detachment. FASEB J. 17, 896–898. https://doi.org/10.1096/fj.02-0824fje

Tang, J., Kern, T.S., 2011. Inflammation in Diabetic Retinopathy. Prog. Retin. Eye Res. 30, 343. https://doi.org/10.1016/J.PRETEYERES.2011.05.002

Tang, W.H., Martin, K.A., Hwa, J., 2012. Aldose reductase, oxidative stress, and diabetic mellitus. Front. Pharmacol. 3 MAY. https://doi.org/10.3389/FPHAR.2012.00087/FULL

Tarr, J.M., Kaul, K., Chopra, M., Kohner, E.M., Chibber, R., 2013. Pathophysiology of diabetic retinopathy. ISRN Ophthalmol. 2013, 343560. https://doi.org/10.1155/2013/343560

Thanos, S., 1991. The Relationship of Microglial Cells to Dying Neurons During Natural Neuronal Cell Death and Axotomy-induced Degeneration of the Rat Retina. Eur. J. Neurosci. 3, 1189–1207. https://doi.org/10.1111/J.1460-9568.1991.TB00054.X

Theurl, M., Song, D., Clark, E., Sterling, J., Grieco, S., Altamura, S., Galy, B., Hentze, M., Muckenthaler, M.U., Dunaief, J.L., 2016. Mice with hepcidin-resistant ferroportin accumulate iron in the retina. FASEB J. 30, 813–823. https://doi.org/10.1096/fj.15-276758

Tian, R., Luo, Y., Liu, Q., Cai, M., Li, J., Sun, W., Wang, J., He, C., Liu, Y., Liu, X., 2014. The effect of claudin-5 overexpression on the interactions of claudin-1 and -2 and barrier function in retinal cells. Curr. Mol. Med. 14, 1226–1237. https://doi.org/10.2174/1566524014666141015160355

Timpl, R., Wiedemann, H., Van Delden, V., Furthmayr, H., Kühn, K., 1981. A network model for the organization of type IV collagen molecules in basement membranes. Eur. J. Biochem. 120, 203–211. https://doi.org/10.1111/J.1432-1033.1981.TB05690.X

Toda, R., Kawazu, K., Oyabu, M., Miyazaki, T., Kiuchi, Y., 2011. Comparison of drug permeabilities across the blood-retinal barrier, blood-aqueous humor barrier, and blood-brain barrier. J. Pharm. Sci. 100, 3904–3911. https://doi.org/10.1002/JPS.22610

Todorich, B., Zhang, X., Slagle-Webb, B., Seaman, W.E., Connor, J.R., 2008. Tim-2 is the receptor for H-ferritin on oligodendrocytes. J. Neurochem. 107, 1495–1505. https://doi.org/10.1111/j.1471-4159.2008.05678.x

Toussaint, D., Dustin, P., 1963. Electron microscopy of normal and diabetic retinal capillaries. Arch. Ophthalmol. (Chicago, Ill. 1960) 70, 96–108. https://doi.org/10.1001/ARCHOPHT.1963.00960050098015

Treuting, P.M., Dintzis, S.M., 2012. Comparative Anatomy and Histology: A Mouse and Human Atlas, in: Comparative Anatomy and Histology: A Mouse and Human Atlas. pp. 46–51.

Tucker, W.D., Mahajan, K., 2018. Anatomy, Blood Vessels, StatPearls.

Ugarte, M., Grime, G.W., Lord, G., Geraki, K., Collingwood, J.F., Finnegan, M.E., Farnfield, H., Merchant, M., Bailey, M.J., Ward, N.I., Foster, P.J., Bishop, P.N., Osborne, N.N., 2012. Concentration of various trace elements in the rat retina and their distribution in different structures. Metallomics 4, 1245–1254. https://doi.org/10.1039/C2MT20157G

Ugarte, M., Grime, G.W., Osborne, N.N., 2014. Distribution of trace elements in the mammalian retina and cornea by use of particle-induced X-ray emission (PIXE): localisation of zinc does not correlate with that of metallothioneins. Metallomics 6, 274–278. https://doi.org/10.1039/C3MT00271C

Valença, A., Mendes-Jorge, L., Bonet, A., Catita, J., Ramos, D., Jose-Cunilleras, E., Garcia, M., Carretero, A., Nacher, V., Navarro, M., Ruberte, J., 2021. TIM2 modulates retinal iron levels and is involved in blood-retinal barrier breakdown. Exp. Eye Res. 202, 108292. https://doi.org/10.1016/j.exer.2020.108292

Valsania, P., Warram, J.H., Rand, L.I., Krolewski, A.S., 1993. Different Determinants of Neovascularization on the Optic Disc and on the Retina in Patients With Severe Nonproliferative Diabetic Retinopathy. Arch. Ophthalmol. 111, 202–206. https://doi.org/10.1001/ARCHOPHT.1993.01090020056023

Van Buskirk, E.M., 1989. The anatomy of the limbu. Eye 3, 101–108. https://doi.org/10.1038/eye.1989.16

Van Der Wijk, A.E., Wisniewska-Kruk, J., Vogels, I.M.C., Van Veen, H.A., Ip, W.F., Van Der Wel, N.N., Van Noorden, C.J.F., Schlingemann, R.O., Klaassen, I., 2019. Expression patterns of endothelial permeability pathways in the development of the blood-retinal barrier in mice. FASEB J. 33, 5320–5333. https://doi.org/10.1096/FJ.201801499RRR

Vecino, E., Rodriguez, F.D., Ruzafa, N., Pereiro, X., Sharma, S.C., 2016. Glia-neuron interactions in the mammalian retina. Prog. Retin. Eye Res. 51, 1–40. https://doi.org/10.1016/J.PRETEYERES.2015.06.003

Villarroel, M., Ciudin, A., Hernández, C., Simó, R., 2010. Neurodegeneration: An early event of diabetic retinopathy. World J. Diabetes 1, 57. https://doi.org/10.4239/WJD.V1.I2.57

Vinores, S.A., 2010. Breakdown of the Blood–Retinal Barrier. Encycl. Eye 216. https://doi.org/10.1016/B978-0-12-374203-2.00137-8

Wang, J., Pantopoulos, K., 2011. Regulation of cellular iron metabolism. Biochem. J. 434, 365. https://doi.org/10.1042/BJ20101825

Wang, J., Xu, E., Elliott, M.H., Zhu, M., Le, Y.Z., 2010. Müller cell-derived VEGF is essential for diabetes-induced retinal inflammation and vascular leakage. Diabetes 59, 2297–2305. https://doi.org/10.2337/DB09-1420

Wang, S., Ma, W., Yuan, Z., Wang, S.M., Yi, X., Jia, H., Xue, F., 2016. Association between obesity indices and type 2 diabetes mellitus among middle-aged and elderly people in Jinan, China: a cross-sectional study. BMJ Open 6, e012742. https://doi.org/10.1136/BMJOPEN-2016-012742

Wang, X., Liu, X., Ren, Y., Liu, Y., Han, S., Zhao, J., Gou, X., He, Y., 2019. PEDF protects human retinal pigment epithelial cells against oxidative stress via upregulation of UCP2 expression. Mol. Med. Rep. 19, 59–74. https://doi.org/10.3892/MMR.2018.9645

Wang, Y., Wang, S., Sheibani, N., 2006. Enhanced proangiogenic signaling in thrombospondin-1-deficient retinal endothelial cells. Microvasc. Res. 71, 143–151.

https://doi.org/10.1016/j.mvr.2006.02.004

Wang, Z., Liu, C.H., Huang, S., Chen, J., 2019. Assessment and characterization of hyaloid vessels in mice. J. Vis. Exp. 2019. https://doi.org/10.3791/59222

Ward, R.J., Zucca, F.A., Duyn, J.H., Crichton, R.R., Zecca, L., 2014. The role of iron in brain ageing and neurodegenerative disorders. Lancet. Neurol. 13, 1045. https://doi.org/10.1016/S1474-4422(14)70117-6

Warpeha, K.M., Chakravarthy, U., 2003. Molecular genetics of microvascular disease in diabetic retinopathy. Eye 17, 305–311. https://doi.org/10.1038/SJ.EYE.6700348

Watanabe, D., Suzuma, K., Suzuma, I., Ohashi, H., Ojima, T., Kurimoto, M., Murakami, T., Kimura, T., Takagi, H., 2005. Vitreous levels of angiopoietin 2 and vascular endothelial growth factor in patients with proliferative diabetic retinopathy. Am. J. Ophthalmol. 139, 476–481. https://doi.org/10.1016/J.AJO.2004.10.004

Weber, J., Peng, H., Rader, C., 2017. From rabbit antibody repertoires to rabbit monoclonal antibodies. Exp. Mol. Med. 2017 493 49, e305–e305. https://doi.org/10.1038/emm.2017.23

Weller, M., Clausen, R., Heimann, K., Wiedemann, P., 1990. Iron-binding proteins in the human vitreous: lactoferrin and transferrin in health and in proliferative intraocular disorders. Ophthalmic Res. 22, 194–200. https://doi.org/10.1159/000267023

WHO (World Health Organization), 2021. Diabetes [WWW Document]. URL https://www.who.int/news-room/fact-sheets/detail/diabetes (accessed 2.18.22).

WHO (World Health Organization), 2020. Strengthening diagnosis and treatment of Diabetic Retinopathy in SEA Region [WWW Document]. URL https://apps.who.int/iris/handle/10665/334224 (accessed 2.18.22).

Wichaiyo, S., Yatmark, P., Morales Vargas, R.E., Sanvarinda, P., Svasti, S., Fucharoen, S., Morales, N.P., 2015. Effect of iron overload on furin expression in wild-type and β-thalassemic mice. Toxicol. Reports 2, 415–422. https://doi.org/10.1016/J.TOXREP.2015.01.004

Wickström, S.A., Alitalo, K., Keski-Oja, J., 2002. Endostatin associates with integrin α5β1 and caveolin-1, and activates Src via a tyrosyl phosphatase-dependent pathway in human endothelial cells. Cancer Res. 62, 5580–5589.

Worwood, M., Aherne, W., Dawkins, S., Jacobs, A., 1975. The characteristics of ferritin from human tissues, serum and blood cells. Clin. Sci. Mol. Med. 48, 441–451. https://doi.org/10.1042/CS0480441

Wu, W., Yuan, J., Shen, Y., Yu, Y., Chen, X., Zhang, L., Huang, K., Zhan, J., Dong, G.P., Fu, J., 2020. Iron overload is related to elevated blood glucose levels in obese children and aggravates high glucose-induced endothelial cell dysfunction in vitro. BMJ Open Diabetes Res. Care 8, e001426. https://doi.org/10.1136/BMJDRC-2020-001426

Xu, J., Chen, L.J., Yu, J., Wang, H.J., Zhang, F., Liu, Q., Wu, J., 2018. Involvement of Advanced Glycation End Products in the Pathogenesis of Diabetic Retinopathy. Cell. Physiol. Biochem. 48, 705–717. https://doi.org/10.1159/000491897

Yamaguchi, N., Anand-Apte, B., Lee, M., Sasaki, T., Fukai, N., Shapiro, R., Que, I., Lowik, C., Timpl, R., Olsen, B.R., 1999. Endostatin inhibits VEGF-induced endothelial cell migration and tumor growth independently of zinc binding. EMBO J. 18, 4414–4423. https://doi.org/10.1093/EMBOJ/18.16.4414

Yan, H.T., Su, G.F., 2014. Expression and significance of HIF-1 α and VEGF in rats with diabetic retinopathy. Asian Pac. J. Trop. Med. 7, 237–240. https://doi.org/10.1016/S1995-7645(14)60028-6

Yang, X., Cao, J., Du, Y., Gong, Q., Cheng, Y., Su, G., 2019. Angiopoietin-Like Protein 4 (ANGPTL4) Induces Retinal Pigment Epithelial Barrier Breakdown by Activating Signal Transducer and Activator of Transcription 3 (STAT3): Evidence from ARPE-19 Cells Under

Hypoxic Condition and Diabetic Rats. Med. Sci. Monit. 25, 6742. https://doi.org/10.12659/MSM.915748

Yau, K.W., Baylor, D.A., 1989. Cyclic GMP-activated conductance of retinal photoreceptor cells. Annu. Rev. Neurosci. 12, 289–327. https://doi.org/10.1146/ANNUREV.NE.12.030189.001445

Yi, X., Schubert, M., Peachey, N.S., Suzuma, K., Burks, D.J., Kushner, J.A., Suzuma, I., Cahill, C., Flint, C.L., Dow, M.A., Leshan, R.L., King, G.L., White, M.F., 2005. Insulin receptor substrate 2 is essential for maturation and survival of photoreceptor cells. J. Neurosci. 25, 1240–1248. https://doi.org/10.1523/JNEUROSCI.3664-04.2005

Yoshida, Y., Yamagishi, S.I., Matsui, T., Jinnouchi, Y., Fukami, K., Imaizumi, T., Yamakawa, R., 2009. Protective role of pigment epithelium-derived factor (PEDF) in early phase of experimental diabetic retinopathy. Diabetes. Metab. Res. Rev. 25, 678–686. https://doi.org/10.1002/DMRR.1007

Young, R.W., 1967. The renewal of photoreceptor cell outer segments. J. Cell Biol. 33, 61–72. https://doi.org/10.1083/JCB.33.1.61

Yurchenco, P.D., Schittny, J.C., 1990. Molecular architecture of basement membranes. FASEB J. 4, 1577–1590. https://doi.org/10.1096/FASEBJ.4.6.2180767

Zhang, A.-S., Enns, C.A., 2008. Iron Homeostasis: Recently Identified Proteins Provide Insight into Novel Control Mechanisms *. J. Biol. Chem. 284, 711–715. https://doi.org/10.1074/jbc.R800017200

Zhang, C., Asnaghi, L., Gongora, C., Patek, B., Hose, S., Ma, B., Fard, M.A., Brako, L., Singh, K., Goldberg, M.F., Handa, J.T., Lo, W.K., Eberhart, C.G., Zigler, J.S., Sinha, D., 2011. A developmental defect in astrocytes inhibits programmed regression of the hyaloid vasculature in the mammalian eye. Eur. J. Cell Biol. 90, 440–448. https://doi.org/10.1016/j.ejcb.2011.01.003

Zhang, C., Gehlbach, P., Gongora, C., Cano, M., Fariss, R., Hose, S., Nath, A., Green, W.R., Goldberg, M.F., Zigler, J.S., Sinha, D., 2005. A potential role for β- and γ-crystallins in the vascular remodeling of the eye. Dev. Dyn. 234, 36–47. https://doi.org/10.1002/dvdy.20494

Zhang, D., Lv, F.L., Wang, G.H., 2018. Effects of HIF-1α on diabetic retinopathy angiogenesis and VEGF expression. Eur. Rev. Med. Pharmacol. Sci. 22, 5071–5076. https://doi.org/10.26355/EURREV_201808_15699

Zhang, L., Knez, M., 2011. Spherical nanoscale protein templates for biomedical applications : A review on ferritin. Jorunal Nanosci. Lett. 2, 1–13.

Zhang, M., Lv, X.Y., Li, J., Xu, Z.G., Chen, L., 2008. The characterization of high-fat diet and multiple low-dose streptozotocin induced type 2 diabetes rat model. Exp. Diabetes Res. 2008, 704045. https://doi.org/10.1155/2008/704045

Zhang, X., Zeng, H., Bao, S., Wang, N., Gillies, M.C., 2014. Diabetic macular edema: new concepts in patho-physiology and treatment. Cell Biosci. 2014 41 4, 1–14. https://doi.org/10.1186/2045-3701-4-27

Zhang, Y., Stone, J., 1997. Role of astrocytes in the control of developing retina1 vessels. Investig. Ophthalmol. Vis. Sci. 38, 1653–1666.

Zhao, L., Li, Y., Song, D., Song, Y., Theurl, M., Wang, C., Cwanger, A., Su, G., Dunaief, J.L., 2014. A High Serum Iron Level Causes Mouse Retinal Iron Accumulation Despite an Intact Blood-Retinal Barrier. Am. J. Pathol. 184, 2862–2867. https://doi.org/10.1016/j.ajpath.2014.07.008

Zhao, T., Guo, X., Sun, Y., 2021. Iron Accumulation and lipid peroxidation in the aging retina: Implication of ferroptosis in age-related macular degeneration. Aging Dis. 12, 529–551. https://doi.org/10.14336/AD.2020.0912

Zhao, Y., Singh, R.P., 2018. The role of anti-vascular endothelial growth factor (anti-VEGF) in the

management of proliferative diabetic retinopathy. Drugs Context 7. https://doi.org/10.7573/DIC.212532

Zhi, K., Raji, B., Nookala, A.R., Khan, M.M., Nguyen, X.H., Sakshi, S., Pourmotabbed, T., Yallapu, M.M., Kochat, H., Tadrous, E., Pernell, S., Kumar, S., 2021. Plga nanoparticle-based formulations to cross the blood-brain barrier for drug delivery: From r&d to cgmp. Pharmaceutics 13. https://doi.org/10.3390/PHARMACEUTICS13040500

Zhou, J., Xie, Z., 2022. Endostatin Inhibits Blood-Retinal Barrier Breakdown in Diabetic Rats by Increasing the Expression of ICAM-1 and VCAM-1 and Decreasing the Expression of VEGF. Comput. Math. Methods Med. 2022, 1–9. https://doi.org/10.1155/2022/5105866

Zhou, L., Sun, X., Huang, Z., Zhou, T., Zhu, X., Liu, Y., Wang, J., Cheng, B., Li, M., He, C., Liu, X., 2018. Imatinib Ameliorated Retinal Neovascularization by Suppressing PDGFR-α and PDGFR-β. Cell. Physiol. Biochem. 48, 263–273. https://doi.org/10.1159/000491726

Zhou, Z.D., Tan, E.K., 2017. Iron regulatory protein (IRP)-iron responsive element (IRE) signaling pathway in human neurodegenerative diseases. Mol. Neurodegener. 12. https://doi.org/10.1186/S13024-017-0218-4

Zhu, X., Li, A., Brown, B., Weiss, E.R., Osawa, S., Craft, C.M., 2002. Mouse cone arrestin expression pattern: Light induced translocation in cone photoreceptors. Mol. Vis. 8, 462–471.

Zihni, C., Mills, C., Matter, K., Balda, M.S., 2016. Tight junctions: From simple barriers to multifunctional molecular gates. Nat. Rev. Mol. Cell Biol. 17, 564–580. https://doi.org/10.1038/NRM.2016.80

Zudaire, E., Gambardella, L., Kurcz, C., Vermeren, S., 2011. A computational tool for quantitative analysis of vascular networks. PLoS One 6. https://doi.org/10.1371/journal.pone.0027385

Universitat Autònoma
de Barcelona

FACULTAT DE
VETERINÀRIA

Centre de
biotecnologia
animal i teràpia gènica